UNIVERSITÀ DEGLI STUDI
DI TRENTO

DEPARTMENT OF INFORMATION ENGINEERING AND COMPUTER SCIENCE
ICT International Doctoral School

Advanced Methodologies for Planning and Scheduling Payload Operations for Planetary Exploration Missions

Stefano Paterna

Advisor
Prof. Lorenzo Bruzzone
University of Trento

Co-Advisors
Ing. Massimo Santoni
University of Trento
Prof. Roberto Iuppa
University of Trento

July 2021

A mia madre, a mio padre, a me stesso.

Abstract

Missions for planetary exploration are unique opportunities to provide very meaningful and high-valuable data about the analysed celestial bodies. These missions can characterize many aspects of them, thanks to the different remote sensing instruments included in their science payload. However, the observations in this context are influenced by complex constraints (e.g., limited resources, environment characteristics) and limitations, thus limiting the availability of acquisition opportunities. Hence, an accurate planning and scheduling of the acquisition operations by the science payload instruments of a Planetary Exploration mission is a crucial task in the mission design. This requires the development of automatic methodologies to aid this delicate phase, which are capable of considering all the different constraints, the science requirements and the characteristics of the instruments in order to produce feasible observation schedules that are optimized with respect to the acquisition quality. In this context, this thesis provides two main contributions related to: i) the analysis and the scheduling of the acquisitions by a single instrument and ii) the extension of the study to the simultaneous scheduling of the observations by multiple instruments.

The first novel contribution presents a methodology for the automatic scheduling of the acquisition operations of a single instrument for planetary exploration missions. The presented methodology is based on 2 main phases and it uses a multi-objective optimization technique to produce an acquisition schedule, optimized with respect to the scientific requirements and the characteristics of the considered sensor and the mission constraints. The second contribution addresses the complexity of automatically generating and harmonizing observation schedules for multiple instruments simultaneously. The proposed method models the problem as a bilevel optimization task. At the lower level the acquisition schedule for each sensor is produced and evaluated, considering all the instrument-related requirements and limitations. At the upper level the harmonization of the individual sensor schedules is performed, considering all the mission- and resource-related constraints and maximizing the overall quality and science return.

The proposed methods have been applied considering in detail the operations of radar sounder instruments. In particular, the first methodology has been tested on the observations by RIME, radar sounder of the JUICE mission and the second considered RIME and three other instruments of the same missions. The obtained results show the effectiveness of the proposed techniques, which aim at increasing the level of automation in the data acquisition planning and scheduling phase in Planetary Exploration missions.

The work compiled in this thesis was supported by the Italian Space Agency (ASI) in the framework of "Attività scientifiche per JUICE fase C/D" under Grant No. 2018-25-HH.0.

Contents

List of Tables

List of Figures

List of Abbreviations

2D	2-Dimensional
3D	3-Dimensional
ACO	Ant Colony Optimization
AOI	Area Of Interest
APGEN	Activity Plan GENerator
ASPEN	Automated Scheduling and Planning ENvironment
CO	Combinatorial Optimization
CReMA	Consolidated Report on Mission Analysis
DAG	Directed Acyclic Graph
DR	Data Rate
DLO	Down-Link Opportunity
DTO	Data Take Opportunity
DV	Data Volume
EA	Evolutionary Algorithms
EO	Earth Observation
EOS	Earth Observation Satellite
ESA	European Space Agency
ESOC	ESA Science Operation Center
GA	Genetic Algorithm
GALA	GAnymede Laser Altimeter
GCO-500	Ganymede Circular Orbit (500Km altitude)
GUI	Graphic User Interface
HGA	Hybrid Genetic Algorithm
IEOSS	Integrated Earth Observation Satellite Scheduling
JANUS	Jovis, Amorum ac Natorum Undique Scrutator
JAXA	Japanese Aerospace Exploration Agency
JPL	Jet Propulsion Laboratory
JUICE	JUpiter ICy moons Explorer

LRS	Lunar Radar Sounder
MAJIS	Moons And Jupiter Imaging Spectrometer
MAPGEN	Mixed-initiative Activity Plan GENerator
MAPPS	Mission Analysis and Payload Planning System
MARSIS	Mars Advanced Radar for Subsurface and Ionosphere Sounding
MCS	Mission Control Segment
MOC	Mission Operation Center
NAIF	Navigation and Ancillary Information Facility
NASA	National Aeronautics and Space Administration
NSGA-II	Non-dominated Sorting Genetic Algorithm
P&S	Planning and Scheduling
PE	Planetary Exploration
PI	Principal Investigator
PSO	Particle Swarm Optimization
RADAR	RAdio Detecting And Ranging
REASON	Radar for Europa Assessment and Sounding: Ocean to Near-surface
RIME	Radar for Icy Moons Exploration
SA	Simulated Annealing
SGS	Science Ground Segment
SHARAD	SHAllow RADar
SNR	Signal to Noise Ratio
SPICE	Spacecraft, Planet, Instrument, C-matrix, Event
SOC	Science Operations Center
SRS	Subsurface Radar Sounder
SWT	Science Working Team
TS	Tabu Search

List of Symbols

Radar Sounder Operations

$\epsilon_{r,i}$	Relative dielectric permittivity of the i-th subsurface layer.
$P_{ss,j}$	Power received from the j-th subsurface layer interface.
P_t	Power associated to the transmitted pulse.
G	Antenna gain.
λ	Wavelength associated to the central frequency f_c of the transmitted pulse.
$\Gamma_{j,j+1}$	Reflection coefficient at the interface between layer j and layer $j+1$, (layer 0 is usually free space or the planet atmosphere).
A_{ill}	Illuminated area, corresponding to the radar antenna footprint on the ground.
α	Attenuation constant of the material.
h	Orbit altitude of the platform (spacecraft) on which the sounder is mounted with respect to the ground.
z_j	Depth of the interface between layer j and $j+1$.
SNR_j	Signal to Noise Ratio of the j-th subsurface layer.
P_n	Noise power.
k_b	Boltzmann constant.
T_r	Radar receiver noise temperature.
T_g	Galactic noise temperature.
B	Transmitted pulse bandwidth.
T_p	Transmitted pulse duration.
SWL	Radar receiving window length.
σ_1 and σ_2	Topographic margins.
σ_h	Spacecraft trajectory uncertainty.
z_{max}	Maximum penetration depth.

T_{iono}	Ionosphere-induced delay of the transmitted pulse travel time.
M_s	Security margin applied to the receiving window length.
f_s	Radar receiver sampling frequency.
PRF	Pulse repetition frequency.
N_bit	Number of bits to represent each received echo sample.
N_p	Presumming factor.

Single Instrument Scheduling

Φ	Full considered time interval (i.e., the time span of a particular mission phase).
$\Phi_f = \{\phi_1^f, \phi_2^f, ..., \phi_P^f\}$	Set of time intervals in which the acquisition is feasible with respect to the analyzed instrument capabilities and limitations.
$S = \{s_1, s_2, ..., s_N\}$	Set of the acquisition segments in which Φ_f is subdivided.
s_i	i-th acquisition segment.
$S^* \subset S$	Subset of acquisition segments that constitute the acquisition schedule, resulting from the selection phase.
N	Number of acquisition segments $s \in S$.
$\mathbf{x}$	Vector of the variables (x_i) associated to the acquisition segments and used in the selection phase.
$x_i = x(s_i)$	Binary variable ($x_i \in \{0, 1\}$) associated to the i-th acquisition segment, determining if that segment is included in the acquisition schedule ($x_i = 1$) or not ($x_i = 0$).
$st(s_i)$	Start time of the i-th acquisition segment.
$et(s_i)$	End time of the i-th acquisition segment.
$time(s_i)$	Duration of the i-th acquisition segment.
$day(s_i)$	Day in which the acquisition identified by s_i would take place.
$a(s_i)$	Area covered by the i-th acquisition segment.
$e(s_i)$	Energy consumption associated to the data acquisition operation performed from $st(s_i)$ to $et(s_i)$.
$m(s_i)$	Storage memory consumption associated to the data acquisition operation performed from $st(s_i)$ to $et(s_i)$.
En	Available energy on board the spacecraft.
Mem	Available storage memory on board the spacecraft.
$dat_d(\mathbf{x})$	Acquisition time associated to day d, given the candidate schedule expressed by $\mathbf{x}$.

$\mathbf{g}_d = \{g_{d,1}, g_{d,2}, ..., g_{d,N}\}$	Vector used as support to define $dat_d(\mathbf{x})$.
$g_{d,i} = \{0, 1\}$	Component of $\mathbf{g}_d$.
A	Total surface to be covered with the acquisitions performed by the considered instrument.
A_s	Surface covered by the acquisition segments included in the considered schedule.
A_o	Total overlap surface of the influence areas $a(s_i)$ associated to the segments included in the considered schedule.
$t(s_i)$	Metric to support the proposed mutation operator, expressing how well adding the segment s_i to the considered solution improves the total coverage.
$r(s_i)$	Metric to support the proposed mutation operator, expressing how well removing the segment s_i from the considered solution reduces the coverage overlap.
q_i	Generic quality metric of the observation associated to the segment s_i.

Multiple Instruments Scheduling (Extension of the Formalization to the Multi-Instrument case)

I	Total number of considered instruments.
Φ	Full considered time interval (i.e., the time span of a particular mission phase).
$\Phi_{f,j} = \{\phi_1^{f,j}, \phi_2^{f,j}, ..., \phi_{P_j}^{f}\}$	Set of time intervals in which the acquisition is feasible with respect to the capabilities and limitations of the j-th instrument ($j = 1, ..., I$).
$S_j = \{s_{1,j}, s_{2,j}, ..., s_{N_j,j}\}$	Set of the acquisition segments in which $\Phi_{f,j}$ is subdivided.
$s_{i,j}$	i-th acquisition segment associated to the j-th instrument.
$S_j^{*,\mathbf{w}_j} \subset S_j$	Subset of acquisition segments associated to the j-th instrument that constitute the acquisition schedule, resulting from the instrument level segment selection phase, given the set of weights $\mathbf{w}_j$.
N_j	Number of acquisition segments $s_{i,j} \in S_j$.
$\mathbf{x}_j$	Vector of the variables ($x_{i,j}$) of the instrument-level scheduling problem, associated to the acquisition segments.

$x_{i,j} = x(s_{i,j})$	Binary variable ($x_{i,j} \in \{0, 1\}$) associated to the i-th acquisition segment and the j-th instrument, determining if that segment is included in the instrument acquisition schedule ($x_{i,j} = 1$) or not ($x_{i,j} = 0$).
$\mathbf{w}_j$	Vector of the variables ($w_{i,j}$) of the global level scheduling problem and passed to the instrument level to guide the instrument-level segment selection, associated to the acquisition segments.
$w_{i,j} = w(s_{i,j})$	Variable ($w_{i,j} \in [0; 1]\}$) associated to the i-th acquisition segment and the j-th instrument, determining the weight and thus the importance of segment $s_{i,j}$.
$F(\mathbf{x}_1, ..., \mathbf{x}_I, \mathbf{w}_1, ..., \mathbf{w}_I)$	Objective function of the global level observation scheduling problem.
$f_j(\mathbf{x}_j, \mathbf{w}_j)$	Objective function of the instrument level observation scheduling problem, expressing the quality of the observation schedule produced for the j-th instrument.
$st(s_{i,j})$	Start time of the i-th acquisition segment associated to the j-th instrument.
$et(s_{i,j})$	End time of the i-th acquisition segment associated to the j-th instrument.
$time(s_{i,j})$	Duration of the i-th acquisition segment associated to the j-th instrument.
$day(s_{i,j})$	Day in which the acquisition identified by s_i associated to the j-th instrument would take place.
$a(s_{i,j})$	Area covered by the i-th acquisition segment associated to the j-th instrument.
$e(s_{i,j})$	Energy consumption associated to the data acquisition operation performed from $st(s_{i,j})$ to $et(s_{i,j})$.
$m(s_{i,j})$	Storage memory consumption associated to the data acquisition operation performed from $st(s_{i,j})$ to $et(s_{i,j})$.
En	Available energy on board the spacecraft.
Mem	Available storage memory on board the spacecraft.
$pen = pen_e + pen_m + pen_i$	Penalty factor assigned to the global level objective function, expressing constraint violations of all considered types (energy, memory and inter-instrument limitations).
$q_{i,j}$	Generic quality metric of the observation associated to the segment $s_{i,j}$.

ρ_{sub}	Substitution factor employed in the instrument level scheduling task, implemented with local search.
$a_o(s_{l,j}, s_{k,j})$	Segment overlap area parameter, employed in the instrument level scheduling task, implemented with local search.
$wsm(s_{l,j}, s_{k,j})$	Weighted surface maintainance parameter, employed in the instrument level scheduling task, implemented with local search.

Introduction

This Chapter provides an introduction to the PhD thesis. In the first part the main motivations of the thesis are provided. The second part reports the main objectives of this thesis with a brief description of each proposed novel contribution. Finally, the structure of the thesis is schematized.

Motivations of the Thesis

Missions for planetary exploration have attracted a large interest. These missions represent quite unique opportunities to provide very meaningful and high-valuable data about the analysed celestial bodies, characterizing many different aspects of them, such as their surface, the composition of their atmosphere, their geology and geophysics characteristics, their magnetosphere, etc. This kind of analysis allows to improve our knowledge about how planetary systems are generated and how they evolve, but it can also permit to verify the existence of habitable environments other than the Earth. Many different features can be evaluated, associated to the different aspects and peculiarities of the investigated planets, natural satellites or asteroids and they can lead to very important discoveries.

The numerous and diversified aspects to analyze on a considered celestial body are usually studied by the different instruments included in science payload designed for them. This is for example the case of ESA's JUpiter ICy moons Explorer (JUICE) mission [1]. JUICE is planned to be launched in 2022 and represents the first European mission to the gaseous giant planet. Its key science goals are the characterisation of Ganymede, Europa and Callisto, three of the Galilean satellites, as planetary objects and the study of their potential habitability, together with the exploration of the whole Jovian system as model for the structure of planetary systems beyond the Asteroid Belt. The study of the three icy moons is of major interest after the discovery, thanks to the Galileo mission [2] (the first detailed orbital exploration of the Jovian system), of evidence for the existence of liquid water oceans, hidden under their icy surface, but also due to their geological features and activity, depending on their position with respect to Jupiter. The mission science objectives will be achieved thanks to its science payload composed of 11 different

instruments.

However, such diversity in the on-board instruments and in their associated objectives does not only give the opportunity for a very detailed analysis of the features of the analyzed celestial bodies, but it also makes it very challenging to define and handle the data acquisition strategies for each considered sensor. Indeed, in order to generate an acquisition strategy capable to exploit as much as possible the performances of the instruments defined for a given mission, we need to consider a very large number of different requirements, specifications and limitations. These include the instrument-specific requirements and observation capabilities, the characteristics of the environment in which data acquisitions should be carried (which could severely limit the acquisition capabilities for some sensors), but also the characteristics of the mission itself, such as the trajectory that the spacecraft will follow during the time span of the mission. Moreover, a fundamental aspect to take into account is the availability of resources on board the spacecraft, such as storage memory, energy to power up the instruments or downlink opportunities. All these resources, which for Planetary Exploration missions are generally quite limited, of course need to be shared among all the instruments on board the satellite. In this context, one of the most delicate and important phases of the design of a PE mission is the planning and scheduling of the operations that have to be performed by the science payload. The goal of this phase is the determination of the feasible options for the data acquisitions of each sensor with respect to the above-mentioned constraints, so that for each of them the associated scientific requirements can be met.

Given the very high scientific relevance that these missions have, an accurate analysis of the operations and in particular of the observations to be performed by the science payload instruments of a Planetary Exploration mission is a crucial as well as a very critical task. The relevance of this task is mainly related to the very complex conditions that need to be taken into account in order for the instruments on board to correctly operate. The process to plan and schedule science operations in a mission is thus a very challenging and long-lasting task. It involves a multitude of different entities concentrating on different aspects, from the ones more related to the system engineering to those more focused on the science and the experiments to be carried out. Figure 1 shows the relationships between the several involved entities.

The authors of [3] provide a detailed description of the operations planning and scheduling procedures of a typical ESA planetary mission. The main actor in such process is the Science Ground Segment (SGS), which addresses the scientific aspects of the observations to be performed by the instruments of the science payload. This entity includes the Science Operations Center (SOC) and all the Principal Investigator (PI) Teams. The

[1]Image reproduced from [3].

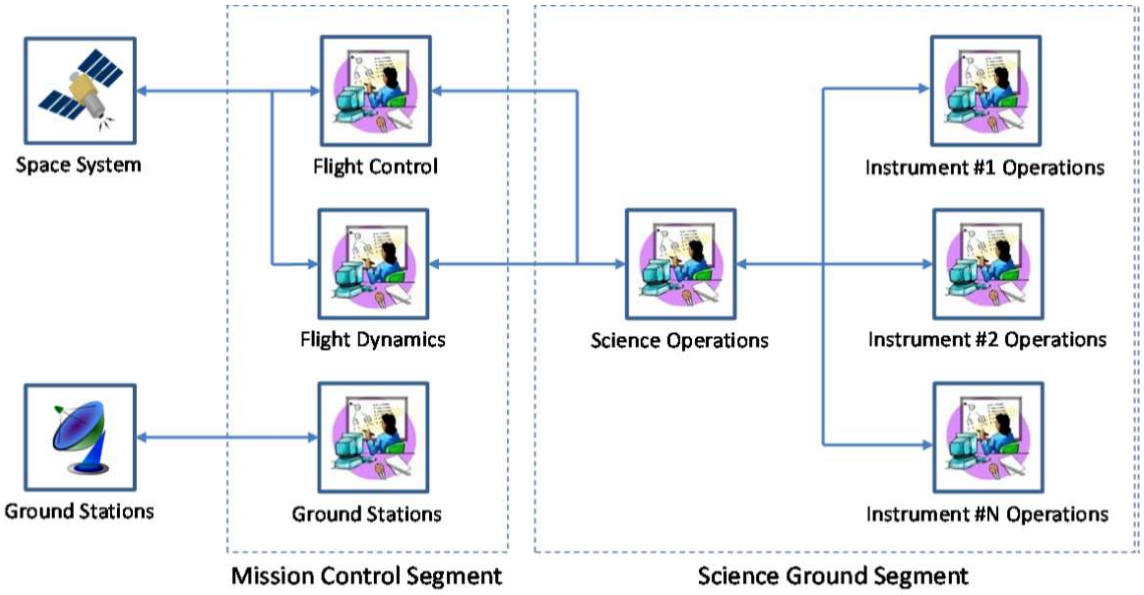

Figure 1: Scheme [1]illustrating different components the complexity of the operation planning and scheduling process and the different entities taking part in it.

role of the PI Teams, besides the study of the instrument design and performances, is that of providing inputs to the SOC on their instrument's operational requirements and limitations. The SOC in turn is in charge of armonizing all these inputs and generate global observation schedules based on them. These schedules and their associated observation operations are then analyzed in depth by the operators of the Mission Control Segment (MCS) and of its main component, the Mission Operation Center (MOC). The tasks of the MCS are mainly related to the overall mission operations and in particular to the spacecraft health, its status and its operations. They are in charge of studying the scheduled observations from an engineering perspective and breaking them down into the series of tasks and the related commands, which have to be fulfilled by the platform and by the instrument in order to perform a given data acquisition.

The planning and scheduling process is a very long and iterative task that takes place over different cycles, which have different length and also different level of detail ([3] [4] [5]). They are usually divided in:

- **Long-term planning cycle**: The first planning cycle is devoted to both the analysis of the overall objectives of the mission (given the spacecraft trajectories) and their feasibility with respect to the general and instrument specific constraints. It allows to define the observation opportunities for each instrument and also to determine a preliminary profile of the observation plans from the point of view of the required resources and of the quality of the observations.

- **Medium-term planning cycle**: The second planning cycle is usually shorter and has the goal to define in more detail the required resources and to allocate them to each instrument on board the spacecraft and the experiments they need to perform.
- **Short-term planning cycle**: The final cycle is devoted to the high detail planning of the science activities and to the definition of the operational command sequences to be executed to realize them.

As shown in detail in Chapter 1, the literature related to the automatic planning and scheduling of observations by remote sensing instruments is mainly focused on the definition of tools for the EOS scheduling problem. It shows significant gaps regarding methodologies and applications devoted to the Planetary Exploration context. Indeed, the tools designed to aid the planning and scheduling phase in PE missions and developed up to the current date have very limited capabilities in the automatic generation of optimized observation schedules. The P&S process itself is iterative, time-consuming and it still requires an extensive presence of human operators and their expertise. Moreover, the methodologies developed in the EO context are usually referred to the acquisitions by a single remote sensing instrument or (in multiple-platform case) by different instruments of the same kind, with almost equal acquisition capabilities and limitations.
Therefore, it is very important to design and develop fully automatic techniques to support the planning and scheduling task, through the detailed study of the observation operations by instruments on board Planetary Exploration missions. These techniques would be valuable during the mission design, since they could significantly reduce the time required to produce operation schedules for each payload instrument and the complexity of this task, while also providing analyses and evaluations on the produced schedules.

Objectives of the Thesis and Novel Contributions

Given the high complexity of the task and the gaps in the literature on this topic, the main goal of this thesis is to study the problem of planning and scheduling operations for Planetary Exploration satellite missions, in order to make it less time-consuming and challenging, by developing and providing methods that increase the level of automation to perform this task. In particular, the steps considered to reach our goal are:

- The definition of a method for analyzing and scheduling observations for a single instrument in the science payload of a PE mission;
- The extension and the generalization of the method for the single instrument to many different instruments of the same mission simultaneously;

- The analysis and the application of these methods to the real case of the observations to be performed by the radar sounder RIME (Radar for Icy Moons Exploration) and other instruments on board the JUICE mission.

Thus, the steps listed above are dealt with in the main contribution of this thesis, which are:

1. A methodology for the analysis and the optimized planning and scheduling (P&S) of data acquisition operations for a single sensor on board a Planetary Exploration (PE) mission;

2. A methodology considering all kinds of constraints for the simultaneous optimized P&S of multiple sensors of Planetary Exploration missions.

A brief description of the two contributions is hereby provided.

An Approach Based on Multi-Objective Genetic Algorithms to Schedule Observations in Planetary Remote Sensing Missions

Observation operations are conditioned by a large number of complex environmental, resource and instrument-specific constraints. This impedes to perform observations at any given time during the mission and with any of the sensors composing the scientific payload for the considered mission. Moreover, due to the complexity of the context, the task of defining a suitable acquisition strategy for a given instrument is still largely performed by human operators. Moreover, for Planetary Exploration missions only a few semiautomatic tools to aid the planning and scheduling phase have been studied and developed, with very limited capabilities of automatic observation schedules generation. Thus, in this work we propose an approach to the automatic scheduling of the acquisition operations of a remote sensing instrument composing the scientific payload of a mission. The presented methodology works by first determining the time intervals in which the acquisitions with the considered instrument are feasible with respect to its operational capabilities and constraints. It then subdivides the determined observation time intervals into shorter segments that are easier to handle. Among this set of observation segments, the proposed system selects a subset, for producing an acquisition schedule, which is optimized with respect to the considered scientific requirements for the instrument, its features and the mission constraints. This scheduling problem (the observation segment selection) is modeled as a multi-objective optimization problem and it is tackled using techniques based on Genetic Algorithms (GAs). GAs have indeed very good capabilities in efficiently exploring the solution space by considering different competing objective functions and reaching high quality solutions. These solutions are observation schedules representing different

optimized tradeoffs among the considered instrument-specific quality metrics. The approach is demonstrated on the operations of RIME (Radar for Icy Moons Exploration), a radar sounder onboard JUpiter ICy moons Explorer (JUICE). The obtained results show the high potential of the proposed methodology.

A Novel Method based on Nested Optimization for the Simultaneous Scheduling of Multiple Instruments Acquisitions in Planetary Exploration Missions

The complexity of the problem addressed in the previous contribution is here extended to the management of the observations to be performed by multiple sensors of the science payload of a PE mission. Indeed, the characteristics, the limitations and the objectives of all the considered experiments on board a mission should be considered in order to produce a unified observation schedule for all of them. The individual instrument operation schedules need to be harmonized and combined with each other, so that the final plan allows all the considered sensors to meet their requirements in an optimized way and without violating any constraint defined at any level. To this purpose a method for the simultaneous scheduling of the observations to be performed by multiple instruments of a mission is proposed. In this method, the scheduling problem is modeled as a bilevel optimization problem. At the lower level the acquisition plans for each sensor are individually generated, exploiting the methodology proposed for the planning and scheduling of the operations of a single sensor. The individual schedule generation is performed with the objective of maximizing ad-hoc observation quality metrics. At the upper level, instead, the system is meant to harmonize the combination of the acquisition plans generated for each sensor. The schedule harmonization considers all the mission- and resource-related constraints and its purpose is to guide the lower level instances toward a unique, feasible and optimized schedule. The final acquisition plan is produced by using Particle Swarm Optimization (PSO) at the upper level, with the goal of maximizing a metric representing the overall aocquisition plan quality of the joint observation schedule over the considered time frame. The approach is demonstrated considering the data acquisition operations of 4 sensors onboard JUpiter ICy moons Explorer (JUICE).

Structure of the Thesis

This Chapter provided a brief introduction to the concept of planning and scheduling acquisition operations in the context of Planetary Exploration missions. It described at high level both the objectives and the main contributions of this thesis. The rest of the thesis is organized in four chapters. Chapter 1 provides an analysis of the state of the art regarding the planning and scheduling task in PE missions and in EO missions, underlining

the differences between the 2 scenarios. Chapter 2 focuses on the features of the acquisition operations performed by radar sounders, which have been especially taken into account for the development of the 2 main contributions. The first contribution is presented in Chapter 3, which describes the proposed methodology for the scheduling of the operations for one single instrument composing the science payload of a PE mission. Chapter 4 describes instead the proposed approach to simultaneaous planning and scheduling of the observations to be performed by multiple instruments of a PE mission. Finally, the last Chapter draws the conclusions of this thesis and provides a brief analysis on the possible future developments of the presented contributions.

Chapter 1

Fundamentals and Background: Planning and Scheduling in Planetary Exploration and Earth Observation Missions

This Chapter[1] *presents a review of the fundamental concepts and of the literature in the context of operation planning and scheduling in satellite missions. The first part provides an overview of the tools used during the acquisition planning and scheduling tasks in Planetary Exploration missions. The second part is devoted to the analysis of the literature on methods and tools for the automatic creation of schedules for remote sensing instruments in Earth Observation missions, which are an interesting inspiration for applications in the Planetary Exploration context.*

1.1 Methodologies and tools for Planetary Exploration Applications

The accurate analysis of the operations and in particular of the observations to be performed by the science payload instruments is crucial for any satellite mission. This is notably true for Planetary Exploration missions, due to the very complex conditions in which they need to work. The process to plan and schedule operations in such missions

[1]Part of this chapter appears in:
[J1] S. Paterna, M. Santoni, L. Bruzzone, "An Approach Based on Multiobjective Genetic Algorithms to Schedule Observations in Planetary Remote Sensing Missions," in IEEE Journal of Selected Topics in Applied Earth Observations and Remote Sensing, vol. 13, pp. 4714-4727, 2020, doi: 10.1109/JSTARS.2020.3015284.

is thus a very challenging and long-lasting task. Executing the planning and scheduling task still requires an extensive responsibility of human operators. There are a few tools that have been used for past missions and that are currently used, but the most widely used ones are mainly devoted to the in-depth analysis of candidate operational schedules rather than to the automatic and optimized generation of them.

Tools like MAPPS [3] or SciBox [4] are usually exploited especially to aid the medium- and short term planning cycles. Their main feature is the capability to take as input a set of mission- and instrument specific constraints (e.g., the instrument pointing, illumination conditions, particular environmental factors such as the presence of known sources of interference) and objectives, together with spacecraft trajectory information and preliminary operation schedules, and to provide as output a visualization and a manually modifiable schedule, in which constraint violations are pointed out. Moreover, they can transform the set of scheduled science operations into command sequences and activities that have to be executed to perform the observation. MAPPS is able to simulate the input schedules, providing a detailed profile of resources consumption versus time caused by the scheduled science operations. Moreover, it provides 2D projection maps, showing geometric features of the observations and the associated data with respect to the target body surface (i.e., the projection of the instrument field-of-view on a surface map). SciBox provides similar visualization capabilities, but it also implements an automatic schedule building methodology. The method starts by defining all observation opportunities related to determined objectives and their characteristics. These observations are then ranked on the basis of the related quality metrics (e.g., illumination of the scene, resolution of the collected data), which can be extracted from the spacecraft trajectory and pointing information. Observations are added to the schedule based on their rank until any constraint gets violated, thus using a so-called greedy strategy in order to generate a first feasible observation schedule to further manually modify.

Another tool, similar to MAPPS and SciBox, is MAPGEN [6], developed at NASA Ames Research Center and Jet Propulsion Laboratory. Like the two engines mentioned above, MAPGEN provides the user with timeline visualization capabilities and is able to produce feasible schedules of top-level science operations in planetary missions. Thanks to the APGEN engine, the top-level operations defined by the user are translated into lower-level activities based on an activity dictionary. This means that any observation operation, initially provided as input just with a start- and an end-time, is broken down to the whole sequence of operations to be performed by the instrument and by the platform (e.g., warming up the instrument to be used, adjust the satellite attitude, etc.). This enables a thorough analysis of both the operations impact on resource consumption and thus the constraint compliance. Based on the mission global constraints defined in the

planner domain and on further user-defined limitations, MAPGEN is able to generate feasible acquisition strategies that can be further manually modified thanks to the GUI implemented in the planning tool. MAPGEN requires the user to specify the initial plan state, observation goals and their priority scores, apart from the above mentioned rules and constraints on the observation sequence construction. In particular, the user-specified priorities are exploited in order to solve any constraint violation in the generated schedule, removing partially or totally the observation with lower scores. The tool also offers the opportunity to the user to manually modify the produced schedules, in order to make them more appropriate to their requirements. As in the case of SciBox, the methodology employed by MAPGEN to build schedules is a simple greedy strategy, which allows to sort the different observation opportunities based on the metrics listed above (and in particular a priority score, specified by the user) and select the best ranked opportunities that allow not to exceed any considered constraint.

Thus, both SciBox and MAPGEN have schedule generation capabilities, using simple techniques, but their main purpose is the handling of constraints and therefore the generation of schedules that are feasible with respect to any instrument-related or global limitation. The goal of building an observation schedule that allows to maximize the science return for each instrument in the science payload and therefore the quality and the value of the whole mission is thus usually left to the human knowledge and expertise.

A more advanced methodology, in order to better consider the total schedule quality is employed in ASPEN [7], developed by the Jet Propulsion Laboratory. Its main goal, similarly to the tools presented previously, is the handling of mission constraints and the automated reparation of any violation occurring in an acquisition schedule provided in input. This task is performed based on a technique introduced in 1993 called iterative repair [8]. Using this methodology, the constraint violations in the input pre-built complete schedules are detected and individually addressed one-by-one, until a feasible operation schedule is produced. The operations causing these conflicts are therefore modified (e.g., an observation generating an excessive data volume might be reduced in its duration or some instrument parameters might be changed to ensure a lower storage memory occupation), moved to another time interval or eliminated from the schedule. ASPEN also has a submodule dedicated to the improvement of the quality of input operation schedules. The approach is similar to the one of iterative repair and it exploits *preferences*, which are quality metrics associated to the different activities or operations. Activities with low preference values are thus detected and individually addressed, until the global value for a given preference is improved with respect to the input plan. The approach used to complete this task is therefore local and it does not guarantee an optimized overall observation schedule quality.

In conclusion, the tools and the methodologies addressed in this section have very limited capabilities in the automatic generation of optimized observation schedules. Conversely, this aspect has been widely discussed and tackled in the context of Earth Observation missions, in which quick planning tools are vital in order to efficiently respond to the multitude of acquisition requests and accurately plan the daily observations.

1.2 Methodologies and tools for Earth Observation Applications

Given the need of tools being able to provide optimal daily acquisition schedules promptly and the very large number of satellites monitoring different features of our Planet, the problem of observation planning and scheduling has been largely addressed, formalized, modeled and tackled in the context of Earth Observation missions.
However, before the description of the methodologies developed in the EO context, it is important to point out the main variables that characterize the differences of performing the P&S task between the EO and the PE cases and most, especially regarding the methodologies for the automatic generation of observation schedules and the phase of the mission design in which they are employed:

- *The drivers.* The main drivers for the acquisition planning and the use of automatic planning and scheduling techniques in the EO case are acquisition requests of well-defined targets, that can be represented either as point targets or as areas-of-interest (AOIs). Indeed, the automatic techniques that will be described in this section are employed to optimize the satisfaction of acquisition requests that are received daily and that are characterized by well specified target areas. While AOIs (also called regions-of-interest, ROIs) can often be defined also in the Planetary Exploration context, the main objective of the science payload instruments in PE missions is very often the global mapping of the analyzed celestial body.

- *The dimensions of the problem and the moment in which it is addressed.* The tools used to aid the operation planning and scheduling phase for PE missions, as well as the techniques that we propose in this thesis, are required to perform the operation analysis and scheduling process already well in advance with respect the mission launch. Furthermore, they should consider long time horizons, in order to thoroughly analyze and plan observations for long mission phases or over the full mission extent. As briefly addressed in the previous point, the automatic scheduling methods designed for EO missions instead usually work at regular intervals, considering short time windows (usually the contemplated window lasts 24 hours), while the mission is ongoing, in order to face the daily acquisition requests and thus sched-

ule the activities over the day. Thus, most of the automatic techniques for EO have been developed for the short-term planning and scheduling tasks, in order to build feasible schedules in a fast way, as previously mentioned.

- *The complexity of the constraints.* The conditions of the environment in which observations have to be performed in PE missions are usually quite different from those faced performing data acquisitions on Earth. These may severely constrain one or more instrument working capabilities, thus limiting the total number of acquisition opportunities and therefore complicating the achievement of the foreseen scientific requirements for the mission. Moreover, the extremely larger distance of the platform from Earth critically impacts the resource availability on board the spacecraft. Indeed this condition seriously decreases the number of opportunities in which the data can be downlinked to the Ground Stations, making the on-board memory management more challenging. It also influences the capability of the platform to recharge its batteries, which provides the energy to power the science payload instruments, further limiting the possibilities of performing observations. This is especially critical for missions with the objective of studying and analyzing celestial bodies in the Outer Solar System, due to their very large distance from the Sun. In the context of EO, constraints to the observations surely need to be specified and considered, but they are usually less complex and strict, because of the well-known environment in which the observations are performed.

These reasons make the approaches studied for the Earth Observation case non ideal to be applied to the PE context. Nonetheless, the formalizations of the planning and scheduling problem and the observations on it defined in the studies dedicated to the EO case are relevant and can be extended to any satellite-based remote sensing mission.
A general description of the problem at hand is offered in [9], considering generic surface-imaging sensors. The authors treat the problem in the multi-platform case, considering one single type of instrument on board each considered satellite. Acquisition requests are modeled as sets of tasks that need to be completed during the analyzed time horizon (24 hours usually). A priority value is usually associated to each request *a priori*. These requests are characterized by a well defined region called area of interest (AOI), over which data have to be acquired, and by a time window during which the observation should be performed. AOIs are usually defined as point (or spot) regions, which are very limited surface portions that can be observed in a single shot, or as larger areas enclosed by a polygon, which instead need multiple acquisition operations to be fully observed. Given these characteristics, observation opportunities are then determined based on the characteristics of the sensors on board the considered satellites, their field of

view, their visibilty span (i.e., if an instrument can slew its angle with respect to the nadir orientation) and the orbits to be performed during the specified planning horizon. Basic

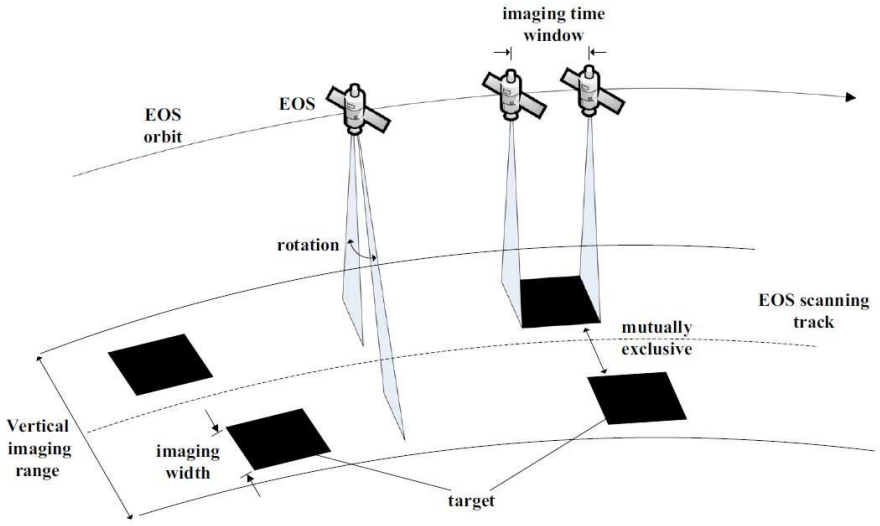

Figure 1.1: Illustration[2]representing EOS imaging opportunities determination for small targets inside the visibility span of the on-board imaging sensor along the satellite orbit.

strips with variable length and fixed width are identified along the satellite ground track trajectory, intersecting them with the AOI boundary coordinates. This allows to clearly identify their associated observation start- and end-time and define the time intervals in which the AOI related to a given request is visible with respect to the considered platform. These intervals and the associated strips can be further subdivided into shorter acquisition segments, in order to have more flexibility in the generation of the observation schedule. The different acquisition segments linked to a given acquisition request identify the single tasks to be scheduled related to it. Relevant attributes are also associated to each task, such as incidence angle, task duration and related time window, satellite orbit and related identifier, and other performance-related metrics (e.g., task AOI coverage, energy consumption, generated data volume). Thus, given a set of acquisition requests, their combined priority values, and a set of imaging opportunities (tasks), the problem is to insert tasks inside the schedule in order to maximize a given acquisition profit metric over the specified planning horizon. This maximization should consider a set of constraints, related to different aspects, such as:

- globally available resources, like on-board memory, energy or downlink opportunities;

[2]Image reproduced from [10].

- temporal limitations, i.e., if a given request needs to be fulfilled within a given time window;
- operational limitations, as for example for a passive instrument like a camera the illumination is fundamental in order to acquire data in a proper way;
- binary constraints on the observations, e.g., if two available observations are associated to overlapping time intervals but need different slewing angles to be performed, atmost one among them can be scheduled.

It is very important to mention that very often further types of constraints can be defined, depending on the specific analyzed mission or instrument. This means that after the determination of all possible observation opportunities, the next step is to select a subset of them in order to optimize a desired objective.
In [11], the authors provide a categorization of the different types of models used to represent the Earth Observation Satellite (EOS) observation scheduling problem. Among them we can find *mathematical programming models* (which guarantee accurate solutions but are quite difficult to build and to generalize to different EOS problem instances), *constraint satisfaction problem models* (which allow to obtain solutions in a fast way, but they do not guarantee that solution to be optimal) and *graph-based model formulations* (which are able to accurately represent the relationships between the different observation opportunities, but are not efficient to solve complex problems). Finally, a largely used model is defined in [12] and analyzed in further detail later also in [13] [14]. This is based on the *multi-dimensional knapsack problem* (MKP) [15] formulation. The objective in general MKPs is to maximize a total profit parameter $f(\mathbf{x})$ associated to a subset of the available objects o_i, given a set of C constraints based on cost coefficients associated to these objects. Each object is linked to a profit coefficient p_i and cost coefficients $c_{j,i}$ that depend on the i-th object and to the j-th constraint. The problem can be generally formulated as follows:

$$\max_{\mathbf{x}}\{f(\mathbf{x})\}, \tag{1.1}$$

$$\text{with } f(\mathbf{x}) = \sum_{i=1}^{N} p_i x_i, \tag{1.2}$$

$$\text{subject to} \sum_{i=1}^{N} c_{j,i} x_i < b_j, j = 1, ..., C, \tag{1.3}$$

$$x_i \in \{0, 1\}, i = 1, ..., N; \tag{1.4}$$

The variables $x_i \in \mathbf{x}$ represent if an object o_i is included in the subset (1) or not (0). In this model, the observation operations are represented by the different objects, which may be included or not in the analyzed observation schedule. The profit coefficients instead can model any of the relevant attributes discussed above, depending on the aspect of the observation schedule that we need to optimize. Finally, the specified constraints can be associated to any kind of instrument-related or mission-related limtation (e.g. the coefficients $c_{j,i}$, could express the required energy to perform a given acquisition, or the data volume generated by it).
The MKP is a particular type of combinatorial optimization problem and it is known to be NP-hard. Even using slightly different models, as in [16], the general observation scheduling problem is highly combinatorial, even with some simplifications, which means that no technique could solve it to optimality in polynomial time with respect to the dimension of the problem at hand. However, this model can efficiently represent the the P&S problem, both for simple and for larger and more complex instances (as we will show in Chapters 3 and 4).

The numerous different approaches published in the literature can be cathegorized not only based on the model used to represent the P&S problem, but also with respect to the type of strategy employed to tackle the EOS observation scheduling problem, which we will hereby discuss in more detail. Namely, we can find methodologies exploiting *exact algorithms*, *heuristics* (constructive or greedy algorithms), or *meta-heuristics* (stochastic optimization techniques).

1.2.1 Exact algorithms

Exact algorithms have the advantage of ensuring to find the optimal observation schedule, but since they need to evaluate any possible combination of the available feasible observations constituting a possible acquisition schedule, they are only able to handle small-scale problems in an acceptable amount of time. An example of this kind of approach can be the use of depth-first branch-and-bound algorithms, as stated in [12]As underlined by the authors, this technique is quite efficient in the exploration of the solution space, as it iteratively subdivides it in subspaces and stops exploring the ones for which it estimates a lower bound of the employed objective function (considering a minimization problem) which is higher than the best known objective function value of the solutions explored up to that point. Thus, it does not need to explicitly evaluate the whole set of possible solutions, even if, depending on the first evaluated solutions and the subsequent subdivisions of the solution space, it might still need to enumerate a large portion of it.
Another work in which this technique is used is [17]: first the acquisition opportunities

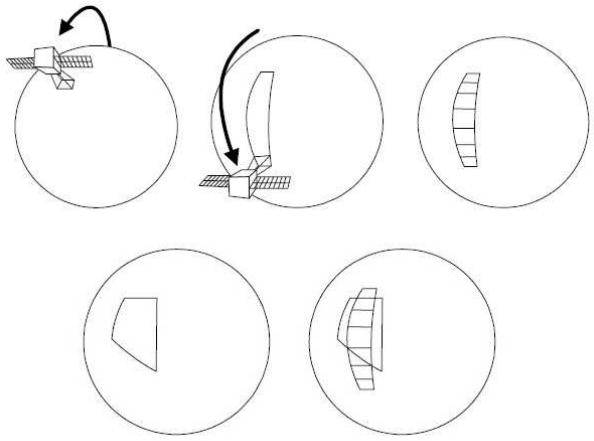

Figure 1.2: Illustration [3]of the projection of the sensor field of view on the ground, the subdivision in segments and the intersection of them with a target AOI.

among which to perform the selection are identified by intersecting the areas-of-interest with the swaths formed by projecting the field-of-view of the considered instrument on the Earth surface, then the target AOIs are subdivided into so-called shards, which are subsections of the targets that can be acquired. They can be easily formed by intersecting the edges of the swath segments and the target polygons, as shown in Figure 1.2. Each of the shards has an associated reward value (which, for example, can be the area covered by the shard), while the segments (the time intervals in which a given shard can be imaged) carry with them the information about their cost (for example, the memory capacity required to store the data associated to that segment). This formulation allows one to update the available capacity depending on the selection or rejection of a segment. The node ordering heuristic, starting from an empty solution, takes a partial solution **R'** and the available segments $s \in \mathbf{R}$ (where **R** includes all the segments associated to their downlink opportunity), s $\notin$ **R'** and orders them accordingly. The basic approach is to calculate the reward/cost associated to the inclusion of each set not yet included in the solution.

Other approaches include the search of the multiple criteria optimal path in a graph, as in [18]. Here the nodes of the graph (called *feasibility graph*) are the observations to be performed in one day (previously defined, similarly to the approaches discussed above) and the arcs represent the precedence relationships between the possible observations. The optimal paths are found following criteria such as the maximization of satisfied requests and of the number of high-priority acquisitions performed in the candidate schedule, as

[3]Image reproduced from [17].

well as the minimization of the satellite resources utilization. A further method is described in [19] and applied to general Valued Constraint Satisfaction Problems (VCSPs, another type of model used to describe the EOS P&S problem). It uses an extention of the approach in [17], the Russian Doll Search. Indeed in this methodology the depth-first branch and bound technique is employed n times on n nested subproblems, where n is the number of variables (in our case, the available acquisition opportunities). The subproblems are formed iteratively, after a sorting of the variables, starting from the last variable alone and adding the variables one by one until the first one is reached, so that the i-th subproblem contains the variables from the $(n-1+1)$-th to the last.

1.2.2 Heuristics

The second category includes the approaches using heuristics to solve the EOS observation scheduling problem. Techniques such as constructive or greedy algorithms appear very appealing especially due to their reduced required computational time even dealing with large-scale instances of the problem. In these approaches the observation schedules are iteratively built by following one or more problem-specific metrics that need to be optimized and usually adding the observation operations that best improve the considered metrics to the candidate acquisition schedule. This is done until any constraint (e.g., resource-related limitations) is violated. Two very similar approaches to the scheduling problem using heuristics are presented in [20], regarding the acquisitions with ASTER (on board NASA EOS-AM1 satellite), and in [21], regarding the observations with the synthetic aperture radar on board DLR's TerraSAR-X satellite. In both cases, as usual, the AOIs are intersected with the swathes determined by the observation capabilities of the sensing instruments during the orbit of the spacecraft. This intersection defines the observation opportunities, associated with determined time intervals, that the scheduling algorithm can select. For both mentioned algorithms, the selection of the opportunities is based on a priority score. In [20], observation opportunities are first subdivided into shorter parts, called scenes, each of which is characterized by a score, determined by the quality of the observations over that particular portion of the surface and by the degree of priority of the related acquisition request. The overall priority score for the opportunity is then calculated by summing the scores of all its scenes. In [21], instead, the priority of an opportunity is defined by assigning a score between 0 and 9 to the related acquisition request. The opportunities are ranked based on the priority score. Both algorithms iteratively select the opportunity with the highest priority, assess its resource consumption and add the opportunity to the schedule, following therefore a so-called greedy approach. A constraint check is performed and if any resource constraint is violated by adding the

considered acquisition opportunity to the schedule, the opportunity is deleted and will no longer be considered for the following steps. Both methods consider a scheduling time-frame of one day, but the algorithm described in [21] is executed every 12 hours.
A further very interesting approach in this category is the one shown in [22], devoted to the acquisition operations of the satellite constellation COSMO-SkyMed, mounting SAR sensors. Here, in a similar fashion, all the available acquisition opportunities (called Data Take Opportunities - DTOs) are previously determined with respect to the data acquisition requests, provided with a priority score (*high*, *medium*, or *low*), defining for each of them well specified starting and end time and the observable portion of the surface. The method also takes into account Down-Link Opportunities (DLOs) in the scheduling process. The employed methodology is a constructive technique based on time with both look-ahead and back-tracking capabilities, exploited in order to control and maintain the constraint compliance of the resulting observation schedule. First, the satellite that has to be active at a given time is selected among the four platforms composing the COSMO-SkyMed constellation. Then the type of activity to be performed at that time is singled out among the three possible activities (acquisition, transmission on Channel 1 and transmission on Channel 2, since the COSMO-SkyMed satellites are provided with two possible communication channels), based on the characteristics of the available DTOs and DLOs. If an acquisition operation is selected and if the analyzed DTO is deemed feasible with respect to local constraints (possible conflicts due to overlapping DTOs), the system has to decide whether that observation should be performed or not. This decision is taken based on the objective of maximizing the total number of satisfied acquistion requests, considering also that there might be AOIs associated to some requests (called *split* requests), which need a given number of DTOs in order to be completely observed. This process is executed until the whole analyzed time-horizon (which can last up to 16 days, differently from most of the available algorithms) has been planned. During the process, the look-ahead capability is used in order to early detect the presence of a DTO related to a high-priority request and avoid any conflict between it and a down-link operation of a low priority acquisition. The back-tracking capability instead is used when an acquisition schedule under construction violates any resource-related constraint, preventing the satisfaction of a high-priority or a medium-priority request. The plan is thus checked in reverse chronological order, in order to remove the last scheduled DTOs associated to low-priority requests until the higher-priority request satisfaction becomes feasible. After that a further check is performed to see if re-inserting one or more of the previously removed acquisitions could cause any conflict.
Another more recent example of method using constructive techniques is the one presented in [23]. As usual, the set of acquisition opportunities is obtained by determining the time

windows in which the target areas defined by the acquisition requests are observable. Then, given the priority associated to each task, observation schedules are sequentially constructed trying to maximize the total priority score and considering constraints on the maximum exploitable memory storage space and on the maximum total working time. The approaches using heuristics are usually able to reach a feasible schedule in quite a short time. However they are not able to guarantee that the reached solution is optimal with respect to an overall quality metric considering the whole analyzed observation schedule. For this reason, meta-heuristics and stochastic optimization techniques have been often contemplated, both in the Satellite Observation Scheduling context and for other generic combinatorial optimization problems.

1.2.3 Meta-heuristics

Given the combinatorial nature of the general EOS planning and scheduling problem, stochastic optimization techniques have been extensively applied to the problem at hand. These techniques have been used both in their standard form and considering modifications to their operators, but even combining them in order to exploit the best characteristics of each employed method. Among the meta-heuristics employed in the EOS P&S problem we can find Tabu Search (TS) [24][25], Evolutionary Algorithms (EA) like Genetic Algorithms (GAs) [26], Particle Swarm (PSO) [27], Ant Colony (ACO) [28] and Simulated Annealing (SA) [29].

Tabu Search has been among the first employed meta-heuristic techniques, because it is easily applicable to problems such as the EOS observations P&S. Its use started from the pioneering work presented in [12] and it was applied in many further works such as in [13][14][30]. Another example is the one shown in [31]. Starting from an empty schedule, the search for the optimal solution is performed inside a *neighbourhood*. The neighbourhood of a solution is determined by all the elementary modifications to the current solution, like the insertion, the removal or the substitution of a task. In this work also requests indicating stereo observations (two observations need to be done at the same location, at different angles) are considered, so for them a task (or *job*) identifies both observations. The algorithm moves at every iteration to the best solution/schedule present in the neighbourhood, given the objective that is required to be optimized (in this case, the total profit of a given solution). A tabu list, avoiding the reinsertion of a task that was previously removed for a given number of iterations, is also used. A penalty value is computed if a given schedule violates a constraint and subtracted from the objective function. Moreover, also the solutions in the neighbourhood, which do not improve the current best value of the objective function, are penalized so that a higher diversification in the solution search is possible.

ACO has been quite widely employed, mostly with some modifications to avoid stagnation in local optima as for example in [32][33][34]. An example of application of ACO to the EOS planning and scheduling process is shown in [23]. In this approach, the available observation opportunities can be seen as the edges of a graph, similarly to what is presented in [18]. As in the other approach presented in the same paper, the resulting observation schedules are generated in a constructive manner starting from an empty solution and building therefore a path representing a feasible schedule, since the process stops if no more resources or no more tasks are available. The tasks and the time windows in which to perform the given task are selected with a probability value based on the associate pheromone level (calculated with respect to the total priority score of the path) and on the impact of a given observation on the available resources.

SA has been used in a few cases, like [35] or in [36], where the problem of Ground Station Scheduling for EOS is addressed. An example of approach using SA is the one presented in [37], where a set of R_{tasks} requested tasks to be performed on the considered day is taken into account. A set of Orb orbits over which the different tasks can be accomplished is examined. The different acquisition opportunities associated to each task over the different orbits are identified and described by several metrics that define the energy and memory consumption, but also the required sensor slewing angle. In addition to the metrics, constraints on the cost of performing the different data acquisitions are considered: for example, the energy consumption due to the acquisition and the sensor slewing operations over a certain orbit shall not exceed a well defined amount. A very similar constraint is also expressed regarding the memory consumption over a certain orbit. These metrics are then combined in a parameter that expresses the weight of completing the considered task at a particular orbit. The final goal is to construct the schedule that maximizes the total profit associated to the set of tasks scheduled for the considered day, without violating any constraint. The objective function to be optimized is defined as follows:

$$\max\{\sum_{j=1}^{Orb}\sum_{i=1}^{R_{tasks}} y_{i,j}w_i\}, \tag{1.5}$$

where $y_{i,j} \in \{0,1\}$ expresses if the i-th task is scheduled to be performed on the j-th orbit and the weight w_i expresses the above-mentioned combination of metrics describing the score of the acquisition opportunity. The effective selection of the observations to be scheduled on the considered day is performed using a stochastic optimization algorithm based on an Adaptive Simulated Annealing (ASA) with a Dynamic Task Clustering (DTC) rule. The DTC allows to group multiple tasks (this work considers requests with point targets observable in a single shot) if they require the same slewing angle to be observed

and if the total length of the task cluster observation does not exceed a given length threshold. The sense of the task clustering is to reduce the total resource consumption. Thus the clustering of two or more tasks can happen if the resources (energy and memory) used by the clustered tasks are less than the sum of the resources used by the tasks performed individually. Moreover, in this work SA is made adaptive by using an adaptive temperature control, where the temperature parameter rules the search capability of SA, in order to avoid to get stuck in local (which is a common problem for the plain SA algorithm).

Due to the combinatorial nature of the problem, which contrasts with the characteristics of PSO, this technique is not so widely used, but in [38] a discrete valued variant of Particle Swarm is employed. An important variation with respect to the standard PSO procedure is the integration of Russian Doll Search (RDS) to improve the particles' ability of local refinement. In order to use the RDS technique, the variables (as usual, the available acquisition opportunities) are first sorted based on their associated weight or importance. An interesting aspect about this approach is how constraints are handled. Indeed, the fitness function to be optimized (which is in the form of 1.2, maximizing the total weight) is completed with a penalty function emphasizing by how far constraints of any sort are violated.

Finally, among the most extensively used meta-heuristics, we can find the Genetic Algorithms. They have been employed in many different modalities, both using the single-objective ([9][10][39][40][41][42][43][44][45]) and the multi-objective set-up ([46][47][48][49]). Moreover, they have been exploited also to control the scheduling of ground stations for the downlink operations of EO satellites, as in [50][51][52][53]. An example of application of GAs to the EOS scheduling problem is the one reported in [39]. Here, a plain single-objective GA (whose process is explained in 3 in 3.2.2) is utilized to optimize a fitness function in the form of Eq. 1.2, handling binary variables representing if a given observation is included in the schedule or not. The profit parameter associated to each elementary observation here synthesizes the ratio of covered surface with respect to the total surface of the analyzed AOI, the priority associated to the acquisition request (both in terms of importance and of the time window in which the request must be fulfilled) and a profit in monetary terms (a parameter exploited for private satellites). The same profit parameter also incorporates penalty factors related to energy and memory consumption and also a coefficient related to the probability of cloud coverage of the observed area (this is mainly related to passive sensors). Thus, constraints, which are expressed as in Eq. 1.3, are handled in similar way as in [38]. A more interesting and complex methodology exploiting GAs is presented in [9]. In this work, after the usual determination of all available observation opportunities for the considered planning horizon, the acquisitions related to

each orbit are grouped and represented as a *directed acyclic* graph (see Fig. 1.3), similarly to what proposed in [18]. So, for each orbit a path crossing this graph has to be selected.

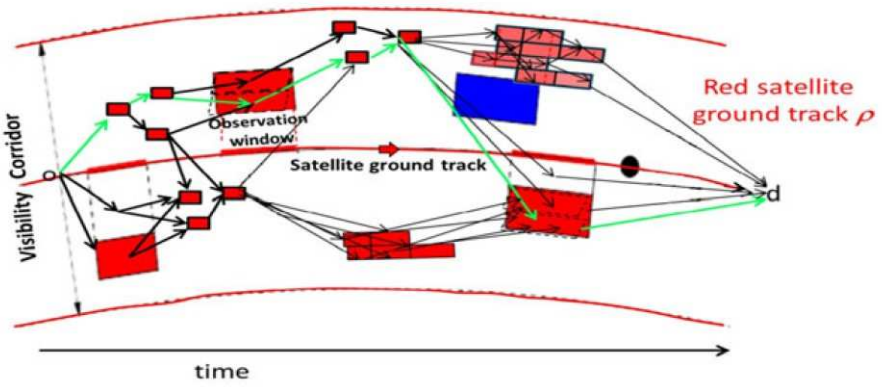

Figure 1.3: Illustration[4]of the directed acyclic graph structure employed to represent the feasible opportunity transition (black arrows) between the different identified observation opportunities in one orbit. The green arrows indicate a possible selected observation sequence, representing a part of the resulting acquisition schedule.

In this way the constraints related to mutually exclusive observations or to not feasible image transitions are easily dealt with, imposing conditions on the imaging opportunity transition variables. The objective to be optimized is given by the priority score of each request totally or partially satisfied by the resulting schedule, weighted by the ratio of the covered surface over the total surface of the AOI related to the given request and by the combined probability of successful observation for each scheduled acquisition operation related to the given request. In the proposed Hybrid Genetic Algorithm (HGA) each individual (candidate schedule) is represented by a binary variable string containing both variables representing the insertion of a given imaging opportunity in the schedule and those representing the transition from a given opportunity to another.

The basic genetic operators (crossover and mutation) are modified to make the solution space more efficient (implementing a local search in the mutation operator) and to adapt to the graph representation. Moreover, in this approach 2 populations are coevolved. The first one uses a fitness function based on the objective described above and for each individual computes the ratio between the individual objective value and the average objective value over the population. The second instead uses the same fitness function, incorporated with the computation of the average resource exploitation by the individuals (schedules) of the second population. At each iteration the best individuals of each population are migrated in the other, in order to enhance the diversity in the solution

[4]Image reproduced from [9].

search.

A further approach using GA is reported in [10], which addresses the Integrated EOS Scheduling (IEOSS) problem that is the scheduling of both acquisition and downlink operations simultaneously. The problem includes not only the satellite (or the satellite constellation) provided with an imaging sensor, but also further satellites acting as relays for the communication of the acquired data to the ground. Once again the problem is represented through a DAG in order to handle many different constraints in a simple way and to represent the feasible schedules as paths crossing the graph. What is really interesting is the type of employed optimization approach. Namely, if in the previously described work some modifications to the basic operators and to the population structure were applied, this time the ability of rapidly exploring new solutions in GA is combined with the characteristics of SA. Thus, a first search in the solution space is performed using GAs and after that, with a rule specifying when to switch algorithms, the neighbourhood of the population generated by the GAs is further explored with SA. The algorithm switching rule is based on the improvement rate, which in GAs is usually very high in the first iterations, but starts declining after a while. The inverse usually happens using SA. The improvement rate, which is quite stable in the first iterations for SA, is computed and when the initial search with GAs reaches the same improvement rate as SA, the algorithms are switched. A multi-objective GA is instead used in [47]. The considered objectives are the total profit of the selected acquisitions related to a set of acquisition requests, as usual, and the fairness between users, which are the entities that materially formulate the acquisition requests. The fairness is expressed as a function of the difference of the profits associated to the requests related to a pair of users. What in this approach differs from the commonly used multi-objectives versions of GAs, is use of local search at each iteration. More in detail, at each iteration of the multi-objective GA, the non-dominated solution set is determined. After that, for each member of the non-dominated set a local search step is conducted (based on the 2 objectives) to see if the non-dominated set can be improved, in order to improve the hill-climbing capability of GAs and thus avoid to get stuck in local optima. If so, the non-dominated set is updated with the improved solutions and the successive iteration can start.

In conclusion, meta-heuristics are very valid techniques to solve general satellite observation scheduling problems and represent a very promising alternative to heuristics and exact methods thanks to their flexibility and easy application to different problems. When the dimensions of the problem at hand become too large, some modifications to the basic execution of these techniques often succeed in making the solution search more efficient and lead to better results with small additional effort.

Almost all the different contributions described in this previous subsections consider the EOS planning and scheduling (P&S) problem with the availability of different satellites. However, these different platforms all carry the same types of instruments, where the only difference is often the image quality that they can acquire. Considering instead the P&S problem for Planetary Exploration missions, multiple different types of instruments need to be taken into account, with their own limitations and characteristics and all their different associated requirements. Ideally, all of these aspects should be taken into account simultaneously, carefully handling the resources, in order to maximize the global science return and that of the single experiments and sensors. This, together with all the aspects listed at the beginning of Section 1.2 in the context of PE missions, greatly increases the complexity of the definition of a framework being able to plan and schedule the acquisitions of multiple instruments (ideally a full science payload) at the same time.

Chapter 2

Acquisition Operations of Radar Sounder Instruments in Planetary Exploration Missions

This Chapter [1] *introduces radar sounder instruments and analyzes their operations in Planetary Exploration missions. In the first part a brief introduction to radar sounders and their working principles are presented. In the second part indications on how to define and estimate the acquisition quality for the observations performed by these instruments are provided.*

2.1 Introduction

In recent years, radar sounding systems are more and more considered as relevant sensors to be included in the science payload of Planetary Exploration missions. Many missions included or will include a radar sounder in their scientific payload. Examples of such systems are MARSIS (Mars Advanced Radar for Subsurface and Ionosphere Sounding) on the ESA Mars Express mission [54] and SHARAD (SHAllow RADar) on the NASA Mars Reconnaissance Orbiter [55], which are employed to survey the subsurface of Mars. Another important radar sounder system is LRS (Lunar Radar Sounder) on board the

[1] Part of this chapter appears in

[J1] S. Paterna et al., "An Approach Based on Multiobjective Genetic Algorithms to Schedule Observations in Planetary Remote Sensing Missions," in IEEE Journal of Selected Topics in Applied Earth Observations and Remote Sensing, vol. 13, pp. 4714-4727, 2020, doi: 10.1109/JSTARS.2020.3015284

and in

[C2] L. Bruzzone, F. Bovolo, S. Thakur, L. Carrer, E. Donini, C. Gerekos, S. Paterna, M. Santoni, E. Sbalchiero, "Envision Mission to Venus: Subsurface Radar Sounding", 2020 IEEE International Geoscience and Remote Sensing Symposium (IGARSS), Waikoloa, HI, USA, 2020, doi: 10.1109/IGARSS39084.2020.9324279.

JAXA Kaguya/SELENE mission [56] [57]), which has been used to investigate the subsurface of the Moon. Moreover, sounders like RIME (Radar for Icy Moons Exploration) on the ESA JUICE mission [58], REASON (Radar for Europa Assessment and Sounding: Ocean to Near-surface) on board the NASA Europa Clipper mission [59] and SRS (Subsurface Radar Sounder), part of the science payload of the ESA recently selected EnVision mission [60] will be used to probe the Jovian Icy Moons (Ganymede, Europa and Callisto) and Venus in the next years. The growing interest about this kind of radars is due to their unique features and capabilities. These features allow them to investigate the characteristics of the subsurface of the analyzed celestial bodies and study their stratigraphy and their geological structure, with direct and non-invasive measurements. Given their particular operative characteristics and the growing presence of sounders in Planetary Exploration missions science payloads, it is important to understand how these instruments work and how to determine the quality of both a single observation and a full acquisition campaign.

2.2 Fundamentals of Radar Sounding

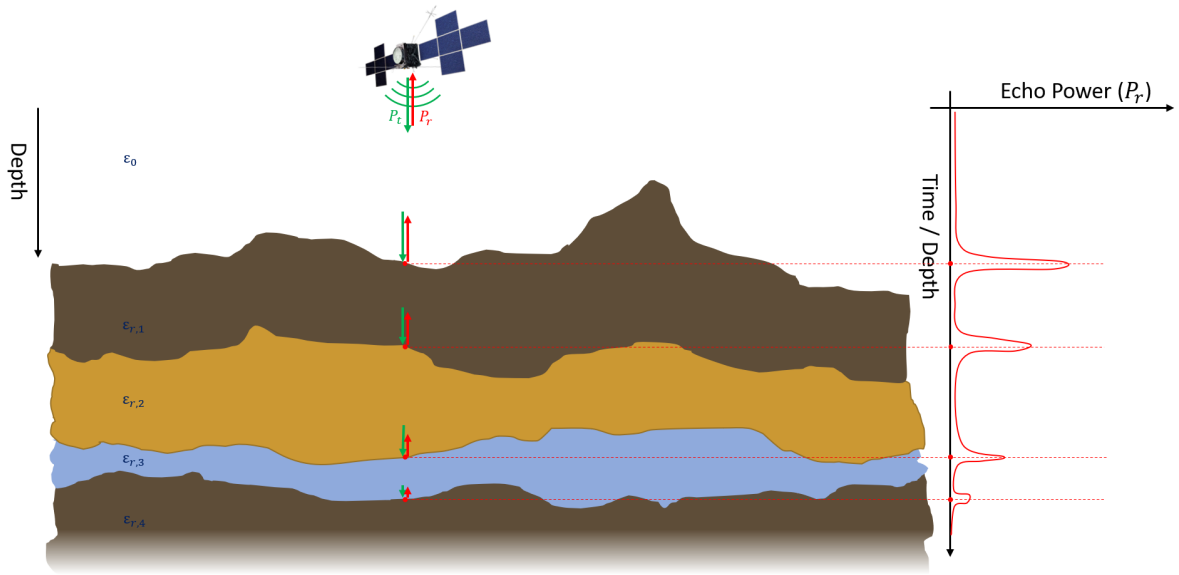

Figure 2.1: Illustration of the radar sounder acquisition geometry. Radar sounders are nadir-pointing pulsed radars. The transmission of a single pulse and the related response from the surface and subsurface layers interfaces are qualitatively depicted. The different subsurface layers are identified through their relative dielectric permittivity ($\epsilon_{r,i}$), which affects the radar response.

Radar sounders have a particular acquisition geometry and specific observation capabilities, as illustrated in Fig. 2.1 and 2.2. They are nadir-looking pulsed radars that are able to penetrate the ground and therefore to perform direct measurements on the subsurface of the observed body. The penetration capabilities are strictly connected to the relatively low frequency of the electromagnetic pulses that they emit, which is in the range between 1 and 300 MHz. The characterization of the subsurface structures is obtained by measuring the reflections caused by interfaces between targets or layers with different dielectric properties and representing them as radargrams.

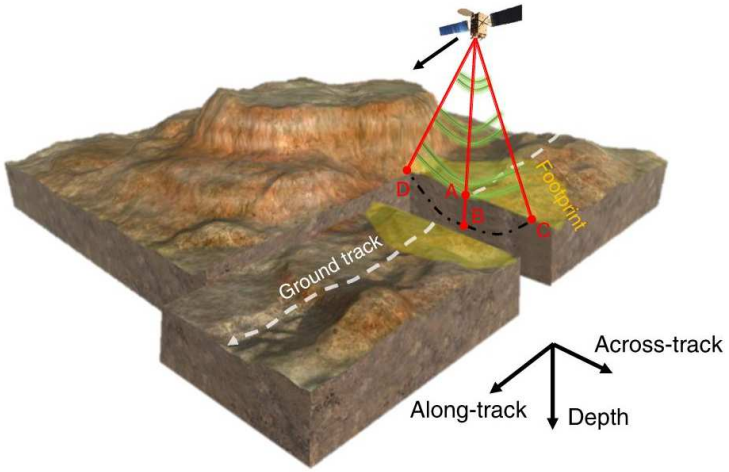

Figure 2.2: Illustration of the radar sounder data acquisition process[2]. Radar sounders produce tomographies of subsurface features (B), below the regions identified in the figure as ground tracks (A), exploiting the platform movement. Points C and D are off-nadir sources of non-desired echoes, which might interfere with the characterization of subsurface features placed long the nadir direction.

A single radargram represents a vertical profile of the subsurface of the illuminated area on the body's surface. This is obtained by acquiring consecutive columns along the direction of movement of the platform on which the radar is mounted. In the produced image, the backscattered signals are mapped on the vertical direction, transforming the information relative to the time interval between the pulse transmission and the signal reception into the distance of the scattering object from the platform. By performing multiple acquisitions on different ground tracks over a certain area on the ground, it is possible to collect a detailed information on the subsurface of the observed body and on the subsurface features distribution. The ground tracks are identified by nadir-projecting the position of the satellite in time on the celestial body surface and they identify the target positions that are observed in the acquired data. In order to better understand the

[2]Image reproduced from [61].

features and the parameters that determine the quality of a single continuous observation and then of an entire acquisition campaign, we need to address and summarize some fundamental quantities that are associated to the radar sounder working principles.

2.3 Acquisition Parameters and Data Quality

The first performance parameter that we consider is the amount of power that is received by the radar antenna from each of the subsurface layer interfaces. This quantity and its expression are very important, as they underline the capability of the instrument of detecting the different subsurface layer interfaces and of recognizing the depth and the material composing each subsurface layer. The power received from each layer interface is expressed as follows [62]:

$$P_{ss,j} = \frac{P_t G^2 \lambda^2 \Gamma_{j,j+1}^2 A_{ill} \prod_{i=0}^{j-1} (1 - \Gamma_{i,i+1}^2)^2 e^{-4\alpha z_j}}{(4\pi)^3 (h + z_j)^4}, \tag{2.1}$$

The meaning of each parameter is here reported:

- P_t represents the power associated to the transmitted pulse. This is a crucial design parameter, strictly linked to the instrument energy consumption and thus it has to be accurately defined also with respect to the energy availability on board the spacecraft;
- G is the antenna gain due to its particular radiation pattern;
- λ is the wavelength associated to the central frequency f_c of the transmitted pulse;
- $\Gamma_{j,j+1}$ is the reflection coefficient at the interface between layer j and layer $j+1$, where layer 0 is usually free space or the planet atmosphere. It determines the amount of power that is reflected towards the radar antenna, with respect to the incident power at the interface. It is strictly related to the ratio between the relative dielectric permittivities $\epsilon_{r,j+1}$ and $\epsilon_{r,j}$ associated to the two interfacing materials;
- A_{ill} is the illuminated area, corresponding to the radar antenna footprint on the ground (shown in yellow in Fig. 2.2);
- α is the attenuation constant of the material, which strictly depends on the pulse frequency and on the dielectric properties of the material;
- h is the orbit altitude of the platform (spacecraft) on which the sounder is mounted with respect to the ground. This quantity greatly impacts on the received signal power and therefore on the radar sounder performances. Thus, during the design

of the trajectory to be performed by the spacecraft on which the considered radar sounder is mounted, this variable has to be accurately taken into account, also with respect to the acquisition capabilities of other instruments included in the science payload;

- z_j is the depth at which we can find the interface between layer j and $j+1$.

Based on the above defined parameters, it is possible to express a fundamental performance metric, which is one of the main drivers of the instrument design: the Signal to Noise Ratio (SNR). Given the noise power, indeed, through this quantity we can estimate the performances of the radar, for example in terms of maximum penetration depth. Moreover, it determines how well it is possible to detect and recognize the surface and subsurface structures through radar sounder observations. Following the definition of the power received from each subsurface layer interface $P_{ss,j}$, it can be expressed for each interface as follows [62]:

$$SNR_j = \frac{P_{ss,j}}{P_n}, \tag{2.2}$$

where P_n is the noise power. In general, the main sources of noise that should be considered and that can interfere with radar sounder observations are the thermal noise caused by the radar receiver and the isotropic galactic noise, which can be characterized similarly to the thermal noise. Thus, in general $P_n = k_b T B$ [62], where k_b is the Boltzmann constant, $T = T_r + T_g$ is the overall noise temperature obtained as the sum of the receiver noise temperature T_r and the galactic noise temperature T_g, and B is the transmitted pulse bandwidth. However, if a high-quality receiver is designed for the radar system, we have that the temperature T_g is order of magnitudes larger than T_r, thus we can approximate the overall noise temperature as $T \approx T_g$.
Besides the modification of the design parameters (e.g., P_t, B, f_c,...), which are limited by technical or budget constraints, different techniques can be employed in order to improve the SNR. Indeed, the use of a linear frequency modulated pulse (also called a *chirp*) allows to apply a processing technique on the received signal called range compression, which produces an SNR gain that directly depends on the transmitted pulse bandwidth B and its duration T_p. Moreover, the motion of the platform during the data acquisition performed by the radar sounder can be exploited in order to apply a synthetic aperture processing on the received echo signal. This procedure allows to obtain a further SNR gain that depends on the transmitted signal wavelength λ, the platform height h, the radar system pulse repetition frequency (PRF) and the spacecraft speed with respect to the ground v_s. This type of processing also allows to enhance the data resolution in the along-track direction (i.e., the flight track).

Despite the application of these signal processing techniques there are cases in which further sources of intense interferences strongly influence the SNR, potentially destroying the information content of the acquired data. An example of such strong interference is the radiation emitted by Jupiter (the Jovian Decametric Radiation) [63], which has been carefully taken into account in the design of the radar sounders RIME and REASON on board the JUICE and Europa Clipper missions, in the evaluation of its performances [64] and, later, in the determination of the available observation opportunities. As briefly explained in Chapter 3, Section 3.3.1, the JUICE mission will include a phase called GCO-500, in which the spacecraft will perform a circular orbit around Ganymede with an altitude of about 500 Km from the surface. The presence of this source of powerful noise reduced the possibility of subsurface mapping of Ganymede during the GCO-500 phase only to the time intervals in which Jupiter is eclipsed by Ganymede with respect to the JUICE spacecraft. Given the orbital characteristics of Ganymede, this results in a limited operational area over which data acquisitions are feasible, as shown in Figure 2.3. Only a small number of observations are foreseen outside this operational area, due to the sporadic nature of these emissions.

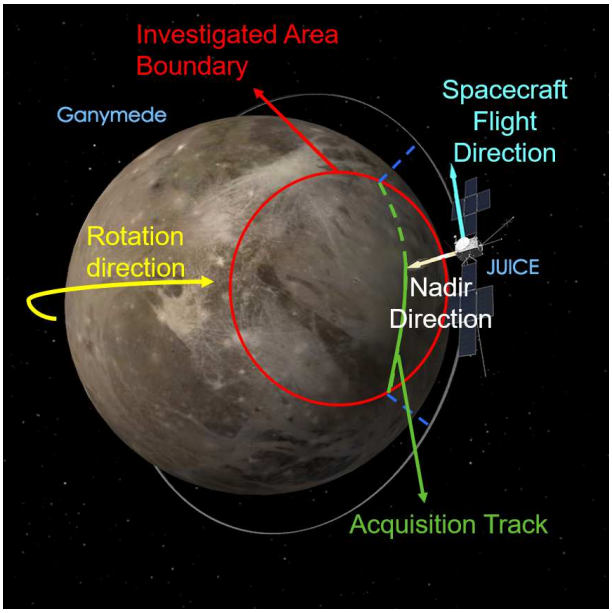

Figure 2.3: RIME acquisition scenario at Ganymede. The red circular area defines the portion of the surface in which acquisitions with the radar sounder RIME are not affected by Jupiter radio emissions.

However for the case of RIME, by thoroughly studying the characteristics of the Jovian Decametric Radiation, the possibility of exploiting this radiation as an illumination source has been studied [63] [65]. Thus *passive* sounding acquisitions could be implemented, in

order to expand the observable area on Ganymede and the number of available acquisition opportunities for RIME.
Another example is related to the acquisitions to be performed by SRS on board the EnVision mission to Venus. In this case, the main source of interference intensively influencing the acquisitions SNR is due to the bursts of solar radio emissions, which becomes critical at relatively short distance from the Sun. Moreover, besides the problems related to the direct radiation from the Sun to the SRS antenna, the solar emissions also have an impact on the ionosphere of Venus depending on the incidence angle between the ionosphere and the zenith direction (Solar Zenith Angle - SZA). Indeed, radio propagation through the ionosphere can distort the received signal by introducing echoes' time delays and causing a loss of peak power and range resolution (the capability of discriminating different targets along the depth direction for radar sounder systems). This depends on the ionosphere Total Electron Content (TEC) that is affected by the solar radio emissions. For this reason, the observations to be performed by SRS on Venus are preferred to be on the night side, when the EnVision spacecraft is shadowed by Venus from the Sun, in order to maximize the detection performances.

Another source of disturbance of the acquired data is the clutter, which for radar sounder observations is represented by off-nadir surface echoes, caused by the large footprint that characterizes the type of antenna usually employed for radar sounder systems, the dipole. However, this variable won't be considered in detail as it is not the main focus of this thesis.

Further parameters need to be taken into account to characterize the resource exploitation associated to each data acquisition operation, especially from the point of view of the generated data volume. The requirements of the data volume, indeed, are one of the most delicate variables to consider when dealing with missions that have a large number of science instruments, since all of them need to exploit and share the available memory and telemetry resources. In order to determine the data volume associated to each observation, we first need to define the length of the time window during which the received echo signal is recorded (SWL) after each pulse transmission. The SWL can be expressed as follows:

$$SWL = \frac{2}{c_0}(\sigma_1 + \sigma_2 + \sigma_h + z_{max}\sqrt{\epsilon_{r,av}}) + 2M_s + T_{iono} + T_p. \tag{2.3}$$

The meaning of the different terms of this expression is hereby reported:

- c_0 is the speed of light in vacuum;
- σ_1 and σ_1 represent a positive and a negative margin related to the topographic

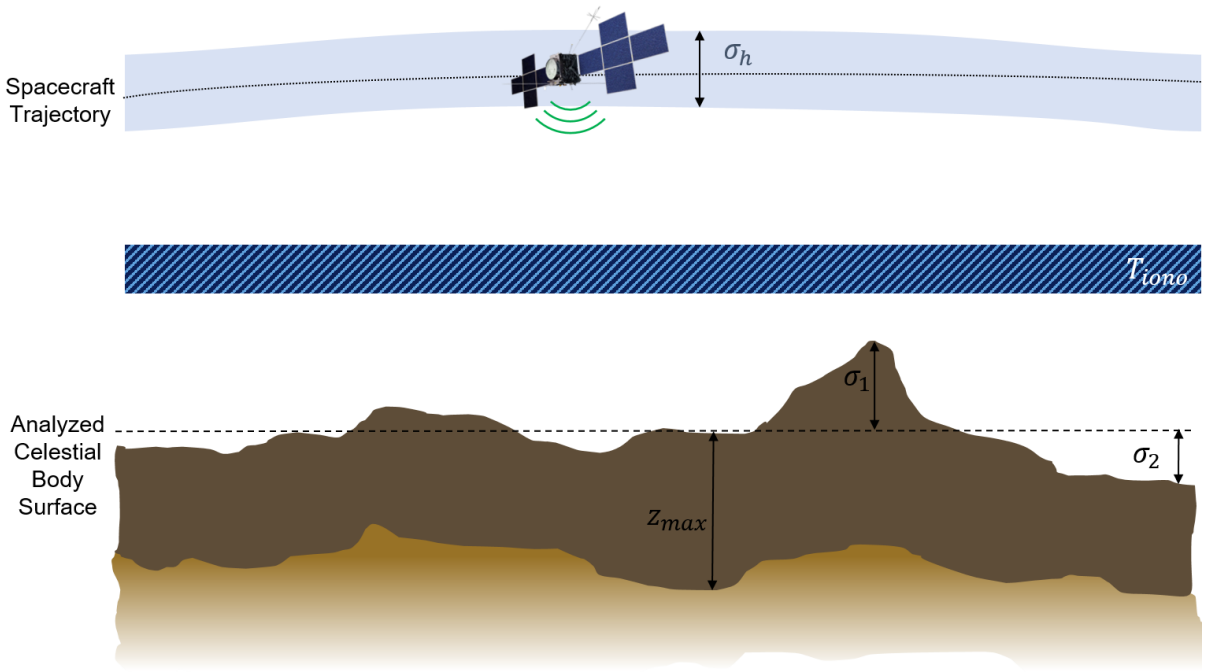

Figure 2.4: Illustration of the variables associated to the acquisition scenario influencing the radar sounder acquisition generated data rate.

characteristics of the surface of the area to be analyzed respectively, given a reference quota, calculated based on the ellipsoid used to represent the considered celestial body;

- σ_h is associated to the position uncertainty related to the spacecraft trajectory, which has an impact on the actual height of the platform from the ground. Around the trajectory defined for the considered spacecraft, an uncertainty "tube" can be defined based on the probability of the spacecraft to be in a given position with respect to the nominal trajectory and σ_h is the diameter of this "tube";
- z_{max} is the estimation of the expected maximum penetration depth that the analyzed radar sounder can reach, based on the design variables values and on the hypotheses of the subsurface composition;
- $\epsilon_{r,av}$ is the average dielectric permittivity of the subsurface materials along the depth direction. It is useful to estimate the pulse propagation velocity and thus the pulse travel time through the subsurface layers;
- T_{iono} is the estimated delay in the transmitted pulse travel time, caused by the propagation through the ionosphere;

- T_p is the transmitted pulse length in time;

- M_s is a further security margin that is applied to the receiving window length SWL to ensure that important unforeseen features can still be detected.

The components related to the particular acquisition scenario are depicted in Figure 2.4

After the definition of the SWL, it is possible to express the data rate DR associated to the acquisitions to be performed by the considered radar sounder system, which simply represents the amount of data per second that a given data acquisition generates. DR can be formulated as follows:

$$DR = \frac{2SWL \cdot f_s \cdot PRF \cdot N_{bit}}{N_p}, \tag{2.4}$$

where:

- f_s is the frequency at which the receiver of the considered radar sounder system samples the received analog echo signals;

- PRF is the pulse repetition frequency designed for the the considered radar sounder system;

- N_{bit} is the number of bits that are employed to represent each sample of the received echo signal;

- N_p is the so-called *presumming* factor.

The presumming operation is a lossy compression that can be employed in order to reduce the data rate of an observation at the cost of a reduced quality of the resulting radargram. It sums N_p consecutive echo signals. However, given that the echo signals are complex (they have an in-phase and an in-quadrature component), it is very important that the echoes that get summed in the presumming operation are coherent. A large phase difference could induce a high loss on the information content of the echo signals. Thus, this operation can be performed only on acquisitions over areas where the topography does not have a high variability, reducing the total amount of data to be recorded on the spacecraft memory storage and to be downlinked to the ground stations.
As briefly addressed before, the data rate and data volume reduction, where feasible, becomes particularly important in missions with a large science payload.

2.4 Quality Parameters in Radar Sounder Acquisitions

Once we have defined the parameters to describe the performances of a radar sounder for a single observation, we need to analyze the characteristics of a full acquisition schedule or strategy, which is the way to completely assess the compliance with the mission science requirements associated to this type of instrument. In order to define the quality of the acquisition strategy of planetary radar sounders in general, given the available observation opportunities, the following variables can be considered:

1. *Uniformity in space of the data acquisitions.* In general, given the acquisition geometry and capabilities of radar sounder instruments, the observations performed by this sensors do not have a 2D surface coverage. Indeed they provide a vertical tomography of the subsurface in correspondence of the ground tracks, as shown in Figure 2.2. Thus, in order to globally sample the subsurface of the analyzed celestial body in the best possible way, the ground tracks associated to the different scheduled observations should be uniformly distributed. This is done because in general it is not possible to have a priori a direct information on the subsurface structure, even if different hypotheses can be made, which help in the operations design. To control the spatial uniformity of the observations, the distance between the different associated ground tracks should be checked. Moreover the desired distance between the ground track should be defined. This distance is a trade-off between the resources exploitation by the radar sounder and the achievable level of detail of the characterization of the subsurface, which of course is higher if a lower distance between ground tracks is defined, thus requiring a larger number of observations;

2. *Number of intersection points between the ground tracks and their position and distribution on the surface.* A more detailed analysis of the subsurface structure of the investigated celestial body can be done by acquiring data over intersecting ground tracks. The intersections allow for an improved calibration of the acquired data but, more importantly, they provide an additional dimension to the set of acquisitions thanks to the data acquired along different directions. The more intersection points we can reach with the observations we include in the acquisition schedule and the more uniformly they are distributed on the celestial body surface, the more accurately we can characterize and reconstruct its subsurface structure and stratigraphy.

3. *Presence of regions of interest (ROIs).* The acquisitions to be performed over particular selected target areas have to be managed with specific attention. In order to support the interpretation of the data acquired over them, uninterrupted observations of these target areas are desired. Moreover, a higher acquisition density could

also be required, in order to better analyze and characterize the subsurface. This objective could be pursued, for example, also by increasing the bandwidth (where possible) of the transmitted pulses, thus improving the radargram resolution along the depth direction.

In specific missions, additional variables might constrain the acquisitions, as for example environmental conditions or the compatibility with the observations performed by other instruments included in the science payload of the considered mission.
In the case of PE missions, the above-mentioned variables need to be carefully harmonized with the requirements of all other instruments composing the science payload, increasing the complexity of the definition of a feasible and high quality acquisition strategy for any sensor.

2.5 Conclusion

In this chapter we have briefly summarized some of the most important features and parameters involved in radar sounder acquisition, in order to provide useful metrics to describe the quality of their observations, given their unique observation geometry and capabilities.
The parameters to describe the quality of a single observations can be obtained and designed deterministically, even if some uncertainties, mostly regarding the subsurface structure, still need to be faced. The determination of the quality of a full acquisition strategy and schedule and their optimization for planetary radar sounder observations instead, as well as for other instruments, is a very complex combinatorial problem. It is based on a very large number of variables, especially if we need to take into account the acquisitions to be performed by all other instruments composing the science payload of the considered PE mission. For this reason, the methodologies presented in Chapters 3 and 4 have been studied and developed to deal with the complex and multifaceted problem of automatically plan and schedule observations of science payload instruments for Planetary Exploration missions.

Chapter 3

An Approach Based on Multi-Objective Genetic Algorithms to Schedule Observations in Planetary Remote Sensing Missions

This chapter[1] *presents an approach to the automatic scheduling of the acquisition operations of a remote sensing instrument included in the scientific payload of a mission. The presented methodology first subdivides the long available observation time intervals into shorter segments and then performs a selection of them, producing an acquisition schedule, optimized with respect to the scientific requirements, the instrument characteristics and the mission constraints. The scheduling problem is modeled as a multi-objective optimization problem and solved by using Genetic Algorithms (GAs). GAs are able to efficiently explore the solution space by considering different competing objective functions, reaching high quality solutions. These solutions represent different optimized tradeoffs among the considered instrument-specific quality metrics. The approach is demonstrated on the operations of RIME (Radar for Icy Moons Exploration), a radar sounder onboard JUpiter ICy moons Explorer (JUICE). The obtained results show the high potential of the proposed methodology.*

[1]Part of this chapter appears in

[J1] S. Paterna et al., "An Approach Based on Multiobjective Genetic Algorithms to Schedule Observations in Planetary Remote Sensing Missions," in IEEE Journal of Selected Topics in Applied Earth Observations and Remote Sensing, vol. 13, pp. 4714-4727, 2020, doi: 10.1109/JSTARS.2020.3015284,

and in

[C1] S.Paterna, M. Santoni, L. Bruzzone, "An Automatic Planning and Scheduling Method Based on Multi-Objective Genetic Algorithms for Planetary Radar Sounder Observations," 2020 IEEE International Geoscience and Remote Sensing Symposium (IGARSS), Waikoloa, HI, USA, 2020, doi: 10.1109/IGARSS39084.2020.9324270.

3.1 Introduction

As stated in the introductory Chapter, remote sensing instruments provide high-valuable data, characterizing the surface, composition and structure of the analyzed celestial body. This is possible by exploiting the data acquired by the science payload designed for the considered mission and the related spacecraft. The science payload is usually composed of different instruments, each one devoted to the analysis of a particular variable (or a set of variables) of the considered environment. This often results in a challenging handling of the data acquisition strategy. Indeed, as illustrated in Chapter 1 the management of acquisitions requires to consider a large number of complex constraints and specifications. These include the scientific objectives associated with each instrument and the related requirements, the environmental conditions that may limit the observation capabilities of certain types of sensors, and the resources that are available on board the spacecraft (e.g., power, memory storage space, downlink data rate) that have to be shared among all the instruments composing the payload. In general, the resources available for a mission and the trajectory to be followed by the spacecraft in the different phases of the mission are defined on the basis of the science objectives and the related operational requirements of the payload in the early stages of the mission design. Nonetheless, technological issues and cost boundaries limit the resources available to each single instrument. This results in constraints on both the total acquisition time allowed to each instrument and the time distribution of the acquisitions, with the risk to affect the mission science return.
In this context, one of the most important phases of the mission is the scheduling of the operations of the science payload. It is aimed at determining the possible options for data acquisitions with respect to the above-mentioned constraints. A very important input to this phase is the planned mission trajectory that defines and characterizes the feasible observation opportunities of a certain sensor over a well defined portion of the target body.
The planning and scheduling phase is therefore aimed to produce a scientific payload operations schedule, over a well-defined time frame, which is feasible with respect to both global limitations and the constraints concerning the acquisitions of single sensors. This schedule should optimize the performances of the different instruments in terms of data acquisition quality, resources consumption and compliance to the scientific requirements. In particular, for missions that comprehend orbital phases, this means that during the planning and scheduling process it is mandatory to select a subset of the many observation opportunities. The selection has to be based on a set of metrics that express the quality of the data collection operations performed in each specific time window and in the whole considered time frame.

In the general context of data acquisitions planning and scheduling for planetary exploration missions, the typical planning procedures are described in [3] [4]. The process is usually quite long and complex and requires multiple iterations (or cycles) to progressively increase the level of detail of the planning and finally converge to an overall schedule. During these cycles, the instrument teams provide inputs in terms of acquisition requirements and constraints to a mission planning team, which is in charge of collecting the inputs and define the acquisition scenarios for the whole scientific payload. Both the overall schedule and the requests from the instrument teams are iteratively refined during the whole process. Thus, the planning phase requires a high percentage of human interaction in the definition of the science operations schedules, even if tools like MAPPS or SciBox (described more in detail in Chapter 1) are available, which can support:

1. the definition of the observation strategy;
2. the constraint checking phase;
3. the translation of the schedules into command sequences to be executed by the spacecraft and its payload.

Further steps towards the development of automatic methods for the planning and scheduling process have been done on Earth Observation missions, which, however, are significantly different from planetary missions in terms of both constraints and scale of the problem. These methods, as we showed in Chapter 1, can be used as an inspiration for addressing the challenges of planetary missions under the assumption of major adaptation and refinements.
In this chapter, we present an approach to the automatic observation planning and scheduling based on multiobjective Genetic Algorithms to be used in complex planetary remote sensing missions. The main goal of the proposed approach is to provide a tool being able to speed up the usually time-consuming observations scheduling process for planetary missions by automatically generating optimal (or nearly-optimal) schedules, considering the mission and the instrument-specific constraints. The proposed technique consists of two main stages, i.e. the segmentation and the selection stages, during which all feasible acquisition intervals (with respect to the considered instrument capabilities) are determined, analyzed and evaluated to generate the observation sequence for a given sensor over the input time horizon. The segmentation splits the input time horizon into well-defined shorter acquisition intervals, following a time-based or a target-based criterion (namely, the start- and end-time of the interval are determined as the window in which the whole considered target is visible). In the selection phase, an NSGA-II-based engine explores the space of the solutions related to the combinations of the acquisition

segments, by analyzing different objectives expressed by competing metrics. A similar approach was used also in the context of Earth Observation missions, as shown in Chapter 1. However, with respect to the technique presented in [47], we here tackle a problem of larger scale and we do it by directly working on the genetic operators that characterize the GAs. Indeed, two slightly modified versions of NSGA-II [66] have been considered: one exploits the mission constraints so that no unfeasible solutions can be generated and evaluated to minimize the computational time; the other implements a local-search-based strategy to better guide the solution space exploration. At convergence, the system provides operation schedules that are optimized (in the Pareto front sense) with respect to different objectives like data acquisition quality, resources consumption and compliance to the scientific requirements. To validate our approach, we studied the real case of the operations planning and scheduling for the JUpiter Icy Moons Explorer (JUICE) mission of the European Space Agency (ESA), which is focused on the analysis of the Jovian System and of Jupiter's Icy Moons. In detail, we focused our attention on the observations of the Radar for Icy Moons Exploration (RIME), the radar sounder designed for JUICE.

This chapter is structured as follows. Section 3.2 illustrates the proposed methodology in general considering neither any specific instrument nor any specific mission. Section 3.3 presents the application of the proposed methodology to RIME in the context of the JUICE mission, the experimental setup, the specific choices in terms of constraints and objective functions and the results are shown and discussed, given the indications presented in Chapter 2. Finally, Section 3.4 draws the conclusions of this Chapter.

3.2 Proposed Planning and Scheduling Approach

The methodology that we propose to automate the planning and scheduling process consists of two main phases (see Figure 3.1) : the **segmentation** and the **selection**. The segmentation phase takes as input the whole set of feasible acquisition time intervals (contained in the total considered time interval Φ), splits them into shorter segments, following a user-defined criterion, and extracts a set of significant metrics describing each of the acquisition segments. These metrics are then exploited in the selection phase, in which they are combined in suitable cost/fitness functions that express the acquisition schedule quality. The selection phase is aimed at building an optimized acquisition schedule. This result is obtained by using an optimization algorithm, which efficiently explores the solution space and selects an appropriate subset of acquisition segments, given the science and instruments requirements, the acquisition quality metrics and the mission constraints.

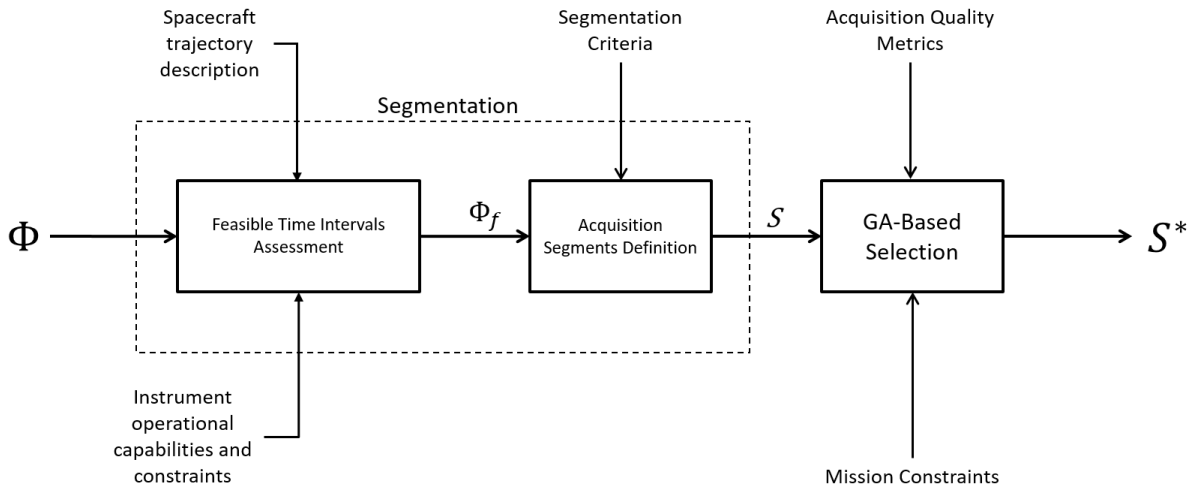

Figure 3.1: Illustration of the steps of the proposed methodology: here Φ represents the total time interval that we are taking into account (i.e. a particular phase of the considered mission) and $\Phi_f \subset \Phi$ is the set of time intervals $\phi_i^f \in \Phi$ in which the data acquisition with the specified instrument is feasible. S is the result of the subdivision of Φ_f in shorter time segments $s_i \in S$ which are easier to handle and analyze. Finally, $S^* \subset S$ represents an optimal subset of S with respect to the instrument specific quality metrics and general constraints.

3.2.1 Segmentation Phase

As shown in Figure 3.1, the inputs to the whole system are the total considered interval Φ and the description of the trajectory that the spacecraft will follow during its orbit around the target celestial body. The latter is defined using kernel files that contain the state vector (describing position and speed) of the satellite in time, using a format that is the standard *de facto* for the description of the trajectories of spacecrafts. The interface to these kernel files is provided by dedicated libraries, which allow to extract all the useful information about the spacecraft motion around the celestial body to be investigated and about the acquisition scenario. An example of these libraries are the ones created by NAIF (NASA's Navigation and Ancillary Information Facility), called SPICE [67] [68]. On the basis of the orbit data, it is possible to perform a first filtering of the time intervals, removing all the time intervals in which the acquisitions with the analyzed instrument are not feasible due to the characteristics of the instrument with respect to the environmental conditions (e.g., an optical camera can only acquire images on the illuminated side of the considered celestial body) and to other mission-related limitations that might prevent any instrument from performing acquisitions. This filtering can be done by exploiting the dedicated function libraries (e.g., SPICE) mentioned above. Indeed, using those conditions and limitations as input to these functions, it is possible

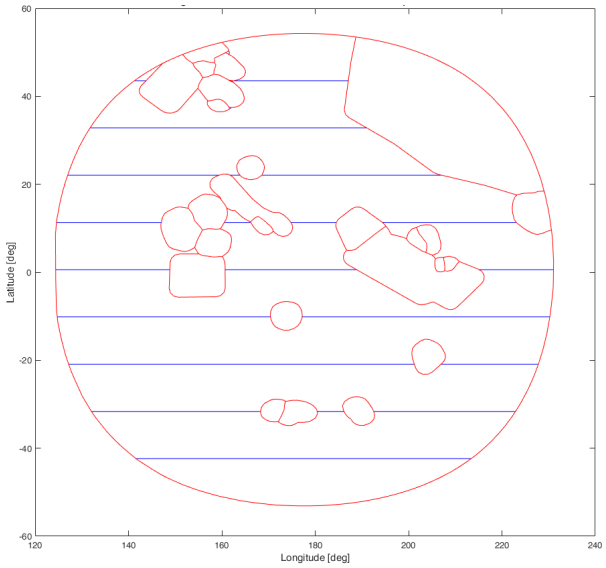

Figure 3.2: Example of segmentation grid of the "operative" zone for the orbital phase at 500 km altitude around Ganymede (GCO-500) of the JUICE mission. The borders of the higher-relevance areas are shown in red, while the rest of the surface is subdivided in latitude bands (in blue). This grid is used to segment the whole set acquisition opportunities, once that their relative position on Ganymede's surface has been determined.

to easily recognize the time intervals in which they are verified and remove them from the time horizon Φ. After this filtering phase that produces the set Φ_f of time intervals in which the acquisition operations of the considered instrument are feasible, the next step is to determine the area that we can observe at each time instant. If we consider an instrument with fixed pointing, this is possible by simply projecting the position of the spacecraft on the surface of the target body along the pointing direction. Figure 2.3 shows how this operation is performed for the case of the radar sounder RIME, which is the study case we consider in this work (see Section 3.3 for more details).

The resulting opportunities and the ground tracks related to the time intervals Φ_f are often too long to be acquired in a single continuous observation. Therefore the successive step is to subdivide them into shorter acquisition segments s, which can be more easily managed during the mission operation. We can define these segments as single uninterrupted time intervals in which different desired conditions are verified. These conditions for the segmentation should be given as input to the framework, as shown in Figure 3.1. An easy condition, following which we might want to subdivide the long acquisition time intervals in Φ_f, could be the duration, creating therefore a set of segments with equal or similar time span. Moreover, once the pointing of the instrument is fixed (also

the information regarding the pointing is contained in the kernel files), it is straightforward to translate the time instants in Φ_f into observable positions on the target's surface (expressed as latitude and longitude coordinates). Thus, it is possible to perform the segmentation directly on the related ground tracks to take into account high-interest areas on the target body's surface. Indeed, it is convenient to perform the acquisitions over these important areas in a continuous way, to ease the interpretation and the extraction of information from the acquired data. After the identification of these high-interest areas and the determination of their coordinates, the remaining portion of the surface to be observed can be further subdivided in a uniform way. Thus, we can create a particular mapping of the analyzed celestial body surface that we call a *segmentation grid*. Figure 3.2 shows an example of a segmentation grid as applied to the test case described in Section 3.3. The single areas in which the surface to be observed is subdivided (both the target areas and the other remaining surface portions) are called *cells* and the long acquisition tracks are split at the edges of them. Therefore, in this case the conditions to be verified are spatial: we define the acquisition segments as the individual time intervals in which the observable portion of the surface is delimited by a particular cell. Thus, the start- and end-time of each segment are determined as the time instants in which the observable portion of the surface crosses the border of one of the cells.
The output of the segmentation stage is a set of acquisition segments $S = \{s_1, s_2, ...s_N\}$, where N is the total number of resulting segments.
These acquisition segments, are then described by a set of metrics. The most important and general segment metrics are as follows:

- $st(s_i)$ and $et(s_i)$ identify the beginning and the end of the acquisition segment s_i from the temporal point of view. They are defined as a result of the temporal or spatial segmentation described above;
- $time(s_i) = et(s_i) - st(s_i)$ is derived from the previous metrics and determines the temporal duration of segment s_i;
- $a(s_i)$ is the portion of surface covered by segment s_i. It is obtained by merging the projection of the instrument field of view on the surface in correspondence of the spatial coordinates between the instants $st(s_i)$ and $et(s_i)$;
- $e(s_i)$ and $m(s_i)$ represent the energy and the memory consumption associated to the acquisition operation of segment s_i, respectively. They are defined on the basis of the instrument characteristics in terms of energy and memory consumption rates.

Further metrics to describe the acquisition segment could be specifically created and extracted, based on the charateristics of the considered instrument, of the analyzed mission

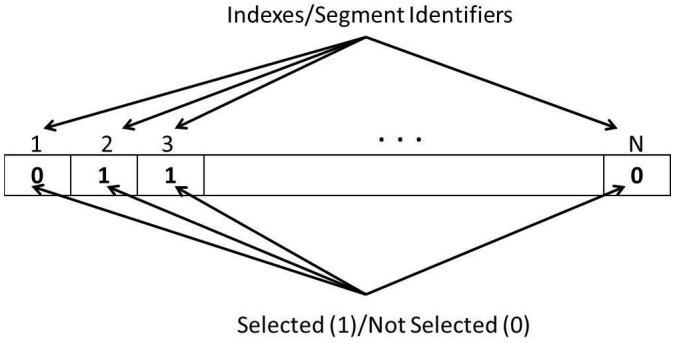

Figure 3.3: Binary vector representation of the scheduling problem in the phase of selection of acquisition segments

and of the environment in which the instrument should operate.

3.2.2 Selection Phase

Following the definition of the metrics that describe each acquisition segment and the whole acquisition strategy (based on the segment metrics), in the selection phase the subset S^* of segments that satisfies the scientific requirements in the best possible way should be selected without violating any constraint. We can represent a possible schedule as a binary vector $\mathbf{x}$ ($\mathbf{x} = \{x_1, x_2, ..., x_N\}$), in which every position i identifies one of the acquisition segments s_i, and the value x_i ($x_i \in \{0, 1\}$) of the i-th position of the solution vector $\mathbf{x}$ expresses if that particular acquisition is inserted in the schedule (1) or not (0). This is a combinatorial problem that can be modeled as a particular type of multi-dimensional 0-1 knapsack problem [37], as also shown in Chapter 1. Multi-dimensional knapsack problems [15] are a very good example of combinatorial problem in which the objective is to maximize a total profit parameter associated to a subset of the available objects, given a set of constraints based on cost coefficients associated to these objects. Each of these objects has associated both a profit coefficient and costs coefficients that depend on the different constraint.
In general, different metrics to be optimized can be considered simultaneously. However, often these metrics express objectives that might be conflicting between each other. Accordingly, in the proposed approach we address this issue by exploiting a multi-objective optimization approach.
The result of such optimization is a set of different solutions that represent the Pareto front, i.e., the set of the non-dominated solutions [69]. For a multi-objective maximization problem, a given solution $\mathbf{x}_1$ of the optimization problem dominates another solution $\mathbf{x}_2$ if $f_j(\mathbf{x}_1) \geq f_j(\mathbf{x}_2)$ $(\forall j = 1, 2, ..., O)$ and $f_k(\mathbf{x}_1) > f_k(\mathbf{x}_2)$ at least for one objective

$f_k(\mathbf{x})$ $(k = 1, 2, ..., O)$ [70], where $f_j(\mathbf{x}), f_k(\mathbf{x})$ are different objectives that are taken into account and O is the total number of analyzed objectives. It is worth noting that a single-objective approach can not ensure the control on all the metrics that describe the quality of the acquisition campaign, even if we combine different quality metrics in one single cost/objective function. The multi-objective approach, instead, has the advantage of producing solutions that represent multiple optimal tradeoffs between the different objectives. In the case of the segment selection problem, this results in a set of optimal acquisition schedules, which are all non-dominated solutions with respect to the considered quality metrics. Thus, any of these solutions could potentially be selected as the final observation schedule for the considered instrument. The final choice is only guided by the desired trade-off between the selected quality factors. Moreover, since we are taking into account the acquisition operations of a single instrument in missions that usually have a large scientific payload, having different optimal solutions with different tradeoffs can be very useful to choose the strategy that better adapts to the acquisition requirements and schedules of other instruments.

Let $\mathbf{x} = \{x_1, x_2, ..., x_N\}$ be the vector of the decision variables, $F(\mathbf{x}) = \{f_1(\mathbf{x}), ..., f_l(\mathbf{x}), ..., f_O(\mathbf{x})\}$ be the set of objectives/fitness functions that are related to the quality metrics we need to optimize, $f_l(\mathbf{x}) \in F$ be one of the functions indicating the quality of the schedule identified by $\mathbf{x}$, and q_i be a generic quality metric associated to the segment s_i. In the case we are analyzing, a possible quality metric q_i could be the parameter $a(s_i)$. We formulate the segment selection problem as follows:

$$\max_{\mathbf{x}}\{F(\mathbf{x})\}, \tag{3.1}$$

$$\text{with } f_l(\mathbf{x}) = \sum_{i=1}^{N} q_i x_i, \tag{3.2}$$

$$\text{subject to} \sum_{i=1}^{N} c_{j,i} x_i < b_j, j = 1, ..., M, \tag{3.3}$$

$$x_i \in \{0, 1\}, i = 1, ..., N; \tag{3.4}$$

The cost coefficient $c_{j,i}$ $(j = 1, 2, ..., M,\ i = 1, 2, ..., N)$ is associated to the j-th constraint and to the i-th position of the solution vector (i.e., to the i-th acquisition segment s_i). The parameter b_j is a component of the vector $\mathbf{b}$ $(\mathbf{b} = \{b_1, b_2, ..., b_M\})$, which contains the values of the bounds associated to each of the M constraints. Moreover, we have a set of multiple global constraints that should guide us in the selection of the correct subset of segments also based on their associated metrics. The global quality function $f(\mathbf{x})$ can in general be more complex than the one shown in Eq. 3.2, but that formulation is a good representation for many acquisition schedule quality metrics.

In order to solve this kind of problem, given that in general the number of acquisition segments is very high, we use stochastic optimization techniques that can explore the solution space in an efficient way, without the need to explicitly evaluate the whole set of possible combinations of acquisition segments. A suitable option is to use a technique based on Genetic Algorithms (GAs), which have been used in a variety of applications (i.e., [71]), providing very good results.

GAs have also been applied to specific satellite scheduling problems, for scheduling the downlink from the satellite to a ground station, given the visibility intervals and the possible ground stations on Earth [51] [50]. Note that the structure used to represent the different solutions in GAs, the *chromosome*, is intrinsically suitable to the representation of our problem in form of a binary vector. Another important property of GAs is that genetic operators, crossover and mutation, allow for a good exploration of the solution space by generating new solutions combining the current ones or slightly modifying a small number of variables of them. In general, the mutation operator randomly modifies one or more of the components x_i of the solution vector $\mathbf{x}$ to a certain extent, in the case of a binary solution vector it simply changes the value of x_i from 0 to 1 or from 1 to 0. In our case this results in adding the related segment s_i to the schedule we are building, or removing s_i from it, respectively. The crossover operator instead produces new solutions taking in input pairs of solution vectors of the previous iteration. It subdivides the input solution vectors into two or more components in correspondence with the crossover points. Considering to have one crossover point, two new solution vectors are generated. The first solution is made by joining the first component of the first input solution vector and the second component of the second input solution vector. The first component of the second input solution vector and the second component of the first input solution vector constitute the second new solution generated by crossover.

Since we formulated the acquisition segment selection as a multi-objective optimization problem, a suitable algorithm to solve it is NSGA-II [66], which is one of the most effective multi-objective versions of GAs. The algorithm is initialized either with a randomly generated or with a custom population of candidate schedules, modeled as binary vectors. At iteration h, for each member of the current population Pop_h the values of all the cost/objective functions are computed. The members of Pop_h are sorted following the non-domination criterion based on the values of the considered quality metrics, assigning a rank to each member based on its non-domination front (or level). A further metric controlling the density of the population members in the objective function space (which is the crowding distance) is also computed for each candidate acquisition schedule in Pop_h. The offsprings (new candidate schedules) O_h are created by selecting members from Pop_h via binary tournament selection and using them as input to the crossover and

mutation functions. The binary tournament selection is based on the rank (the lower, the better) and in case two members with same rank are picked, the one with larger crowding distance will be selected, to ensure that the final solutions of the optimization will be well distributed along the Pareto front. Moreover, NSGA-II implements the concept of elitism: indeed, in order to create Pop_{h+1}, the offsprings O_h are considered together with the members of Pop_h. The members of $Pop_h \cup O_h$ are ranked following the non-domination criterion, after the evaluation of the objective functions for the members of O_h. Pop_{h+1} is created by picking the best $|Pop_h|$ candidate schedules from $Pop_h \cup O_h$ based on their rank (non-domination level) and using the crowding distance as a tie-breaker to decide between candidate solutions with the same rank.
However, given the dimension of the problem, NSGA-II would not be able to easily converge to a good set of solutions close to the Pareto front, despite the potentialities given by its features. Thus we need to modify the algorithm, implementing hybrid strategies to improve the way in which we explore the solution space. A possible strategy is to modify the way in which new candidate solutions are generated, implementing constraints inside the evolutionary operators (crossover and mutation), so that only feasible solutions are generated. In general, constraints can be represented in matricial representation as:

$$C\mathbf{x} < \mathbf{b}, \tag{3.5}$$

where $C \in \mathbb{R}^{M \times N}$ is the matrix that represents all the cost coefficients associated to each variable of the solution vector $\mathbf{x}$ and each constraint that we need to apply (e.g., energy, memory, time). The cost coefficient $c_{j,i}$ defined above represents the generic component of the matrix C. The constraints that can be introduced in the scheduling process should be carefully designed, depending on the characteristics of the mission, of the considered instrument and of the acquisition environment. However, as an example of constraint that could be useful in general we can use the segment metric $m(s_i)$ that has been described in the previous section, regarding the memory consumption. We can define the vector $\mathbf{c}_j$ (being $\mathbf{c}_j$ a row of the matrix C) as:

$$c_{j,i} = m(s_i), \tag{3.6}$$

and formulate the constraint as:

$$\sum_{i=1}^{N} c_{j,i} x_i < Mem, \tag{3.7}$$

where Mem identifies the amount of storage memory that is available between two consecutive downlink windows and thus the amount of data that can be downlinked in a specific downlink window. We can easily associate each segment s_i to the downlink window in which the datavolume generated between $st(s_i)$ and $et(s_i)$ $(m(s_i))$ is effectively

transmitted to the ground station. Thus, given this association, the constraints on the memory consumption can be defined for each downlink window and therefore considering only the segments related to the specific downlink window. This allows to better control the state of the memory storage on board the spacecraft throughout the whole considered time frame. This formulation is inserted in the genetic operators, in order to check the generated solutions and, if any constraint violation is detected, to correct the non-feasible solutions changing the value of some of the associated variables from 0 to 1 or from 1 to 0, accordingly. This introduces a first limitation on the exploration of the solution space. Another possibility to increase the efficiency of the exploration is to further modify the mutation operator in order to perform a smarter exploration of the solution space. The operator should modify the input solution vectors such that this modification is guided towards solutions that are better from the point of view of the specified objectives.
This should be done by exploiting our knowledge of the problem and of the characteristics of each segment $s_i \in S$. In particular, inspired by the local search strategy proposed in [16], by maintaining the randomness of the GA, a higher weight (and therefore a higher probability to be selected) can be given to the variables/segments that improve the considered solution/schedule if added or removed from it. Based on the metrics that can be extracted for each acquisition segment, further metrics can be calculated based on the scenario represented by the input solution vector. More in detail, we can identify 3 possible actions:

- Adding segments to the schedule;
- Removing segments from the schedule;
- Replacing a segment in the schedule (a mixture of the previous two actions).

For modeling this last case it is useful to define two additional sets of segments:

- $S_{in} = \{s_i \in S : x_i = 1\}$, which is the set of segments included in the input schedule/solution vector;
- $S_{out} = \{s_i \in S : x_i = 0\}$, which is the set of segments not included in the input schedule.

Initially the action to be performed is randomly selected. Given the action to perform, one should focus on either S_{in} (for the removal action) or on S_{out} (for the addition action) and compute metrics that guide the search towards better solutions. These metrics are then used in order to implement a *roulette wheel selection* mechanism, to decide which segments should be added, removed or substituted to improve the characteristics of the input observation schedule. For example, in our case we can extract the information

regarding the area $a(s_i)$ covered by each acquisition segment. Considering an acquisition schedule modeled as the binary vector $\mathbf{x}$ as input to the modified mutation operator, if the selected action is to add a segment to the schedule, the goal can be to increase the total surface covered by the segments $s_i \in S_{in}$. We can define A as the total surface that has to be covered and A_s as the surface covered by the current solution:

$$A_s = \bigcup_i \{a(s_i) : s_i \in S_{in}\}. \tag{3.8}$$

We can therefore define for each $s_j \in S_{out}$ a metric of "surface improvement" as follows:

$$t(s_j) = a(s_j) \cap (A - A_s), \forall s_j \in S_{out}. \tag{3.9}$$

The higher the value of $t(s_j)$, the higher the probability of s_j to be included in the output schedule. The values of $t(s_j)$ are calculated for each of the segments in S_{out} and then used to pick the segments to be added to the output acquisition schedule. A similar situation happens if the selected action is to remove segments from the input schedule: in this case the goal might be to reduce the overlapping between all the $a(s_i)$ with $s_i \in S_{in}$. For this case we can therefore define the total overlap area A_o as:

$$A_o = \bigcup_{i,j} \{a(s_i) \cap a(s_j) : i \neq j, s_i, s_j \in S_{in}\}. \tag{3.10}$$

We can therefore define for each $s_i \in S_{in}$ a metric of "overlap reduction" as follows:

$$r(s_i) = a(s_i) \cap A_o, \forall s_i \in S_{in}. \tag{3.11}$$

Again, the higher the value of $r(s_i)$, the higher the probability of s_i to be excluded from the output schedule. The values of $r(s_i)$ are calculated for each of the segments in S_{in} and used to pick the segments to be removed from the output acquisition schedule. Further details on how this modified mutation operator is used and on the metrics that have been exploited are given in Section 3.3.

3.3 Experimental Results

For the validation of the proposed approach we considered the planning and scheduling of the acquisitions of a planetary radar sounder, analyzing a real case. We used as test case the operations of the radar sounder RIME [64] [58] onboard the JUICE mission [1]. The JUICE mission, which includes 11 instruments in its scientific payload, is aimed to study the Jovian System. Its main objectives are the analysis of the Icy Moons of Jupiter: Ganymede, Europa and Callisto.

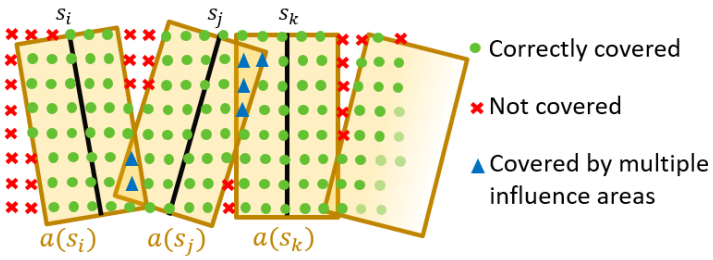

Figure 3.4: Scheme representing the concept of influence area for radar sounder acquisition opportunities. The area "covered" by each identified continuous observation opportunity (s_i) is here represented as a dense set of points. This representation helps simplifying the calculation of the total area covered by all the scheduled observation opportunities inserted in a given data acquisition schedule.

3.3.1 Test Case Considered: RIME and the GCO-500 phase

In our experiments we considered the GCO-500 phase of the mission. During this phase the JUICE spacecraft will be in a nearly polar circular orbit around Ganymede at 500 Km altitude (the real altitude ranges from 470 to 530 Km). This part of the mission will last 130 days. The acquisitions of RIME are constrained by an important environmental factor. Indeed, Jupiter is a source of radio emissions, which can strongly interfere with the acquisitions and reduce the SNR of the acquired data, thus damaging their information content. For this reason, the acquisitions of RIME should be performed when the JUICE spacecraft is occulted by Ganymede with respect to Jupiter. Moreover, Ganymede is in *tidal locking* with Jupiter, meaning that its rotation period and its revolution period are almost the same. Thus, Ganymede always has the same side directed towards Jupiter. These conditions reduce the analysis to about a 30% of Ganymede's surface, which is still large.
The analysis of the RIME observation operations has been carried out using the proposed approach. The main requirements for the solution of this problem are:

- To achieve uniform coverage of the surface of Ganymede in the investigated area;
- To select segments of acquisition tracks spaced among each other of about 50km.

A further guideline to take into account is to try to limit bursts of resources consumption, which may limit the acquisitions performed by the other instruments. Thus, an additional variable that has been considered in the definition of the scheduling is the daily duration of the acquisitions, with the objective to obtain an almost uniform distribution of this time in the full orbital phase.

Regarding the uniformity in space of data acquisitions, this requirement can be considered by slightly modify the concept of the area $a(s_i)$ covered by the segment s_i, since the instrument does not produce an image of the surface but rather a tomography of the subsurface. $a(s_i)$ can be obtained by enclosing each of the ground tracks related to the acquisition segments s_i in areas that have the same length of the ground tracks and a width equal to the desired distance between tracks. For the radar sounder case, $a(s_i)$ is therefore called *influence area*, and the concept is depicted in Figure 3.4. Thus, using this formulation, we can express the uniformity requirement as a surface "coverage" requirement, similarly to what one can do for other imaging systems, for which $a(s_i)$ can be defined in a more straightforward way considering their imaging capabilities.

3.3.2 Set-up of experiments

The first phase (segmentation) starts by taking as an input the trajectory that the spacecraft will perform during its orbit around Ganymede and the time span of the GCO-500 phase as our Φ. As explained in Section 3.2, the trajectories are defined in a set of kernel files (those of the JUICE mission can be found at [72]) that contain the state vector (made of position and speed) of the satellite in time. For what concerns the JUICE mission, these files are defined by the Operation Center of ESA (ESOC) based on the Consolidated Reports on Mission Analysis (CReMA). We consider the file reported in [73]. The input time interval Φ goes through the assessment of all the feasible observation opportunities: all the time intervals in which the acquisitions with RIME are not feasible are removed. These intervals correspond to instants in which the JUICE spacecraft is not shadowed from Jupiter by Ganymede and thus acquisitions might be affected by the interference produced by the Jovian electromagnetic noise. Moreover, the intervals related to the downlink windows (the information about them is also contained in one of the kernel files mentioned above) are removed. In these intervals the ground segment (situated in Malargüe) is in line-of-sight with the satellite and therefore the resources of the satellite are dedicated to the transmission of the data. No acquisition is possible during these time windows. After the assessment of all the practical observation opportunities we have a set Φ_f of time intervals in which the acquisition with RIME are feasible. Accordingly, we identify the related positions on Ganymede's surface, obtaining the possible long acquisition tracks.

Considering the set of high-interest targets provided by the RIME Science Working Team (SWT) on the analyzed area and subdividing the remaining surface in 10 latitude bands (as shown in Figure 3.2), we could split the acquisition tracks and the related time intervals, thus obtaining the set S of segments to use in the next phase. We also defined a set of uniformly distributed points $P = \{p_1, p_2, \ldots, p_M\}$ on the area over which acquisi-

tions are feasible, which represent a quantization of the surface. Indeed, exploiting P, we can simplify the calculation of the covered surface, keeping also track of the coordinates of the points that are covered by each acquisition segment and of those that are not.

We similarly defined a set $P_t \subset P$ that identifies the points on the surface included in the high-relevance areas. After the segmentation phase, we obtained a set S with more than 5000 segments. For each of them we generated the influence areas $a(s_i)$ (whose width has been set at 50 km) and extracted data such as the number of points covered by each influence area $\{p_k \in a(s_i)\}$, the duration ($time(s_i)$) of the acquisition and the day $day(s_i)$ in which the acquisition defined by each segment should be executed. We assumed that the acquisitions performed by RIME during the GCO-500 phase have a constant generated datarate (DR) and a constant power consumption (P_{acq}). Thus we have $m(s_i) = DR \cdot time(s_i)$ and $e(s_i) = P_{acq} \cdot time(s_i)$. Therefore, we can easily analyze the resource consumption through the evaluation of the acquisition time.
We applied the proposed approach by using the NSGA-II algorithm. We expressed the quality metrics in terms of cost, i.e., better solutions correspond to smaller values of the metrics. Accordingly, the global metrics used for the evaluation of the solutions are defined as follows:

- $unif(\mathbf{x})$: the tracks distribution uniformity, expressed as the percentage of points of the set P that are not covered one and only one time. We can formalize it as follows:

$$unif(\mathbf{x}) = \frac{|P| - L}{|P|}, \tag{3.12a}$$

where:

$$L = \sum_{j=1}^{|P|} h_j, \tag{3.12b}$$

$$h_j = \begin{cases} 1, & \text{if } \sum_{i=1}^{N} k_{j,i} x_i = 1 \\ 0, & \text{otherwise} \end{cases}, \tag{3.12c}$$

$$k_{j,i} = \begin{cases} 1, & \text{if } p_j \in a(s_i) \\ 0, & \text{otherwise} \end{cases} \tag{3.12d}$$

with $p_j \in P$;

- $unif_t(\mathbf{x})$: the tracks distribution uniformity on areas of higher interest, expressed in a similar way as the previous metric, but focusing on the set P_t. We define it as

follows:

$$unif_t(\mathbf{x}) = \frac{|P_t| - Q}{|P_t|}, \tag{3.13a}$$

where:

$$Q = \sum_{l=1}^{|P_t|} v_l, \tag{3.13b}$$

$$v_l = \begin{cases} 1, & \text{if } \sum_{i=1}^{N} w_{l,i} x_i = 1 \\ 0, & \text{otherwise} \end{cases}, \tag{3.13c}$$

$$w_{l,i} = \begin{cases} 1, & \text{if } p_l \in a(s_i) \\ 0, & \text{otherwise} \end{cases} \tag{3.13d}$$

with $p_l \in P_t$;

- $\sigma(\mathbf{x})$: the uniformity in time of the acquisitions. This parameter allows to distribute the acquisitions as evenly as possible on different days. It is possible to define it as follows:

$$\sigma(\mathbf{x}) = std[D(\mathbf{x})] = \sqrt{\frac{1}{N_{days} - 1} \sum_{d=1}^{N_{days}} [dat_d(\mathbf{x}) - \mu(\mathbf{x}))^2]}, \tag{3.14a}$$

where:

$$D(\mathbf{x}) = \{dat_1(\mathbf{x}), dat_2(\mathbf{x}), ..., dat_{N_{days}}(\mathbf{x})\}, \tag{3.14b}$$

$$dat_d(\mathbf{x}) = \sum_{i=1}^{N} g_{d,i} time(s_i), \tag{3.14c}$$

$$g_{d,i} = \begin{cases} 1, & \text{if } x_i = 1 \text{ and } day(s_i) = d \\ 0, & \text{otherwise} \end{cases} \tag{3.14d}$$

$$\mu(\mathbf{x}) = \frac{1}{N_{days}} \sum_{d=1}^{N_{days}} dat_d(\mathbf{x}); \tag{3.14e}$$

with N_{days} being the total number of days.

The requirement on the intersection points between the acquisition tracks was not used in these tests because the considered orbit and the related acquisition tracks present very few intersection points.

3.3.3 Results

We carried out different tests by considering different configurations for the selection stage. For the first tests we implemented the constraints in the proposed solution generation operators, mutation and crossover. Thus, no unfeasible solutions are explicitly evaluated, limiting the search space as explained in Section 3.2. By associating each segment to one of the latitude bands or to one of the higher-interest areas (the cells of the grid used to segment the acquisition opportunities), we defined a set of constraints on the number of segments for each of these areas, so that the uniformity requirement can be more easily achieved:

$$\sum_{i=1}^{N} c_{j,i} x_i \leq b_j \tag{3.15}$$

where x_i is the i-th component of the binary solution vector $\mathbf{x}$ (as shown in figure 3.3), $c_{j,i} = \{0, 1\}$ is in this case the weight associated to the i-th segment and the j-th constraint, while b_j expresses the value of the upper bound in terms of number of chosen segments per area.

For the successive tests, we implemented the modified mutation operator (the guided mutation), without introducing the constraints defined before. The metrics used to guide the generation of new schedules/solutions are the ones described in Section 3.2.2, i.e., $t(s_i)$ and $r(s_i)$.

Figures 3.5, 3.6 and 3.7 show some examples of the results of the tests obtained with the 2 described configurations. The circular area in Figures 3.5a) and 3.6a) is the one that we considered for our analysis. The white edges identify both the high-interest areas on the investigated area on Ganymede and the other portions of the surface considered during the segmentation phase. The different colors show an example for a specific solution, for both test configurations, of how well and how uniformly the considered portion of surface is covered. Figures 3.5b) and 3.6b) show instead the results in terms of daily acquisition time, while Figures 3.5c) and 3.6c) summarize the characteristics of the considered solutions. Both test configurations considered a population size (the number of different solutions evaluated at each iteration) of 100 elements. They took about 3.5 days to reach 50000 generations on a single computing cluster node (24 cores running at 2.4 GHz, 96 GB of RAM). The solutions displayed in Figs. 3.5 and 3.6 obtain very good scores especially in terms of spatial uniformity of the selected segments. Indeed, this is evident both from the graphical representation and from the solution feature summary: for the constrained optimization result we obtain a total coverage of 94.41% of the total investigated area with just a 4.85% of "overcovered" surface. These metrics are even slightly better for the result of the optimization implementing the modified mutation operator: 94.7% coverage of the considered surface with 4.65% of overcovered surface. Very similar percentages of coverage

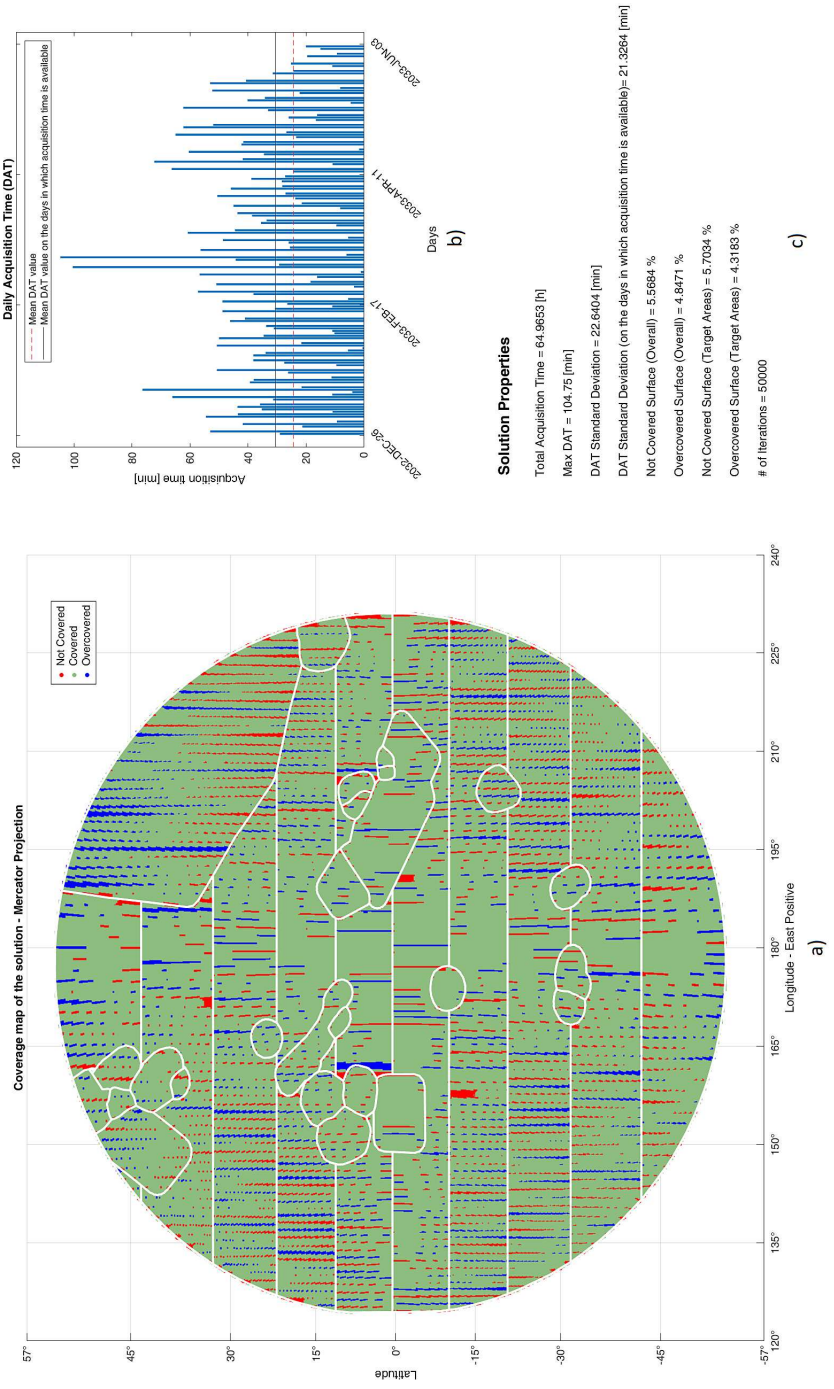

Figure 3.5: Example of a solution of the multiobjective optimization achieved implementing the constraints on the number of segments to be active for each cell. This solution is the best in terms of spatial uniformity of the selected acquisition segments (GCO-500 case). In green, the points that are covered by one and only one of the influence areas of the selected segments. In blue, the points that are covered more than once. In red the points that are not covered.

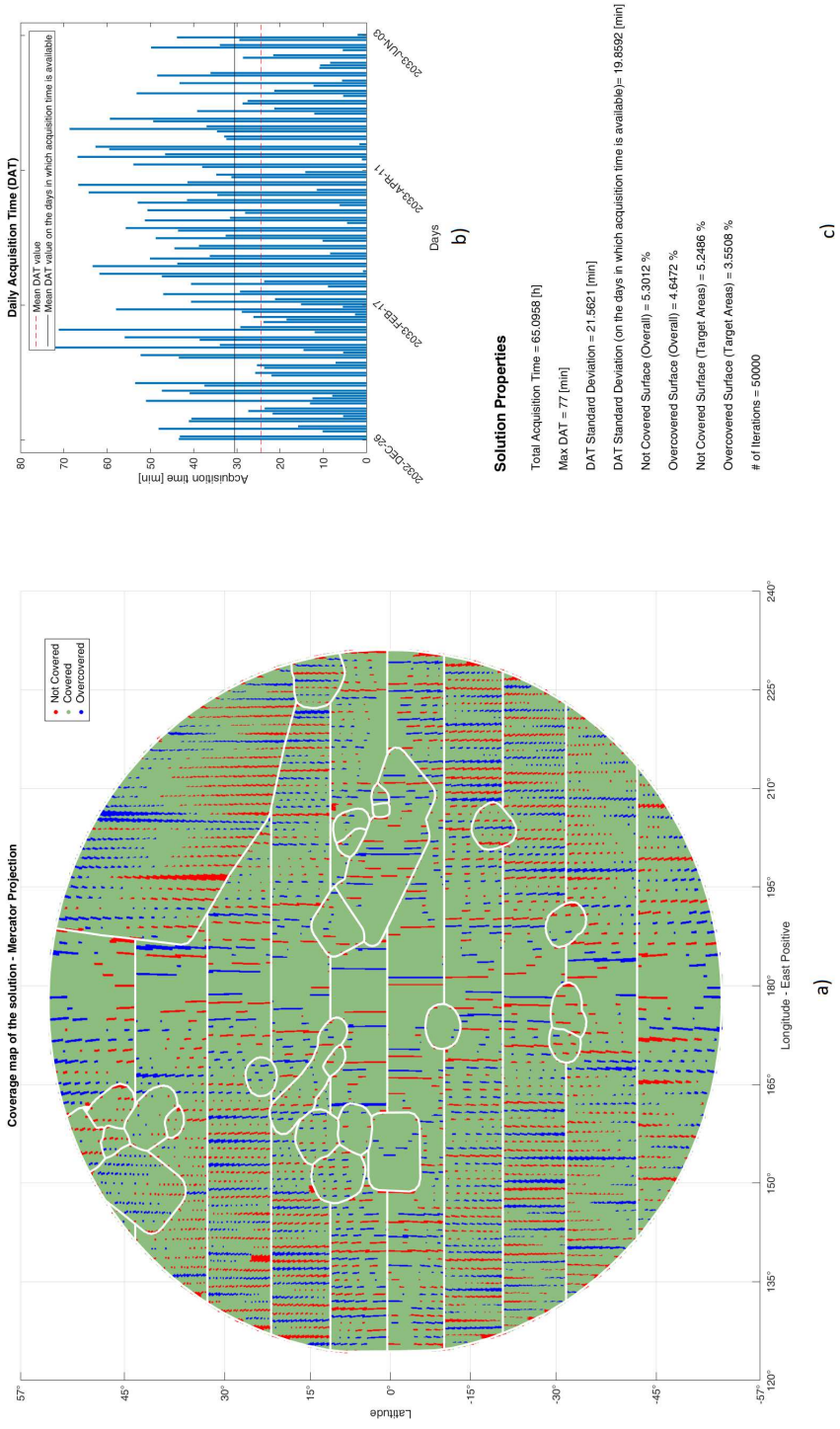

Figure 3.6: Example of a solution of the multiobjective optimization achieved implementing the proposed mutation. This solution is the best in terms of spatial uniformity of the selected acquisition segments (GCO-500 case). In green, the points that are covered by one and only one of the influence areas of the selected segments. In blue, the points that are covered more than once. In red the points that are not covered.

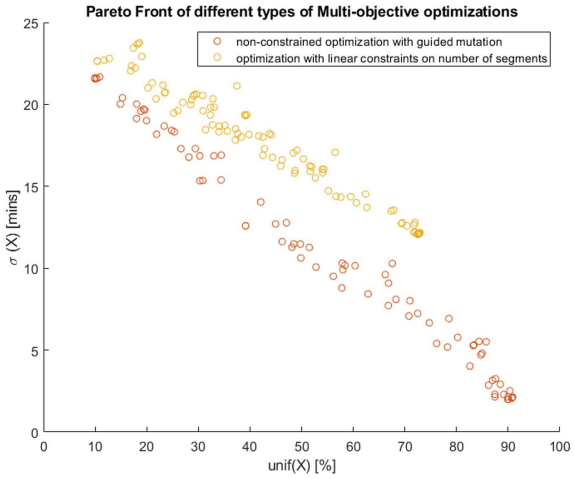

Figure 3.7: Comparison of the 2 sets of solutions obtained after the selection phase with the implementation of the constraints on the number of segments per cell (in yellow) and with the guided mutation (in red). Here one can see how the different solutions are distributed, considering the 2 most important objectives of the experiment: $unif(X)$ and $\sigma(X)$. The solutions obtained with the second method are in general better as they dominate the solutions obtained with the first method

have been obtained for what concerns the high-relevance areas. Interpreting these results in terms of spatial distribution, they mean that on more than 90% of the analyzed surface we obtained the correct distribution of the ground tracks with the required distance. On the remaining portion of the surface, the selected tracks were either slightly too far (causing lack of coverage) or too near (causing the overlap of the considered influence areas and therefore overcoverage) from each other. Moreover, it is possible to see from Figs. 3.5a) and 3.6a) that these conditions are not concentrated in a particular region, but they associated with very small regions, distributed on the investigated area. This emphasizes the fact that the obtained results involve only a small irregularity in the spatial distribution of the selected segments, which is mostly due to the slight difference in the inclination of the available acquisition tracks.
The analysis of the daily acquisition time profiles for the 2 considered solutions also shows that the modified mutation was able to distribute the acquisition time more evenly, but both the analyzed solutions have obtained good and very similar values in terms of daily acquisition time standard deviation. These results should be interpreted considering the different daily constraints on the acquisition time in the time frame we are analyzing, which depends on the satellite orbit characteristics.

Examples of Pareto fronts (i.e., the non dominated solutions of the multi-objective op-

timization) obtained with the two different optimization set-ups are reported in Fig.3.7. These show the obtained solutions in terms of two of the considered objectives, i.e., $unif(\mathbf{x})$ and $\sigma(\mathbf{x})$. Part of these solutions do not show satisfactory results for the analyzed test case. In particular, this is the case of the ones on the right side of the 2 fronts. Nonetheless, the 2 sets of obtained solutions demonstrate that using a multi-objective technique, we can find a good number of candidate acquisition schedules related to multiple different optimal tradeoffs between the specified quality metrics describing the whole acquisition campaign. Moreover, the representation of the two Pareto fronts shows that the one obtained with the proposed guided mutation method is better than the one resulting from the configuration in which we explicitly implemented the constraints on the number of acquisition segments to be selected for each macrocell. Indeed all the solutions of the first front dominate the ones of the second front. This shows the efficiency of the proposed mutation operator for the exploration of the solution space and its potentiality in finding very good solutions for a large-dimensional problem.

3.4 Conclusions

In this chapter we have presented an approach to the automation of the planning and scheduling process for planetary exploration missions. In particular, we have considered the study of the acquisition operations of a single instrument included in the scientific payload of a mission. We have defined and presented an approach based on 2 main steps: the segmentation and the selection, showing its application to the particular case of radar sounder observations.

For the segmentation phase we defined a way to subdivide the long available acquisition time intervals into shorter segments based on a spatial criterion that allows the ground tracks not to be split over high-relevance targets. The resulting schedules are then produced in the selection phase, in which an optimized subset of the previously defined acquisition segment set is derived by using metrics that express the quality of the related acquisition schedule. For the selection phase, we considered two different configurations that use NSGAII-based multi-objective optimization techniques. The first configuration exploits the mission-specific and user defined constraints to limit the otherwise very large search space. The second configuration, instead, implements a modified mutation operator, which performs a local search to more efficiently guide the exploration of the solution space towards high-quality solutions. We analyzed the proposed approach by considering its application to the real study case of the planetary radar sounder RIME on the JUICE mission.

The obtained experimental results are very promising and show the potentialities of the

proposed approach. From the achieved results we can conclude that both configurations can produce high quality solutions. With the first configuration, in fact, it was possible to efficiently limit the search space, avoiding non-satisfactory solutions. With the second one, instead, we could reach a set of solutions that dominates the one obtained with the first configuration, and therefore represents a collection of better tradeoffs of the considered objectives. This was obtained considering the same number of iterations and almost the same computational time. The results also show the importance of using a multi-objective technique, when multiple conflicting objectives are analyzed. Thus, the presented approach represents a good tool to produce optimized schedules for each instrument composing the scientific payload of a planetary exploration mission. Results like the ones presented allow us to further study and apply this approach also in the multi-instrument planning scenario. Of course some modifications are required in order to properly take into account a given number of instruments simultaneously. As shown in Chapter 4 though, many of the concepts and methods developed and shown in this chapter can be easily adapted for the simultaneous acquisition scheduling of multiple science payload instruments with just slight changes in their definition or in their specific application.

Chapter 4

A Novel Method based on Nested Optimization for the Simultaneous Scheduling of Multiple Instruments Acquisitions in Planetary Exploration Missions

This Chapter presents a novel method for the simultaneous scheduling of the observations to be performed by multiple instruments in a Planetary Exploration mission. The scheduling problem is here modeled as a nested/bilevel optimization problem. At the lower level the optimized observation schedule for each sensor is individually produced and evaluated, following the structure described in Chapter 3 and trying to maximize ad-hoc observation quality metrics. At the upper level the harmonization of the individual sensor schedules takes place, considering all the mission- and resource-related constraints and guiding the lower level instances toward a unique, feasible schedule. The final acquisition plan is produced by using Particle Swarm Optimization (PSO) at the upper level, trying to maximize a metric representing the overall quality for the mission over the specified time horizon. The approach is demonstrated on the operations of a set of instruments onboard JUpiter ICy moons Explorer (JUICE). The obtained results show the potential of the proposed methodology.

4.1 Introduction

In the previous chapters we have emphasized the importance of planetary remote sensing. Indeed, thanks to the different remote sensing instruments that usually compose the science payload, PE missions are able to analyze different important characteristics of the considered celestial body, e.g., the composition of the atmosphere, the surface properties and the structure of the subsurface. This diversity in the mission objectives and in the capabilities and limitations of the on-board sensors underlines the importance and the complexity of managing each experiment. As observed in Chapter 3, this complexity deeply affects the handling of the strategies and plans for the data acquisition by each instrument. Thus, the definition of the observation schedules of these sensors should consider a variety of constraints, requirements and objectives, at different levels. Limitations and objectives related specifically to the single instruments can include conditions caused by specific environmental features, which impede the observations (as for example in the case of the operations of RIME, illustrated in Chapter 3), as well as the requirements on the way acquisitions should be performed in order to achieve the specific science goals. Similar indications are also defined regarding the mission in general, from the high-level science objective to the limitations imposed for example by the availability of resources such as energy, memory and acquisition time. Moreover, in the previous chapters we have underlined the importance of the management of the resources on board the spacecraft and how their limited availability also can considerably contribute in limiting the total acquisition opportunities for each instrument. Therefore, given these limitations, the observation opportunities that can be effectively exploited by each sensor are significantly bounded and considerable effort should be made in order to make it possible for each instrument to meet its associated requirements without penalizing the acquisitions by other sensors. Consequently, as observed in the previous Chapters, one of the most critical phases of the mission design is the analysis, the planning and the scheduling of the operations of the science payload. The planning and scheduling task must take into account all the constraints and the requirements discussed above to generate a feasible general acquisition plan over the considered time horizon, which allows each instrument to achieve their objectives and does not violate any general or instrument related constraint. The choice of the observation opportunities to exploit for each sensor on board the mission has to be based on a set of specific measures representing the quality of the data collection operations performed in each specific time window and over the whole considered time frame. As mentioned in Chapter 1 the planning and scheduling procedure for Planetary Exploration missions is a long iterative and complex process. At each iteration the level of detail of the planning is increased thanks to the inputs provided by the

teams developing each instrument to a mission planning team. This long process requires a high percentage of human involvement, even if some methodologies (described in detail in Chapter 1) are available to support the observation schedule generation. However, these methodologies have limited capabilities with respect to the automatic generation of observation schedules. Automatic methods for the planning and scheduling process have been extensively studied in the context of Earth Observation missions. However these missions, as shown in Chapter 1, differ considerably from PE missions in terms of type and entity of constraints and dimension of the problem.

In this chapter we present an approach to the simultaneous automatic observation planning and scheduling for multiple sensors, based on a hybrid nested *bilevel* optimization structure, to be used in complex planetary missions. The goal of the proposed approach is twofold: **a)** to provide a framework being able to consider the acquisition operations of more than one sensor simultaneously, and **b)** to automatize and speed up the usually time-consuming observation scheduling process for planetary missions. This objective is pursued by generating nearly-optimal schedules for each instrument, which are then combined in a total acquisition plan considering the characteristics and limitations of each examined instrument and the mission features and constraints. The proposed technique consists of two main stages, i.e. the segmentation and the schedule optimization and harmonization stages, during which all feasible acquisition intervals (with respect to the considered instruments capabilities) are determined, analyzed and evaluated to generate the observation sequence for the examined sensors over the input time horizon. The segmentation splits the input time horizon into well-defined shorter acquisition intervals, following a time-based or a target-based criterion (namely, the start- and end-time of the interval are determined as the window in which the whole considered target is visible). In the schedule optimization and harmonization phase, a hybrid GA-PSO nested optimization engine is employed to complete 2 tasks. At the lower level a GA-based optimizer explores the space of the solutions related to the combinations of the acquisition segments associated to each instrument to find the observation schedule with the best possible instrument-specific quality metric value and science requirement compliance. At the upper level, instead, the schedules produced for each instrument are combined in a single global acquisition schedule and evaluated. Here a PSO-based engine has the objective of iteratively guiding the search performed at the lower level assigning weights to the acquisition segments associated to each sensor, to avoid any possible violation of mission-related constraints and thus enhance the global schedule acquisition quality. Thus, the output of this technique is a unique acquisition plan over the considered time horizon, which is optimized with respect to the combination of all instrument-specific quality metrics and is ensured to be feasible with respect to any local (instrument-related) or global (usu-

ally resource-related) constraint. To study and validate our approach, we analyzed the real case of the operations planning and scheduling for the JUpiter Icy Moons Explorer (JUICE) mission of the European Space Agency (ESA), which is focused on the analysis of the Jovian System and of Jupiter's Icy Moons. In detail, we focused our attention on the observations of 4 sensors composing the science payload of this mission:

- the radar sounder **RIME** (Radar for Icy Moons Exploration);
- the laser altimeter **GALA** (GAnymede Laser Altimeter);
- the visible camera **JANUS** (Jovis, Amorum ac Natorum Undique Scrutator);
- the visible and near infrared imaging spectrometer **MAJIS** (Moons And Jupiter Imaging Spectrometer);

This chapter is structured as follows. Section 4.2 illustrates the proposed methodology with particular attention to the modeling of the P&S problem as a bilevel optimization problem. Section 4.3 presents the application of the proposed methodology to the 4 instruments of the JUICE mission, the experimental setup, the specific choices in terms of constraints and objective functions and the obtained results. Finally, Section 3.4 draws the conclusions of this chapter.

4.2 Proposed Methodology

The methodology that we propose to automate the simultaneous planning and scheduling process for multiple sensors is an extension of the one presented in Chapter 3. A schematization of it is shown in Figure 4.1. Also this method includes the **segmentation** phase, which is performed for each considered sensor. It takes as input the sets $\Phi_{f,j} \subset \Phi$ with $j = 1, ..., I$ where I is the total number of considered instruments. The sets $\Phi_{f,j}$ include all the time intervals $\phi_i^{f,j} \in \Phi_{f,j}$ in which the data acquisition with the j-th instrument is feasible. The segmentation phase then splits them into shorter segments, following a user-defined criterion that can be different for each sensor, and like for the previously described approach it extracts a series of meaningful metrics characterizing each of the acquisition segments. The significant difference with respect to the proposed single-instrument P&S system lies in how the final schedules are constructed. This is the task of the **schedule optimization and harmonization** block, as depicted in Figure 4.1. Here, the segment-related data are still exploited to define the indicators representing the acquisition quality for each instrument. The actual segment selection for each instrument, though, is not only based and optimized with respect to its own quality measures. It is rather adapted to the characteristics of other instruments' schedules, in an effort

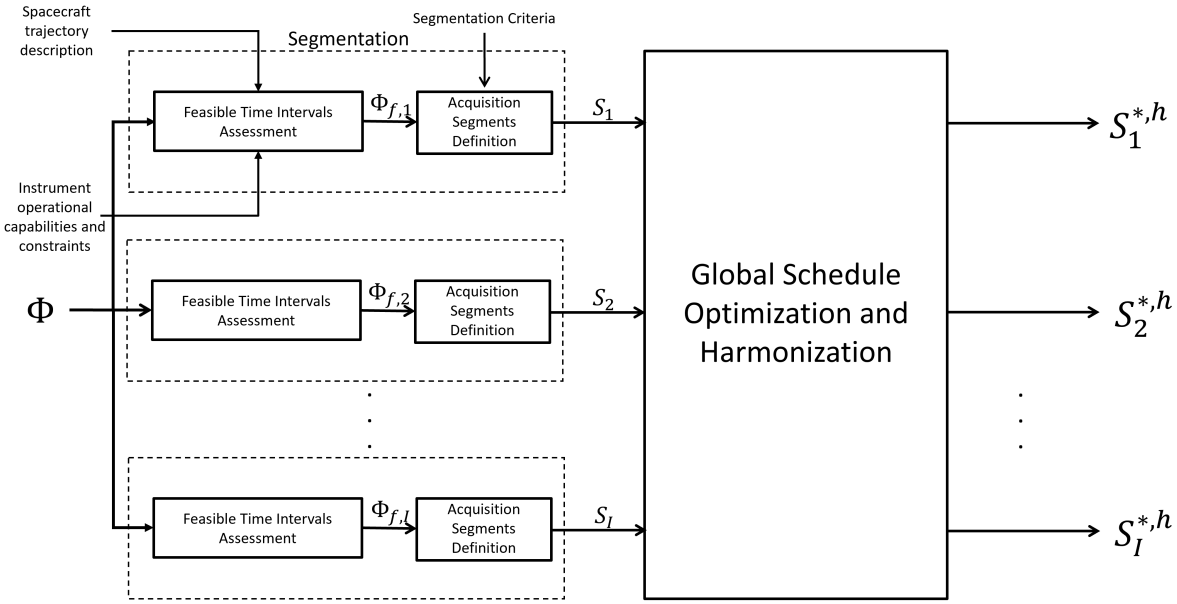

Figure 4.1: Blockscheme for the proposed multi-instrument planning and scheduling methodology. Φ represents the total time horizon over which the planning and scheduling task should be completed (i.e., a particular phase of the considered mission). $\Phi_{f,j} \subset \Phi$ is the set of time intervals $\phi_i^{f,j} \in \Phi_{f,j}$ in which the data acquisition with the j-th instrument is feasible. S_j is the result of the subdivision of $\Phi_{f,j}$ in shorter time segments $s_i^j \in S_j$ which are easier to handle and analyze. Finally, $S_j^{*,h} \subset S_j$ represents a subset of S_j, which is optimal with respect to the instrument specific quality metrics and most importantly harmonized with the optimal subsets related to all other considered sensors. The union of all these subsets constitutes an optimal global acquisition schedule, feasible with respect to all mission constraints.

to obtain the best possible acquisition schedules for each sensor, in terms of quality and requirement compliance, which combined in a global observation plan do not violate any mission-related constraint.

4.2.1 Segmentation

As in the proposed single-instrument P&S methodology presented in Chapter 3, the segmentation plays a fundamental role, as it allows to univocally define and characterize all the available acquisition opportunities for any given sensor. For each of the examined sensors it works exactly in the same way as it was presented in Chapter 3 (Section 3.2.1), but for sake of completeness in the definition of the total methodology, here we provide its synthesized description. This phase starts by considering the total time horizon Φ, over which we want to schedule the acquisitions by the analyzed instruments. The system

also needs the information regarding the trajectory that the considered spacecraft will travel during the specified time horizon and thus its position in time with respect to the celestial body to explore. As previously reported, this information is usually defined via specific files (kernels) with a standard format indicating the state vector (position and speed) of the satellite at any instant. As we anticipated, these files can be handled thanks to specific function libraries. These interfaces allow to identify time intervals in which particular conditions in the operating environment that make observations not feasible are verified and filter them out. This process produces, for each considered instrument, the set $\Phi_{f,j}$ of time intervals in which the observations by the j-th instrument ($j = 1, 2, ..., I$, where I is the total number of considered sensors) are feasible.
We now need to determine the observable portion of the analyzed celestial body for each interval $\phi_i^{f,j} \in \Phi_{f,j}$ associated to the j-th sensor. As we showed for the case of RIME in the previous Chapter, this is possible by simply projecting the field of view of the considered sensor or the position of the spacecraft on the surface of the target body along the sensor's pointing direction, depending on the instrument characteristics. After that, the usually long time intervals $\phi_i^{f,j}$ and the related ground tracks are subdivided into shorter acquisition segments $s_{i,j}$ for the j-th instrument, which represent time intervals in which an uninterrupted data acquisition can take place. The criteria for the subdivision can be temporal, in order to obtain acquisitions with uniform duration, or spatial, in order to take into account specific target regions. The spatial segmentation can be performed for each instrument since we have determined for each available time interval the portion of the celestial body that the instrument can observe. It is executed by using a particular mapping of the analyzed celestial body surface that we call a *segmentation grid*. Each cell of this grid represents a particular region of the surface and the previously defined long ground tracks are split at the edges of them. Thus, the start- and end-time of each acquisition segment associated to a given instrument are defined as the instants in which the portion of the surface observable by the examined sensor crosses the border of a cell. Thus, the segmentation stage produces for each instrument a set of acquisition segments $S_j = \{s_{1,j}, s_{2,j}, ...s_{N_j,j}\}$, where N_j is the total number of resulting segments for the j-th sensor. The definition of a segment is completed by a set of descriptive metrics. Among them the most general and important for the generation of observation are the following (as specified in Chapter 3):

- $st(s_{i,j})$ and $et(s_{i,j})$: the start and the end time of the acquisition defined by segment $s_{i,j}$;
- $time(s_{i,j}) = et(s_{i,j}) - st(s_{i,j})$: the temporal duration of the acquisition segment $s_{i,j}$;
- $a(s_i)$: the portion of surface covered by segment $s_{i,j}$, obtained by merging the pro-

jection of the j-th instrument field of view on the surface in correspondence of the spatial coordinates covered between the instants $st(s_{i,j})$ and $et(s_{i,j})$;

- $e(s_{i,j})$ and $m(s_{i,j})$: the energy and the memory consumption associated to the acquisition operation of segment $s_{i,j}$ by the j-th sensor, respectively. They are determined based on the j-th instrument energy and memory consumption rates.

Additional measures, if needed, could then be specifically extracted for the considered instrument, to further characterize the quality of the observation defined by segment $s_{i,j}$.

4.2.2 Global Schedule Optimization and Harmonization

All the sets of acquisition segments S_j, with $j = 1, 2, ..., I$, are fed to the schedule optimization and harmonization block, as shown in Figure 4.1. The purpose of this block is that of actually generating the observation schedules with the best possible global observation quality and harmonize these acquisition plans, so that the combination of them in the total observation schedule is feasible with respect to any mission-related constraint. This task is broken down into its 2 main processes and goals, namely, the management and the optimization of the observations at the **instrument level** (lower level) and at the **global level** (upper level). However, the 2 levels are strictly interconnected and they both work iteratively, with each level refining its results in time based on the outputs of the other. More in detail, at the instrument level a full acquisition schedule for each considered instrument is produced for each iteration of the global level task. During each iteration of the global level, the combination of the schedules produced at the instrument level is evaluated and a set of metrics is generated in order to guide the task at the instrument level at the next generation.

As briefly anticipated, one of the objectives pursued at the global level is that of providing a guidance to the optimized segment selection processes of the instrument level. This guidance is coded in the $\mathbf{w}_j$ variables, which represent a set of weights $w_{i,j}$ that have to be assigned to each segment $s_{i,j}$ (or to specific groups of segments) associated to the j-th sensor. Their purpose is that of modifying the search space of the instrument level optimized segment selection instances, by facilitating the selection of some acquisition segments and penalizing that of other acquisition segments. The value of the weights $w_{i,j}$ ($w_{i,j} \in [0; 1]$) to be assigned to the acquisition segments has to be decided with the objectives of: i) avoiding any mission-related constraint violation and ii) optimizing the global quality of the total acquisition schedule, obtained as a combination of the individual instrument observation plans.
The purpose of the instrument level, instead, is that of producing observation schedules

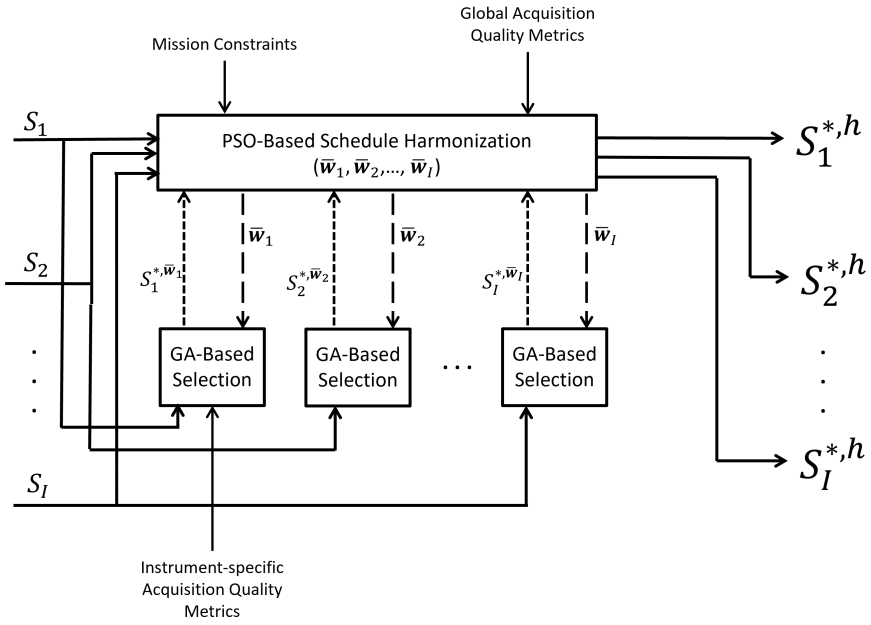

Figure 4.2: Detailed scheme of the Global Schedule Optimization and Harmonization stage of the proposed approach. This stage is modeled as a bilevel optimization instance, where the upper block (the schedule harmonization) represents the upper level of the problem, while the selection blocks in the lower part express the schedule generation processes for each instrument and constitute the lower level of the P&S problem.

for each instrument individually, based on the metrics expressing the quality of the acquisition for the considered instrument, opportunely modified to include the information coded in the weights $\mathbf{w}_j$ coming from the global level. Thus the procedure of the instrument level is very similar to the selection phase of the method described in Chapter 3 (Section 3.2.2). Again, it is possible to express a candidate schedule for the j-th instrument as a binary vector $\mathbf{x}_j$ ($\mathbf{x}_j = \{x_{1,j}, x_{2,j}, ..., x_{N_j,j}\}$), with N_j being the total number of acquisition segments determined for the j-th instrument. Every position i identifies one of the acquisition segments $s_{i,j}$ determined for the j-th instrument, and the value $x_{i,j}$ ($x_{i,j} \in \{0, 1\}$) expresses if the acquisition defined by segment $s_{i,j}$ is inserted in the schedule (1) or not (0). As illustrated in Figure 4.2, the objective at the instrument level is that of selecting the subset $S_j^{*,\mathbf{w}_j}$ of segments that achieves the best possible value of the instrument-specific acquisition quality metric, which can be defined based on the segment metrics. This selection is performed given the guidance provided by the global level block, which is coded in the $\mathbf{w}_j$ variable. At this level the model of the problem for each instrument slightly differs from the one we used in the previous chapter, even if it is still a hard combinatorial problem. This is due to the fact that mission-related

constraints are not explicitly expressed at the instrument level, even if they are implicitly considered anyway thanks to the $\mathbf{w}_j$ variables. However, it can still be modeled as a Multi-dimensional Knapsack Problem (MKP), so that further constraints related to the instrument characteristics, which cannot be solved with the first filtering performed at the segmentation stage, can still be implemented to limit the search at the instrument level. In this case we employ a single-objective optimization strategy. In Chapter 3 we have underlined the benefits of using a multi-objective optimization approach when dealing with the observations by a single instrument. One of them is it can provide a wide set of observation schedules representing optimal trade-offs of the considered objective measures, among which a decision maker can choose. In this approach, though, only one optimal solution for each instrument is required to be used as input to the global level block. The main reason is that here multiple instruments are considered simultaneously and individual schedules can therefore be automatically adapted with respect to those associated to other instruments.

The two levels implicitly share the same variables. Indeed, at the instrument level the weights $w_{i,j}$ produced at the global level directly influence the segment selection task for each sensor. At the global level, instead, the choice of the weights values strictly depends on the joint evaluation of the optimal schedules based on the sets $S_j^{*,\mathbf{w}_j}$ for each sensor, obtained with the segment selection process at the instrument level. This complex structure can therefore be modeled as a particular **bilevel optimization** problem, since the goals and the procedures of the two levels described above cannot be simply tackled individually, but they are clearly deeply dependent and entangled with each other and they have a hierarchical relationship.
Bilevel optimization problems [74] are characterized by two levels of optimization processes related by an intrinsic hierarchy, such that one level can be nested within the other. The outer optimization problem is often referred to as the upper level and the inner one as the lower level. At the same way, as anticipated, we can consider the global level as the upper level of our bilevel problem and the instrument level as the lower level. Following the general expression of a bilevel optimization problem, let us formalize the Global Schedule Optimization and Harmonization task as follows:

$$\max_{\mathbf{x}_1,...,\mathbf{x}_I,\mathbf{w}_1,...,\mathbf{w}_I} \{F(\mathbf{x}_1,...,\mathbf{x}_I,\mathbf{w}_1,...,\mathbf{w}_I)\}; \tag{4.1}$$

$$\text{with } F(\mathbf{x}_1,...,\mathbf{x}_I,\mathbf{w}_1,...,\mathbf{w}_I) = \frac{1}{I}\sum_{j=1}^{I} f_j(\mathbf{x}_j,\mathbf{w}_j), \text{ given } w_{i,j} = 1 \ \forall i = 1,...,N_j, \forall j = 1,2,...,I; \tag{4.2}$$

$$\text{subject to } \mathbf{x}_j \in \underset{\mathbf{x}_j}{\text{argmax}}\{f_j(\mathbf{x}_j, \mathbf{w}_j) : \sum_{i=1}^{N_j} c_{h,i,j} x_{i,j} \leq b_{h,j}, h = 1, ..., H\}, \forall j = 1, 2, ..., I; \tag{4.3}$$

$$\text{with } f_j(\mathbf{x}_j, \mathbf{w}_j) = \sum_{i=1}^{N_j} q_{i,j} w_{i,j} x_{i,j}; \tag{4.4}$$

$$\sum_{j=1}^{I} \sum_{i=1}^{N_j} g_{k,i,j} x_{i,j} \leq b_k \text{ with } k = 1, ..., K, j = 1, 2, ..., I; \tag{4.5}$$

$$x_{i,j} \in \{0, 1\}, w_{i,j} \in [0, 1]. \tag{4.6}$$

where $\mathbf{x}_j = \{x_{1,j}, x_{2,j}, ..., x_{N_j,j}\}$ and $\mathbf{w}_j = \{w_{1,j}, w_{2,j}, ..., w_{N_j,j}\}$ represent vectors of the decision variables described before and here they are the variables vectors associated the lower level (instrument) problem and to the upper level (global), respectively, with N_j being the total number of acquisition segments associated to the j-th instrument. Moreover, $F(\mathbf{x}_1, ..., \mathbf{x}_I, \mathbf{w}_1, ..., \mathbf{w}_I)$ represents the objective function for the upper level, which is the overall acquisition quality function for the combination of all the schedules associated to each instrument j. Here we simply define it as the sum of the acquisition quality metrics for each instrument. Indeed, it's quite easy to determine the global quality of the acquisitions, given the individual success of the observations by each sensor. Moreover, the expression of the upper level objective function with all the weights $w_{i,j} = 1$ means that they are not explicitly used in the computation of the function. However, as we stated earlier, they are needed in order to refine the choice of the variables $\mathbf{x}_1, ..., \mathbf{x}_I$. The functions $f_j(\mathbf{x}_j, \mathbf{w}_j)$ are the objective functions for the lower level instead and they can be generally expressed exactly as they were in Chapter 3 (Equation 3.2) adding the dependency from the weights $w_{i,j}$, with $q_{i,j}$ being a generic quality metric associated to the segment $s_{i,j}$. The constraints for the upper level and for the lower level are expressed again in the same way as we did in Chapter 3 (Equation 3.3). The constraints for the upper level (Eq.4.5) are denoted by the cost coefficients $g_{k,i,j}$ (associated to segment $s_{i,j}$ and to the k-th constraint) and by the bound value b_k associated to the k-th constraint, with K being the total number of upper level constraints. Similarly, the constraints for the lower level (Eq.4.3) are denoted by the cost coefficients $c_{h,i,j}$ (associated to segment $s_{i,j}$ and to the h-th constraint for instrument j) and by the bound value $b_{h,j}$ associated to the h-th constraint for sensor j, with H being the total number of lower level constraints. The hierarchical relationship between the two levels is explicitly expressed: the lower level optimization process is represented as a further constraint to the upper level so as to limit the upper level problem to only consider variables $\mathbf{x}_j$ that are optimized with respect to the lower level requirements and to the assigned weights. These vectors represent optimized observation schedules for the j-th instrument, in other words they

express optimized subsets of the set S_j of the acquisition segments. Therefore they can be expressed as $S_j^{*,\mathbf{w}_j}$, as depicted in Figure 4.2.

Regarding the objective function considered at the upper (global) level, with a formulation such as the one provided in Eq. 4.2 it would be very straightforward to indicate a priority value, so that the observations by a given sensor could be facilitated with respect to the ones of other instruments. However, a more important aspect to take into account for the upper level is the management of the mission constraints (expressed in Eq.4.5), such as the ones related to the resources exploitation. In Chapter 3 we have mentioned how constraint compliance can be checked. Indeed again we can easily associate each coefficient $g_{k,i,j}$ to one of the metrics that have been extracted for each acquisition segment $s_{i,j}$ (e.g., $e(s_{i,j})$ or $e(s_{i,j})$). The coefficients b_k can instead be associated to the upper bounds of the resource consumption over a specified time window, for example. In Chapter 3 the example of the constraint on the maximum data volume generated between 2 consecutive downlink windows was presented. At the same way, we could define a constraint for the energy consumption by the acquisitions included in the total observation schedule over a given amount of time (e.g., one day ore one week) as follows:

$$\sum_{j=1}^{I}\sum_{i=1}^{N_j} e(s_{i,j})x_{i,j} \leq En, j = 1, 2, ..., I; \tag{4.7}$$

where En (specified a priori and dependent on the characteristics of the satellite power supply unit) is the maximum available energy over the specified time interval. Once these constraints, especially those related to energy and memory, have been checked, it's important to decide how to handle a possible constraint violation. As anticipated in Chapter 1, the technique described in [38] employs a penalty factor applied to the considered objective function, which not only expresses if any constraint is violated, but also how severe the violation is. The use of a penalty factor in the calculation of the objective function is indeed an efficient way to handle particularly complex constraints, which are not straightforward to be checked (i.e., they are not linearly related to the single design variables, but to the particular combination of them). This approach is followed also in the proposed methodology and implemented as follows.
We here consider the penalty factor as made of 3 components, related to 3 types of constraints, namely those related to available energy, available memory and inter-instrument acquisition conflicts (i.e., if the acquisition performed by a given instrument makes it impossible for another sensor to acquire data at the same time). For the first type of constraint we can determine the energy penalty factor pen_e as the total time in which the energy constraint is violated. Regarding the memory, we determine the memory penalty

factor pen_m simply considering by how far the memory constraint is exceeded. Finally, for the inter-instrumental conflicts we again determine the inter-instrumental penalty factor pen_i as the total time in which the 2 or more instruments are scheduled to acquire data simultaneously. Thus we can formalize the total penalty factor as $pen = pen_e + pen_m + pen_i$ and accordingly modify the upper level objective function as follows:

$$F(\mathbf{x}_1, ..., \mathbf{x}_I, \mathbf{w}_1, ..., \mathbf{w}_I) = \frac{1}{I} \frac{\sum_{j=1}^{I} f_j(\mathbf{x}_j, \mathbf{w}_j)}{1 + pen(\mathbf{x}_1, ..., \mathbf{x}_I, \mathbf{w}_1, ..., \mathbf{w}_I)}, \tag{4.8}$$

$$\text{with } w_{i,j} = 1 \ \forall i = 1, ..., N_j, \forall j = 1, 2, ..., I; \tag{4.9}$$

With such a formulation, any solution exceeding any type of constraint is strongly penalized, so that the search is efficiently guided towards solutions that comply with all considered constraints.

Bilevel optimization models have been studied especially considering mathematical optimization techniques and associated to problems with particular properties such as continuity and linearity, which our problem does not possess. These conditions may lead to quite easily approximate the problem to a single-level optimization problem, which can then be tackled with the appropriate approaches. For a problem such as the one here described, a possible way to follow is to use a nested methodology, because of its effectiveness, using stochastic optimization techniques at both levels, given the large dimension of both problems. Thus, as we anticipated, at each iteration of the upper level (global) optimization process producing the weights $\mathbf{w}_j$ associated to each instrument, the lower level (instrument) optimization problems should be solved for the given set of weights.

Given the characteristics of the variables $w_{i,j}$ we need to manage at the upper level (which are in general continuous values, even if their discretization could be easily considered), a suitable choice is to use a technique based on Particle Swarm (PSO) [27]. This population-based algorithm is particularly efficient for problems with continuous-valued variables, because of the way the search space is explored. Indeed each member (particle) of the population (called *swarm*) has an associated position (the solution vector, where each value identifies the value of the associated coordinate describing the solution space) and velocity. The velocity determines the position in which the particle will find itself at the successive iteration and therefore the next evaluated candidate solution (in our case, the sets of weights $\mathbf{w}_j$). Moreover, each particle has a "memory", meaning that it remembers the position (candidate solution) with the best value of the considered objective function, both among the ones the particle itself visited (personal best) and among the ones visited by the whole swarm (global best). The velocity at each iteration is thus influenced by the personal and the global best according to two parameters (acceleration

coefficients), which determine if more relevance is given to the global or the personal best for the considered particle in identifying the direction towards which the particle should move. A further parameter (called inertia) is employed to avoid a premature convergence of the algorithm, which terminates after a specified maximum number of iterations or if no significant improvement to the considered objective function can be provided by the positions evaluated in a given number of iterations.
In the upper level optimization problem we should ideally evaluate a single weight for each acquisition segment associated to each considered sensor. This would significantly complicate the problem, having to manage a very large number of continuous valued variables, namely $N = \sum_{j=1}^{I} N_j$. For this reason, taking into account the characteristics of the problem at hand, a possible solution to reduce the dimensionality of the problem is to generate and evaluate, for each sensor, one weight value for a given group of segments. The grouping of the segments could be based on time, for example we can have one weight value associated to all the acquisition segments associated to one instrument taking place in a given day or in a given week. This grouping reduces the flexibility of the system in managing the acquisitions, but it also helps reducing the granularity and the complexity of the problem.

Given the good results obtained by the proposed single-instrument planning methodology presented in the previous chapter, a suitable option to tackle the lower level optimization problem for each of the I considered sensors is to use a method exploiting Genetic Algorithms (GAs). We have underlined how the representation of the observation schedules for each sensor problem in form of a binary vector ($\mathbf{x}_j$) is very useful and naturally exploitable as a *chromosome*, the basic structure of GA, which is used to encode the different solutions. Moreover, we have highlighted the capability of GAs of efficently exploring the solution space. This is made possible by the genetic operators, crossover and mutation. Their strength is to generate solutions at each iteration of the genetic optimization process, by creating combinations of existent candidate solutions or by slightly modifying the value of some of the variables contained in them. Considering a binary solution vector like $\mathbf{x}_j$, the mutation randomly selects a number of variables of the vector and inverts their value, from 1 to 0 or from 0 to 1 accordingly. Given the meaning of $\mathbf{x}_j$, this modification results in either removing an acquisition segment, associated to the modified $x_{i,j}$ variable, from the original observation schedule for the j-th sensor, or in adding a segment to it, respectively. The purpose of the crossover is instead to recombine the variables of two solution vectors, so that the offsprings created by this operator contain part of the chromosome coming from one of the solution, while the other is "inherited" by the second input solution. Considering a simple one-point crossover,

specifying the crossover point, the two original solution vectors are split in 2 parts in the specified point, so that the first offspring vector is composed by the first part of the first original solution vector and the second part of the second input solution vector, viceversa for the second offspring. Also in this case, in order to aid the solution search performed by the GA optimization engine, we modify the standard definition of the mutation. This is done so that the probability of changing a given variable (adding or removing a segment in the analyzed schedule) is not uniformly distributed over all variables, but it's rather dependent on the knowledge of the problem and of the metrics extracted during the segmentation stage for each segment $s_{i,j}$. This strategy, combined with the weights $w_{i,j}$ specified at the upper level, is able to guide the solution search towards good quality solutions in a more efficient way. We remind that the segment selection using the described single-objective GA-based method should be executed for each iteration of the upper level optimization process. Thus, even if the nested optimization approach here described could be considered efficient in producing high-quality and feasible schedules with respect to all considered constraints, it still requires a huge amount of computational resources and time. A suitable way to dramatically reduce the required computational

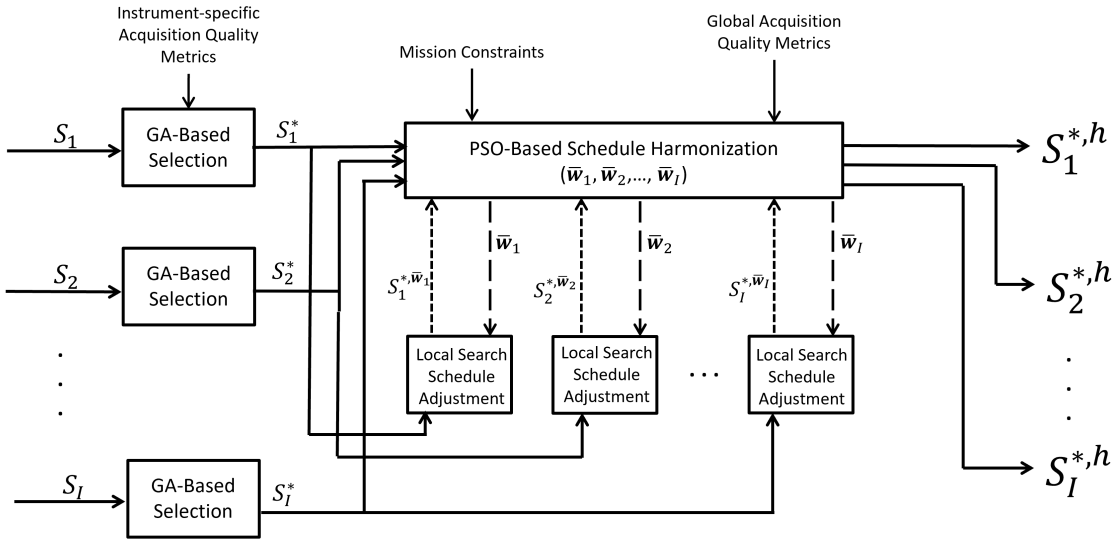

Figure 4.3: Scheme of the simplified version of the Global Schedule Optimization and Harmonization stage. Here, a local search operator applied to the previously obtained optimal schedules for each instrument substitutes the lower level GA-based optimization, which would otherwise need to be entirely executed at each iteration and for each member of the population of the upper level optimization process. This helps dramatically reducing the required computational time.

time is to modify the methodology used for the lower level. Namely, as shown in Figure 4.3, instead of performing an entire GA-based optimization process at each iteration and for each population member of the upper level optimization, it can be run just once for each instrument. This first segment selection for each sensor takes place without using the weights, so that the outcomes S_j^* ideally represent the best observation schedule given just the instrument-specific acquisition quality metrics. We suppose that in a neighbourhood of these optimal schedules (always represented as binary vectors), the instrument-specific quality measure value does not vary significantly. The neighbourhood of an observation schedule can be determined by performing the addition, the removal or the substitution of a small number of segments. Indeed, since for each instrument we deal with a very large number of acquisition opportunities, very long scheduling horizons and usually with very large areas to be observed and covered, changes on a reduced number of segments (which are brief observation intervals) with respect to a given observation schedule for a given instrument just slightly change the total quality of the resulting acquisition schedule. Thus, the optimal schedules S_j^* are then used, at the lower level, as a starting point for a local search technique influenced by the weights produced at the upper level, which instead still works at the same way. We therefore considerably reduce the search space for each of the instrument-level scheduling instances.

More in detail, for each iteration of the global level optimization and for each of its population members, which represent the sets of values of the weights $\mathbf{w}_j$ for all the I considered science payload instruments, all the optimal schedules are modified according to the weights using a local-search-based operator that works similarly to the modified mutation operator described in Chapter 3 (that, as already mentioned, is also inspired by local search techniques). The local-search schedule adjustment (as referred to in Figure 4.3) is hereby illustrated.

The sets of weights $\mathbf{w}_j$ have a fundamental role in guiding the search in the neighbourhood of the initially specified optimal schedules, even more than the one they had in the modified mutation operator. With respect to the modified mutation operator of the previous Chapter, we here only consider one operation, the substitution of an acquisition segment in the considered observation schedule. Indeed, we consider the schedules identified by S_j^* to be optimized already from the point of view of the instrument-specific quality metrics, thus we need to obtain very similar performances but preferring segments that are facilitated by an associated high weight value. Following this idea, we first determine which segments to remove from S_j^*. To do this we first specify a *substitution rate* ρ_{sub}. Let us recall the definition of $S_{in,j} = \{s_{i,j} \in S_j : x_{i,j} = 1\}$, being the set of acquisition segments included in the input schedule/solution vector and of $S_{out,j} = \{s_{i,j} \in S_j : x_{i,j} = 0\}$, being the set of segments not included in the input schedule for the j-th instrument. ρ_{sub} is

simply the percentage of segments we want to replace with respect to the number of active acquisition segments (namely $\left|S_{in,j}\right|$). Once we have determined the number of segments that should be replaced, which is $sub_n = \left\lceil \rho_{sub} \left| S_{in,j} \right| \right\rceil$, using the values of the weights $w_{i,j}$ we rank all the segments $s_{i,j} \in S_{in,j}$ and identify the sub_n acquisition segments with the worst weights (forming the set $S_{sub,j} \subset S_{in,j}$). If we take as example the area $a(s_{i,j})$ covered by each acquisition segment as acquisition quality measure, we need to replace the segments $s_{k,j} \in S_{sub,j}$ with segments $s_{l,j} \in S_{out,j}$ having very similar covered area but associated to weights with high values. Thus we define the segment overlap area $a_o(s_{l,j}, s_{k,j})$ for the observations by the j-th science payload instrument as:

$$a_o(s_{l,j}, s_{k,j}) = a(s_{l,j}) \cap a(s_{k,j}) : s_{l,j} \in S_{out,j}, s_{k,j} \in S_{sub,j}. \tag{4.10}$$

We can therefore define for each $s_{l,j} \in S_{out,j}$ and for each $s_{k,j} \in S_{sub,j}$ a metric of "weighted surface maintainance" as follows:

$$wsm(s_{l,j}, s_{k,j}) = w_{l,j} a_o(s_{l,j}, s_{k,j}), \forall s_{l,j} \in S_{out,j}. \tag{4.11}$$

Thus, each segment $s_{k,j} \in S_{sub,j}$ is replaced by the acquisition segment $s_{l,j} \in S_{out,j}$ with the highest value of $wsm(s_{l,j}, s_{k,j})$.

4.3 Experimental Results

As mentioned in Section 4.1, for validating the proposed approach we considered the planning and scheduling of the acquisitions of multiple instruments analyzing a real case. We used as test case the operations of 4 among the 11 instruments composing the payload of the JUpiter ICy moons Explorer (JUICE) mission [1]. The JUICE mission's aim is the study of Jupiter and of the Jovian System, with particular attention devoted to Jupiter's Icy Moons: Ganymede, Europa and Callisto. The selected sensors for our test are the radar sounder RIME (Radar for Icy Moons Exploration)[64] [58], the laser altimeter GALA (GAnymede Laser Altimeter) [75], the visible camera JANUS (Jovis, Amorum ac Natorum Undique Scrutator) [76] and the visible and near infrared imaging spectrometer MAJIS (Moons And Jupiter Imaging Spectrometer) [77].

4.3.1 Test Case Considered: the GCO-500 phase of the JUICE mission

For our test we once again considered the GCO-500 phase of the JUICE mission under realistic conditions. During this phase the satellite will orbit around Ganymede at 500 Km altitude (the real altitude ranges from 470 to 530 Km). This part of the mission will

last 130 days.
Regarding RIME, a significant limitation to its acquisitions is the fact that Jupiter is a source of radio emissions, which can cause strong interferences during the acquisition operations, as anticipated in Chapters 2 and 3. These interferences might severely reduce the SNR of the data acquired by RIME and therefore destroy their information content. Thus, the acquisitions to be performed by RIME are deemed feasible (for the studied case) only when the JUICE spacecraft is occulted by Ganymede with respect to Jupiter. Due to the characteristics of its rotation and revolution periods, Ganymede is said to be in *tidal locking* with Jupiter. For this reason, only one side of Ganymede is effectively observable by RIME, since the moon always has the same side directed towards Jupiter. The observable area to be covered by RIME's observation is nonetheless quite extended, representing about 30% of the total surface of Ganymede. The main requirements for the data acquisitions by RIME, as pointed out in Section 3.3 are:

- To achieve uniform coverage of the surface of Ganymede in the investigated area;
- To select segments of acquisition tracks spaced among each other of about 50km.

For GALA, JANUS and MAJIS it is important to clarify that the considered requirements and constraints, which are hereby reported, are taken just as an example. Taking into account the observations to be performed by GALA, we consider its objective of covering a set of high-relevance areas, which are more distributed on the surface of Ganymede with respect to the operative area for RIME, but the cumulative area to be covered is still quite large. For these acquisitions we consider requirements that are conceptually similar to those of RIME, also because the acquisition geometry is very similar. Indeed they are nadir-pointing instruments and neither radar sounders, nor laser altimeters produce surface imaging data, but they are rather devoted to characterizing the structure of the subsurface or the local topography respectively, along the flight direction. The investigation of the considered target areas for GALA though requires a higher density of observations, namely, the ground tracks uniformly distributed but with a distance of about 5km.
The characterization of the acquisition to be performed by JANUS and MAJIS instead is easier, given the characteristics of the 2 cameras. They also need to cover the same set of target areas as GALA, considering to be nadir-pointed and performing acquisitions in pushbroom mode, with a ground-projected field of view in the across-track direction of 15 and 30 km respectively (given the 500 km altitude of the platform from the surface of Ganymede). What limits the observations for both JANUS and MAJIS is of course the solar illumination of the observable area in the time intervals in which acquisitions should take place. Observations are thus deemed feasible for the 2 cameras when the Sun is at

an elevation angle of more than 10 and 20 degrees respectively. The sensors and their disposition on board the JUICE spacecraft are shown in Figure 4.4. Given that these instruments are placed all on the same side of satellite and that their operations do not produce any mutual interference, no constraint related to inter-instrument conflict has been considered.

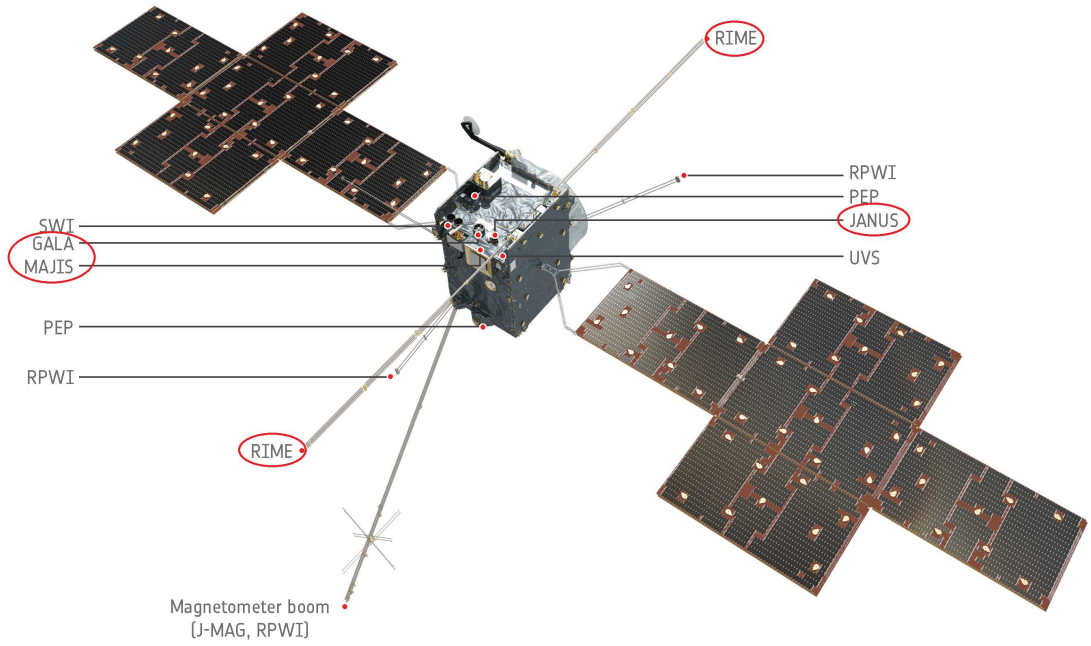

Figure 4.4: Illustration[1] of the instruments composing the science payload of the JUICE mission and their disposition on the spacecraft. The instruments' names circled in red identify the sensors included in our experiments.

4.3.2 Experimental Setup

Similarly to what has been done to test the methodology presented in Chapter 3, the segmentation starts considering the trajectory that the spacecraft will follow the GCO-500 phase and the time horizon over which this phase takes place as our Φ. We remind that the description of the trajectories is defined in a set of kernel files (those of the JUICE mission are available at [72]) that contain the state vector (made of position and speed) of the satellite at each time instant. For the JUICE mission, these kernels are created by the Operation Center of ESA (ESOC) based on the Consolidated Reports on Mission Analysis (CReMA). With respect to the trajectories considered for the tests in Chapter 3, however, we take into account those prepared for the version 5.0 of the CReMA

[1] Image reproduced from [78].

document. Given the instrument capabilities and limitations described above for the 4 considered sensors, for each of the instruments the time intervals in which observations are feasible are determined. We thus obtained the sets $\Phi_{f,j}$ of time intervals in which the acquisition with the j-th sensor are feasible. Given these time intervals and the required pointing angle, which is nadir for all 4 instruments, we identified for each instrument the portions of surface of Ganymede (ground tracks) that can be observed during the possibly long time intervals in $\Phi_{f,j}$. For RIME, the actual segmentation is performed as in Chapter 3, where a particular grid was defined based on the set of targets of high-interest provided by the RIME Science Working Team (SWT) and positioned and located in RIME operative area. For the other instruments (GALA, JANUS and MAJIS), the segmentation was similarly performed, but simply considering the boundaries of the considered target areas (which, we remind, are taken as example), given that they are quite distributed on the surface of Ganymede. Thus for all instruments, the time intervals $\Phi_{f,j}$ and the related ground tracks were subdivided into a set of segments S_j for each considered sensor.
Using the same strategy as described in Section 3.3, we determined for each sensor a set of uniformly distributed points $P_j = \{p_{1,j}, p_{2,j}, \ldots, p_{M_j,j}\}$ on the areas that the instrument needs to cover. These sets represent a quantization of the surface that helps simplifying the calculation of the surface covered by each acquisition segment $s_{i,j}$ as the number of points contained in $a(s_{i,j})$ ($\{p_{k,j} \in a(s_{i,j})\}$). To determine this parameter for all the segments associated to RIME and GALA, we exploited the concept of influence area introduced in Chapter 3, given the similar acquisition geometry, setting their width at 50 and 5 km respectively. For JANUS and MAJIS in an analogous way the areas $a(s_{i,j})$ have been determined considering the specified ground-projected field of view width of 15 and 30 km respectively. We remind that in this case they effectively represent a portion of covered surface, while for RIME and GALA concept of influence area is used to enforce the correct distance between the selected acquisition tracks. For each segment $s_{i,j}$ we then defined other useful data such as the day $day(s_{i,j})$ and the week $week(s_{i,j})$ in which the acquisition defined by $s_{i,j}$ should take place and the duration $time(s_{i,j})$. Moreover, having the information regarding the average generated data rate (DR_j) and the average power (Pow_j) for the acquisitions performed by each instrument (summarized in Table 4.1) we can evaluate the resource consumption by each acquisition segment as $m(s_{i,j}) = DR \cdot time(s_{i,j})$ and $e(s_{i,j}) = Pow_j \cdot time(s_{i,j})$.

After the segmentation stage was performed, the initial GA-based segment selection with the modified mutation operator (which uses the metrics $t(s_{k,j})$ and $r(s_{i,j})$ defined in Section 4.2.2) was executed for each sensor. As acquisition quality metric we considered for all instruments the area covered by the selected acquisition segments, reminding that

for RIME and GALA it identifies the spatial uniformity of the selected acquisition tracks. It can be expressed as the number of points $p_{k,j}$ covered one and only one time plus half the number of points by more than one segment. This solution was employed in order to penalize the solutions for a given instrument, in which some areas are acquired more than once. The metric was expressed in terms of cost (smaller values of the metric correspond to better solutions), thus for each instrument it is defined as follows:

$$cov(\mathbf{x}_j) = \frac{\left|P_j\right| - L - \frac{1}{2}OV}{\left|P_j\right|}, \tag{4.12a}$$

where:

$$L = \sum_{k=1}^{\left|P_j\right|} h_{k,j}, \tag{4.12b}$$

$$h_{k,j} = \begin{cases} 1, & \text{if } \sum_{i=1}^{N_j} l_{k,i,j} x_{i,j} = 1 \\ 0, & \text{otherwise} \end{cases}, \tag{4.12c}$$

and

$$OV = \sum_{k=1}^{\left|P_j\right|} ov_{k,j}, \tag{4.12d}$$

$$ov_{k,j} = \begin{cases} 1, & \text{if } \sum_{i=1}^{N_j} l_{k,i,j} x_{i,j} > 1 \\ 0, & \text{otherwise} \end{cases}, \tag{4.12e}$$

$$l_{k,i,j} = \begin{cases} 1, & \text{if } p_{k,j} \in a(s_{i,j}) \\ 0, & \text{otherwise} \end{cases} \tag{4.12f}$$

with $p_{k,j} \in P_j$. Following this first segment selection phase for each instrument, the Global Schedule Optimization and Harmonization task is performed.

Sensor	**# Acquisition Segments**	**Avg. Memory Usage (Data Rate) [Kb/s]**	**Avg. Power Consumption [W]**	**Starting Schedule Quality Score [%]**
RIME	6242	250	15.19	84.5038
GALA	2664	26	55.69	73.4434
JANUS	1275	550	40	92.7096
MAJIS	378	5740	30	85.5326

Table 4.1: Summary of the employed sensors and of their salient characteristics for the simultaneous planning and scheduling test.

Thus, they are given in input to the proposed "simplified" global schedule optimization and harmonization depicted in Figure 4.3 and described at the end of Section 4.2.2. For the upper level we employed an objective function expressed as in Eq.4.2. Each of the variables used for the upper level (the weights $w_{i,j}$) are associated to all segments $s_{i,j}$ defined for the j-th instrument and related to the same week. Segments associated to different instruments but related to the same week have different associated weights, so that the observations in a given week by a given instrument can be favored with respect to those by another sensor.

4.3.3 Results

As mentioned above, we carried our tests considering the reduced version of the global schedule optimization and harmonization phase. Thus, after the initial GA-based segment selection phase we have obtained the starting observation schedules, given the characteristics of the employed trajectory files and of the resulting avaliable observation opportunities for each sensor. For each sensor, it took about 4 hours to reach 5000 iterations of the optimization, implemented with the described GA approach, on a 16-core AMD Ryzen 9 5950X CPU with 128 GB of RAM. These optimized schedules are then fed to the PSO-based global schedule harmonization block (upper level) and to the instrument-related local-search-based schedule adjustment blocks. The bilevel system built as described was executed for 2500 iterations of the upper level optimization and it took about 3 hours on the same machine. This result in terms of computational time, also compared with the ones shown in the previous Chapter, show how the use of the simplified strategy allowed to reduce the required resources and execution time, which would have been orders of magnitude larger in the case of the approach using GAs at the lower level.

Sensor	**Starting Schedule Quality Score** [%]	**Final Schedule Quality Score** [%]
RIME	84.5038	77.3382
GALA	73.4434	65.7165
JANUS	92.7096	89.6198
MAJIS	85.5326	78.6455

Table 4.2: Summary of the quality scores after the first segment selection for each instrument and after the global schedule optimization and harmonization

The result in terms of individual acquisition schedule quality after the GA-based segment selection and after the application of the whole proposed methodology are summa-

rized in Table 4.2. It is possible to see how for each instrument the associated schedules have gone through a slight degradation of the quality, caused mainly by the effective availability of valid alternatives for the segment replacement performed in the local-search-based schedule adjustment (especially in the case of GALA). Moreover, this is also caused by the constraint violation in terms of memory given by the combination of the initial observation schedules for all the considered sensors, which was corrected by the PSO-based schedule harmonization. However, the produced final schedules still obtain satisfying values in terms of quality and this could be obtained by keeping the substitution rate ρ_{sub} (whose value was determined empirically) as small as possible and thus modifying only a small number of acquisition segments with respect to the original schedules. For the control of the memory limitations we employed a particular threshold, based on the amount of memory that can be downlinked each week and the total available time for the GCO-500 phase, after which no more data can be sent down to Earth. Accordingly, for each week we calculated the cumulative amount of data that cannot be downlinked and checked these values against the threshold that we set.

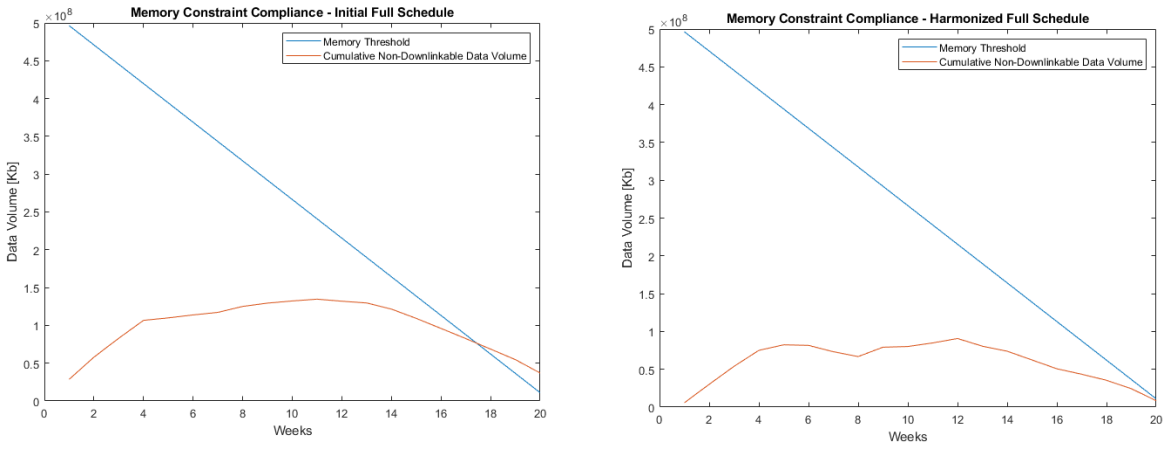

Figure 4.5: Memory constraint checks for the initial and the final combined schedules. It is possible to see how the curve related to the cumulative non-downlinkable data volume has been improved thanks to the weights produced by the PSO-based upper level optimization process.

Figures 4.5 and 4.6 show the profiles obtained for the initial combined observation schedule and the one resulting from the global schedule optimization and harmonization phase both for the cumulative non-downlinkable data volume and for the weekly datavolume. It is possible to see how the weights produced by the global schedule optimization and harmonization process have helped modify the data volume generated for each week in order to correct the final combined schedule, so that no constraint is violated anymore. In the initial combined schedule, indeed, it is possible to see that the curve identifying

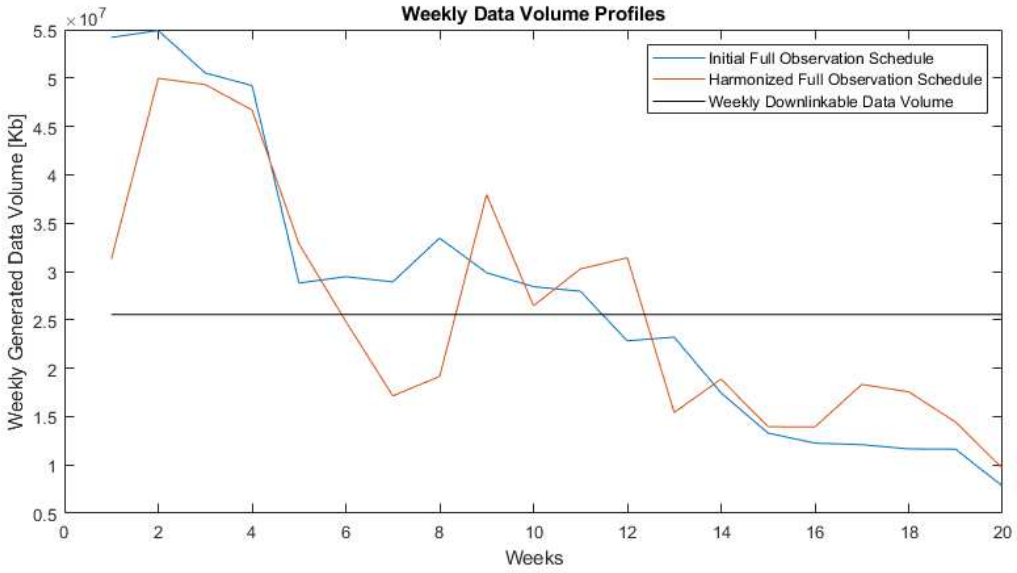

Figure 4.6: Weekly data volume profiles obtained for the initial and the final combined observation schedules, compared with the amount of data that can be downlinked to Earth every week. Also here it is possible to observe how the weights specified at the global level modified the data volume profile for the final joint acquisition plan.

the cumulative non-downlinkable data volume exceeds the threshold that we set, meaning that a part of the whole generated data volume could not be downlinked at all, if that observation schedule would be followed. Thus, it is possible to see that even if the quality of the observation schedules related to each instrument was slightly degraded, the proposed system was efficient in providing a satisfying final solution, which is also feasible with respect to all considered limitations.

4.4 Conclusion

In this chapter we have presented a methodology to automatize the planning and scheduling process for Planetary Exploration missions. In particular, in this case we have considered the study of the acquisition operations of multiple instruments included in the scientific payload of a mission simultaneously. We have defined and presented a methodology which partially exploits the framework developed and presented in Chapter 3 and it extends it in order to take into account the limitations and the objectives of multiple sensors at the same time. The proposed approach is based on 2 main stages: the segmentation and the schedule optimization and harmonization. The second stage is in turn made of 2 deeply interconnected components, devoted to the management of the

operations at the instrument level and at the global/mission level.

For the segmentation phase we exploited the method defined in Chapter 3 to subdivide the long available acquisition time intervals into shorter segments based on a spatial criterion. This way of segmenting the observation opportunities allows the ground tracks not to be split over high-relevance targets and this is particularly important for the data acquired by many types of sensors. The segmentation is applied to each considered sensor, so that we can define in detail the observation opportunities for each instrument and their characteristics. For the schedule optimization and harmonization phase (modeled as a bilevel optimization problem), a hybrid GA-PSO nested optimization technique is considered to complete 2 tasks. At the lower level a GA-based optimizer produces for each considered instrument observation schedules with the best possible instrument-specific quality metric value and science requirement compliance. At the upper level, a PSO-based engine iteratively guides the schedule generation performed at the lower level assigning weights to the acquisition segments associated to each sensor, to avoid violations of global constraints and thus increase the global schedule acquisition quality. Given the complexity of the structure, we also proposed an alternative approach, substituting the GA-based schedule generation to be performed at each iteration of the upper level optimization and for each instrument, with a local search technique acting on previously generated optimal schedules for each instrument. We analyzed the simplified version of the proposed approach by considering its application to the real study case of the operations of 4 different instruments of the science payload of the JUICE mission.

The obtained experimental results are promising and show the potential of the proposed approach in generating good quality schedules and avoid constraint violations. From the achieved results we can conclude that with the simplified version of the proposed approach we were able to just partially degrade the quality of the initial optimal schedules for each considered instrument. At the same time it significantly improved the quality of the resulting joint observation schedule with respect to the resource consumption constraint, producing a final joint schedule that does not violate the memory constraint, which was instead exceeded in by the initial joint schedule. As briefly mentioned in the previous section, a fundamental role in this simplified version of the proposed approach is played by the substitution rate ρ_{sub}, which helped maintaining a good quality for the output instrument observation schedules.Thus, the proposed methodology represents a good tool both to produce optimized schedules for multiple instruments composing the scientific payload of a planetary exploration mission at the same time and to perform analyses on the operations for such missions. Results like the ones presented allow us to try to extend this approach to more instruments, up to consider an entire science payload of a PE mission.

Chapter 5

Conclusions and Future Developments

This Chapter draws the conclusions of the work presented in this thesis. It provides a general discussion regarding the problem that has been dealt with, together with an analysis of the strengths and weaknesses of the proposed contributions. In the second part possible future developments are briefly discussed.

Discussion

In this thesis we addressed the problem of handling the planning and scheduling task for the observations to be performed by the instruments of the science payload of Planetary Exploration missions. We focused our efforts on the development of planning and scheduling methods for instrument observations, which are aimed at increasing the amount of automation of this task, thus reducing the very long time usually required to address this very important part of the mission design.
According to the objectives specified in the introductory chapter, in this thesis two main contributions have been provided:

- Chapter 3 is dedicated to the planning and scheduling of the acquisitions by one single instrument, by addressing the challenges of carefully modelling the objectives and the metrics required to describe an acquisition campaign covering a very large time horizon. It was aimed at characterizing a suitable technique able to handle a very large scale problem, typically required in planetary missions. This was done in order to address the literature gaps regarding the automatic handling of observation operations for PE missions. In this context we proposed an approach, based on multi-

objective Genetic Algorithms, able to identify and characterize a set of acquisition units among which to select multiple subsets representing observation schedules that correspond to optimal tradeoffs of the specified objectives. These objectives measure different potentially conflicting aspects determining the acquisition quality of an acquisition schedule generated for a given instrument.

- Chapter 4 is related to the management of observation operations to be performed by multiple sensors composing the science payload of Planetary Exploration missions instead addressed the very complex challenges of defining a unique methodology for the simultaneous planning and scheduling of the data acquisitions for multiple instruments. In this context we defined and described a suitable model to represent the problem at hand, and we proposed a 2-stage iterative technique. This methodology exploits, extends and generalizes the strategies analyzed in the single instrument context, in order to manage the typically large and complex constraints characterizing a PE mission and the different types of objectives that could be associated to each considered sensor.

- Chapter 2 described the details of the observation operations performed by radar sounders and underlined the characteristics and the peculiarities of the acquisitions of these instruments. In the two Chapters mentioned above, we showed the application of the two proposed methodologies to radar sounder observations and in particular we analyzed the operations of RIME, radar sounder of the JUICE mission.

The novel contribution provided by this thesis is hereby discussed, considering the strengths and the weaknesses of the proposed approaches. In Chapter 3, the main goal of the proposed approach is to automatically generate near-optimal acquisition plans for one sensor in the science payload, considering instrument-specific limitations and quality metrics and thus providing a tool being able to speed up the usually very long planning and scheduling process for planetary missions. The proposed technique consists of two main stages, i.e. the segmentation and the selection, during which all feasible acquisition intervals (with respect to the considered instrument capabilities and the environmental conditions) are defined, analyzed and evaluated to generate observation sequences for a specific sensor over the input (usually large) time horizon. The segmentation subdivides the considered time horizon into well-defined shorter acquisition segments, following a time-based or a space-based criterion. The last one is particularly suitable to take into account the presence of areas of higher relevance. In the selection phase, an NSGA-II-based multiobjective optimization process explores the space of the candidate schedules related to the combinations of the available acquisition segments, by analyzing different objectives expressed by possibly competing metrics. One of the most challenging problems

in the development and the evaluation of such a system is the dimension of the considered problem, which might lead the NSGA-II to early convergence in local optima. However, the implementation of the modified mutation operator exploiting the knowledge that we have regarding the available acquisition opportunities allowed us to generate observation schedules yielding very good quality, thus the obtained results are very promising. However, part of the solutions obtained by the proposed methodology in the produced Pareto front cannot be considered satisfactory for the analyzed test case. A possible way to reduce the number of non-satisfactory solutions and to focus only on the desired portions of the Pareto front could be the use of a technique such as NSGA-III [79]. Indeed, in this technique it is possible to specify a reference point in the objective functions space and the distance of the generated solutions from this point is used as an important parameter to rank them, thus guiding the search of new solutions in a neighbourhood of the reference point. Nonetheless, the two tested versions of the proposed methodology are both able to find a large number of high-quality acquisition schedules. Moreover, from the obtained results it is possible to underline the efficiency of the proposed mutation operator for the exploration of the solution space and its potentiality in finding very good solutions for a large-dimensional problem. Finally, the proposed approach was tested considering a radar sounder instrument, providing a way to easily describe and evaluate the observation quality for an acquisition campaign performed by this kind of instrument that has a very peculiar acquisition geometry. A weak point of the proposed methodology is the need of large computational resources and execution time in order to provide a set of high-quality schedules. However, for the context to which this methodology should be applied this is not a crucial issue, even if less demanding versions of this approach could still be useful to perform an operation analysis in shorter time.

In Chapter 4 we presented a method for the simultaneous automatic observation planning and scheduling for multiple sensors, based on a hybrid (Genetic Algorithms - Particle Swarm Optimization) nested *bilevel* optimization structure, to be used in complex planetary remote sensing missions. The goal of the proposed approach is to provide a method being able to consider the acquisition operations of more than one sensor simultaneously, automatically producing global observation schedules that are optimized with respect to the considered global quality metric and feasible with respect to any kind of constraint. The proposed methodology is made up of 2 main stages and it partially exploits the system described in Chapter 3, especially for the segmentation phase, performed for each considered instrument. In the schedule optimization and harmonization phase, a hybrid GA-PSO nested optimization engine is employed to complete 2 tasks, namely the handling of the observation operations at the instrument level and at the global level, where the global level is meant to guide the generation of the optimal schedules performed at

the instrument level. In the presented approach, we modeled the problem as a bilevel optimization problem, which is very suitable due to the characteristics of the problem at hand. However, if for the first contribution the dimensionality of the problem was a critical issue, here this aspect is even more relevant given the number of sensors that have to be considered simultaneously. To keep this aspect under control, we proposed an alternative reduced version of the methodology that is able to greatly reduce the required computational time and resources. Conceptually, the purely nested approach described in Chapter 4 would be able to perform much better in terms of quality than its reduced version, but in order to execute such a complex and resource-demanding system, a very large execution time and computational power would be required, especially considering to extend the method to a full science payload. An important issue to take into account in order to evaluate the results of the proposed methodology, as pointed out in Section 4.4, are the characteristics of the available acquisition opportunities, depending from the features of the analyzed trajectory and from the limited search space that the local search technique can explore. In this context, as observed in Section 4.3.3, a crucial point to analyze is the substitution rate ρ_{sub}, which was determined empirically. Too small a substitution rate would dramatically reduce the flexibility of the proposed methodology, while a large value of this parameter would make the local search not efficient. In order to obtain better results in terms of quality (and even in terms of constraint compliance in case of very tight resource limitation), its value could be determined adaptively iteration by iteration, based on the characteristics of the solutions produced at the previous iteration. However, the obtained results show how the proposed methodology is still able to correctly guide the generation of the observation schedules for each instrument, until the constraint violations present in the initial combined observation schedule were corrected, showing thus promising performances. The proposed methodology represents therefore a good starting point to further improve the performances of an automatic observation scheduling system for multiple sensors on board Planetary Exploration missions.

Given these considerations, it is possible to conclude that the proposed approaches represent a valuable contribution to the automation of the planning and scheduling task of the acquisition operations to be performed by the science payload instruments in the context of Planetary Exploration missions and in this sense it addresses very open challenges and gaps in the literature for this topic.

5.1 Future Developments

In this thesis we proposed new methodologies for the automation of the planning and scheduling task for acquisition operations, providing an important contribution in this field studying methods in the context of Planetary Exploration missions. However, as briefly pointed out at the end of the previous section, the proposed methodology for the automatic simultaneous scheduling of the observations by multiple instruments represents a starting point for the research in this field, given the scarcity of automatic scheduling applications in the context of PE missions.
In order to improve the performances of the presented methodologies different aspects can be considered:

- Improving the modeling of the requirements and observation capabilities of different types of sensors used in the context of PE missions, in order to ease the definition of instrument-specific metrics to describe the quality of extended acquisition campaigns;
- The possible integration of a system such as the one proposed in Chapter 4 with tools designed specifically to support the science operations definition (such as MAPPS), in order to improve the characterization of the acquisition opportunities, especially from the point of view of the resources exploitation;
- From a more theoretical point of view, it would be interesting to study large combinatorial bilevel optimization problems more in detail, which are deemed to be very complex from a computational point of view, in order to develop methods to tackle and solve these problems, improving the efficiency and the results of a system such as the one presented in Chapter 4;
- Finally, the application of methodologies developed as such to full science payloads of Planetary Exploration missions.

List of Publications

INTERNATIONAL JOURNALS

[J1] **S. Paterna**, M. Santoni, L. Bruzzone, "An Approach Based on Multiobjective Genetic Algorithms to Schedule Observations in Planetary Remote Sensing Missions," in IEEE Journal of Selected Topics in Applied Earth Observations and Remote Sensing, vol. 13, pp. 4714-4727, 2020, doi: 10.1109/JSTARS.2020.3015284.

INTERNATIONAL CONFERENCES

[C1] **S. Paterna**, M. Santoni, L. Bruzzone, "An Automatic Planning and Scheduling Method Based on Multi-Objective Genetic Algorithms for Planetary Radar Sounder Observations," 2020 IEEE International Geoscience and Remote Sensing Symposium (IGARSS), Waikoloa, HI, USA, 2020, doi: 10.1109/IGARSS39084.2020.9324270.

[C2] L. Bruzzone, F. Bovolo, S. Thakur, L. Carrer, E. Donini, C. Gerekos, **S. Paterna**, M. Santoni, E. Sbalchiero, "Envision Mission to Venus: Subsurface Radar Sounding", 2020 IEEE International Geoscience and Remote Sensing Symposium (IGARSS), Waikoloa, HI, USA, 2020, doi: 10.1109/IGARSS39084.2020.9324279.

Bibliography

[1] O. Grasset, M. Dougherty, A. Coustenis, E. Bunce, C. Erd, D. Titov, M. Blanc, A. Coates, P. Drossart, L. Fletcher, H. Hussmann, R. Jaumann, N. Krupp, J.-P. Lebreton, O. Prieto-Ballesteros, P. Tortora, F. Tosi, and T. Van Hoolst, "JUpiter ICy moons Explorer (JUICE): An ESA mission to orbit Ganymede and to characterise the Jupiter system," *Planetary and Space Science*, vol. 78, pp. 1–21, 2013. [Online]. Available: https://www.sciencedirect.com/science/article/pii/S0032063312003777

[2] "Galileo," https://solarsystem.nasa.gov/missions/galileo/in-depth/.

[3] P. Van Der Plas, B. García-Gutiérrez, F. Nespoli, and M. Pérez-Ayúcar, "MAPPS: a Science Planning tool supporting the ESA Solar System Missions," *SpaceOps 2016 Conference*, 2016. [Online]. Available: https://arc.aiaa.org/doi/abs/10.2514/6.2016-2512

[4] T. Choo, S. Murchie, P. Bedini, R. Steele, J. Skura, L. Nguyen, H. Nair, M. Lucks, A. Berman, J. McGovern, and F. Turner, "SciBox, an end-to-end automated science planning and commanding system," *Acta Astronautica*, vol. 93, pp. 490 – 496, 2014. [Online]. Available: http://www.sciencedirect.com/science/article/pii/S0094576512003682

[5] B. Paczkowski and T. Ray, *Cassini Science Planning Process*. [Online]. Available: https://arc.aiaa.org/doi/abs/10.2514/6.2004-544-339

[6] M. Ai-Chang, J. Bresina, L. Charest, A. Chase, J.-J. Hsu, A. Jonsson, B. Kanefsky, P. Morris, K. Rajan, J. Yglesias, B. G. Chafin, W. C. Dias, and P. F. Maldague, "MAPGEN: mixed-initiative planning and scheduling for the Mars Exploration Rover mission," *IEEE Intelligent Systems*, vol. 19, no. 1, pp. 8–12, Jan 2004.

[7] S. Chien, G. Rabideau, R. Knight, R. Sherwood, B. Engelhardt, D. Mutz, T. Estlin, B. Smith, F. Fisher, T. Barrett *et al.*, "ASPEN-Automating space mission operations using automated planning and scheduling," in *SpaceOps 2000*. AIAA Press, 2000.

[8] M. Zweben, E. Davis, B. Daun, and M. Deale, "Scheduling and rescheduling with iterative repair," *IEEE Transactions on Systems, Man, and Cybernetics*, vol. 23, no. 6, pp. 1588–1596, 1993.

[9] M. Barkaoui and J. Berger, "A new hybrid genetic algorithm for the collection scheduling problem for a satellite constellation," *Journal of the Operational Research Society*, vol. 71, no. 9, pp. 1390–1410, 2020. [Online]. Available: https://doi.org/10.1080/01605682.2019.1609891

[10] Z. Waiming, H. Xiaoxuan, X. Wei, and J. Peng, "A two-phase genetic annealing method for integrated earth observation satellite scheduling problems," *Soft Computing*, vol. 23, no. 1, pp. 181–196, Jan 2019. [Online]. Available: https://doi.org/10.1007/s00500-017-2889-8

[11] J. Wang, E. Demeulemeester, D. Qiu, and J. Liu, "Exact and inexact scheduling algorithms for multiple earth observation satellites under uncertainties of clouds," SSRN, 2015.

[12] E. Bensana, G. Verfaillie, J. Agnese, N. Bataille, and D. Blumstein, "Exact &inexact methods for daily man-

agement of earth observation satellite," in *Space Mission Operations and Ground Data Systems-SpaceOps' 96*, vol. 394, 1996, p. 507.

[13] M. Vasquez and J.-K. Hao, "A "logic-constrained" knapsack formulation and a tabu algorithm for the daily photograph scheduling of an earth observation satellite," *Computational Optimization and Applications*, vol. 20, no. 2, pp. 137–157, Nov 2001. [Online]. Available: https://doi.org/10.1023/A:1011203002719

[14] M. Vasquez and J. K. Hao, "Upper bounds for the spot 5 daily photograph scheduling problem," *Journal of Combinatorial Optimization*, vol. 7, no. 1, pp. 87–103, Mar 2003. [Online]. Available: https://doi.org/10.1023/A:1021950608048

[15] J. Puchinger, G. Raidl, and U. Pferschy, "The Multidimensional Knapsack Problem: Structure and Algorithms," *INFORMS Journal on Computing*, vol. 22, no. 2, pp. 576 – 588, Apr. 2010. [Online]. Available: https://doi.org/10.1287/ijoc.1090.0344

[16] M. Lemaître, G. Verfaillie, F. Jouhaud, J. Lachiver, and N. Bataille, "Selecting and scheduling observations of agile satellites," *Aerospace Science and Technology*, vol. 6, no. 5, pp. 367 – 381, 2002. [Online]. Available: http://www.sciencedirect.com/science/article/pii/S1270963802011732

[17] R. Knight and B. Smith, "Optimally Solving Nadir Observation Scheduling Problems," in *Proceedings of the i-SAIRAS 2005 - 8th International Symposium on Artificial intelligence, Robotics and Automation in Space*, September 2005.

[18] V. Gabrel and D. Vanderpooten, "Enumeration and interactive selection of efficient paths in a multiple criteria graph for scheduling an earth observing satellite," *European Journal of Operational Research*, vol. 139, no. 3, pp. 533–542, 2002. [Online]. Available: https://www.sciencedirect.com/science/article/pii/S0377221701001886

[19] G. Verfaillie and T. Schiex, "Russian doll search for solving constraint optimization problems," in *Proceedings of AAAI-96*, 1996, pp. 181–187.

[20] H. Muraoka, R. Cohen, T. Ohno, and N.Doi, "ASTER Observation Scheduling Algorithm," in *Proceedings of the 5th International Symposium on Space Mission Operations and Ground Data Systems (SpaceOps -98)*, 1998, Tokyo, Japan.

[21] E. Maurer, F. Mrowka, A. Braun, M. P. Geyer, C. Lenzen, Y. Wasser, and M. Wickler, "TerraSAR-X Mission Planning System: Automated Command Generation for Spacecraft Operations," *IEEE Transactions on Geoscience and Remote Sensing*, vol. 48, no. 2, pp. 642–648, Feb 2010.

[22] N. Bianchessi and G. Righini, "Planning and scheduling algorithms for the COSMO-SkyMed constellation," *Aerospace Science and Technology*, vol. 12, no. 7, pp. 535–544, 2008. [Online]. Available: https://www.sciencedirect.com/science/article/pii/S1270963808000187

[23] R. Xu, H. Chen, X. Liang, and H. Wang, "Priority-based constructive algorithms for scheduling agile earth observation satellites with total priority maximization," *Expert Systems with Applications*, vol. 51, pp. 195–206, 2016. [Online]. Available: https://www.sciencedirect.com/science/article/pii/S0957417415008477

[24] F. Glover, "Tabu Search—Part I," *ORSA Journal on Computing*, vol. 1, no. 3, pp. 190–206, 1989. [Online]. Available: https://doi.org/10.1287/ijoc.1.3.190

[25] Glover, Fred, "Tabu search—part ii," *ORSA Journal on Computing*, vol. 2, no. 1, pp. 4–32, 1990. [Online]. Available: https://doi.org/10.1287/ijoc.2.1.4

[26] T. Bäck, *Evolutionary Algorithms in Theory and Practice: Evolution Strategies, Evolutionary Programming, Genetic Algorithms*. USA: Oxford University Press, Inc., 1996.

[27] J. Kennedy and R. Eberhart, "Particle swarm optimization," in *Proceedings of ICNN'95 - International*

Conference on Neural Networks, vol. 4, 1995, pp. 1942–1948 vol.4.

[28] A. Colorni, M. Dorigo, and V. Maniezzo, "Distributed optimization by ant colonies," in *Proceedings of the First European Conference on Artificial Life*, Jan 1991.

[29] S. Kirkpatrick, C. D. Gelatt, and M. P. Vecchi, "Optimization by simulated annealing," *Science*, vol. 220, no. 4598, pp. 671–680, 1983. [Online]. Available: https://science.sciencemag.org/content/220/4598/671

[30] N. Bianchessi, J.-F. Cordeau, J. Desrosiers, G. Laporte, and V. Raymond, "A heuristic for the multi-satellite, multi-orbit and multi-user management of earth observation satellites," *European Journal of Operational Research*, vol. 177, no. 2, pp. 750–762, 2007. [Online]. Available: https://www.sciencedirect.com/science/article/pii/S0377221706000051

[31] J. F. Cordeau and G. Laporte, "Maximizing the value of an Earth observation satellite orbit," *Journal of the Operational Research Society*, vol. 56, no. 8, pp. 962–968, 2005. [Online]. Available: https://doi.org/10.1057/palgrave.jors.2601926

[32] L. Xiaolu, B. Baocun, C. Yingwu, and Y. Feng, "Multi satellites scheduling algorithm based on task merging mechanism," *Applied Mathematics and Computation*, vol. 230, pp. 687–700, 2014. [Online]. Available: https://www.sciencedirect.com/science/article/pii/S0096300313013994

[33] G. Wu, J. Liu, M. Ma, and D. Qiu, "A two-phase scheduling method with the consideration of task clustering for earth observing satellites," *Computers and Operations Research*, vol. 40, no. 7, pp. 1884–1894, 2013. [Online]. Available: https://www.sciencedirect.com/science/article/pii/S030505481300049X

[34] Z. Zhang, N. Zhang, and Z. Feng, "Multi-satellite control resource scheduling based on ant colony optimization," *Expert Systems with Applications*, vol. 41, no. 6, pp. 2816–2823, 2014. [Online]. Available: https://www.sciencedirect.com/science/article/pii/S0957417413008282

[35] G. Peng, L. Wen, Y. Feng, B. Baocun, and Y. Jing, "Simulated annealing algorithm for eos scheduling problem with task merging," in *Proceedings of 2011 International Conference on Modelling, Identification and Control*, 2011, pp. 547–552.

[36] F. Xhafa, X. Herrero, A. Barolli, and M. Takizawa, "A simulated annealing algorithm for ground station scheduling problem," in *2013 16th International Conference on Network-Based Information Systems*, 2013, pp. 24–30.

[37] G. Wu, H. Wang, W. Pedrycz, H. Li, and L. Wang, "Satellite observation scheduling with a novel adaptive simulated annealing algorithm and a dynamic task clustering strategy," *Computers & Industrial Engineering*, vol. 113, pp. 576 – 588, 2017. [Online]. Available: http://www.sciencedirect.com/science/article/pii/S0360835217304679

[38] D. Zhang, L. Guo, B. Cai, N. Sun, and Q. Wang, "A hybrid discrete particle swarm optimization for satellite scheduling problem," in *IEEE Conference Anthology*, 2013, pp. 1–5.

[39] S. woo Baek, S. mi Han, K. rae Cho, D. woo Lee, J. sik Yang, P. M. Bainum, and H. dong Kim, "Development of a scheduling algorithm and GUI for autonomous satellite missions," *Acta Astronautica*, vol. 68, no. 7, pp. 1396–1402, 2011. [Online]. Available: https://www.sciencedirect.com/science/article/pii/S0094576510002997

[40] S. mi Han, S. woo Beak, K. rae Cho, D. woo Lee, and H. dong Kim, "Satellite mission scheduling using genetic algorithm," in *2008 SICE Annual Conference*, 2008, pp. 1226–1230.

[41] H. Kim and Y. K. Chang, "Mission scheduling optimization of sar satellite constellation for minimizing system response time," *Aerospace Science and Technology*, vol. 40, pp. 17–32, 2015. [Online]. Available: https://www.sciencedirect.com/science/article/pii/S1270963814002041

[42] Y. Li, M. Xu, and R. Wang, "Scheduling Observations of Agile Satellites with Combined Genetic Algorithm," in *Third International Conference on Natural Computation (ICNC 2007)*, vol. 3, 2007, pp. 29–33.

[43] Z. Zheng, J. Guo, and E. Gill, "Swarm satellite mission scheduling & planning using hybrid dynamic mutation genetic algorithm," *Acta Astronautica*, vol. 137, pp. 243–253, 2017. [Online]. Available: https://www.sciencedirect.com/science/article/pii/S0094576516310396

[44] W. J. Wolfe and S. E. Sorensen, "Three scheduling algorithms applied to the earth observing systems domain," *Management Science*, vol. 46, no. 1, pp. 148–166, 2000. [Online]. Available: https://doi.org/10.1287/mnsc.46.1.148.15134

[45] M. A. Mansour and M. M. Dessouky, "A genetic algorithm approach for solving the daily photograph selection problem of the spot5 satellite," *Computers & Industrial Engineering*, vol. 58, no. 3, pp. 509–520, 2010, supply, Production and Distribution Systems. [Online]. Available: https://www.sciencedirect.com/science/article/pii/S036083520900299X

[46] X. N. Niu, H. Tang, and L. X. Wu, "Multi-satellite observation scheduling for large area disaster emergency response," *The International Archives of the Photogrammetry, Remote Sensing and Spatial Information Sciences*, vol. XLII-3, pp. 1327–1331, 2018. [Online]. Available: https://www.int-arch-photogramm-remote-sens-spatial-inf-sci.net/XLII-3/1327/2018/

[47] P. Tangpattanakul, N. Jozefowiez, and P. Lopez, "A multi-objective local search heuristic for scheduling earth observations taken by an agile satellite," *European Journal of Operational Research*, vol. 245, no. 2, pp. 542–554, 2015. [Online]. Available: https://www.sciencedirect.com/science/article/pii/S0377221715002040

[48] X. Zhai, X. Niu, H. Tang, L. Wu, and Y. Shen, "Robust satellite scheduling approach for dynamic emergency tasks," *Mathematical Problems in Engineering*, vol. 2015, p. 482923, Dec 2015. [Online]. Available: https://doi.org/10.1155/2015/482923

[49] J. Wang, N. Jing, J. Li, and Z. H. Chen, "A multi-objective imaging scheduling approach for earth observing satellites," in *Proceedings of the 9th Annual Conference on Genetic and Evolutionary Computation*, ser. GECCO '07. New York, NY, USA: Association for Computing Machinery, 2007, p. 2211–2218. [Online]. Available: https://doi.org/10.1145/1276958.1277381

[50] V. Kolici, X. Herrero, F. Xhafa, and L. Barolli, "Local search and genetic algorithms for satellite scheduling problems," in *Proceedings of the 2013 Eighth International Conference on Broadband and Wireless Computing, Communication and Applications*, ser. BWCCA '13. USA: IEEE Computer Society, 2013, p. 328–335. [Online]. Available: https://doi.org/10.1109/BWCCA.2013.58

[51] F. Xhafa, J. Sun, A. Barolli, A. Biberaj, and L. Barolli, "Genetic algorithms for satellite scheduling problems," *Mobile Information Systems*, vol. 8, pp. 351 – 377, 10 2012.

[52] L. Barbulescu, J.-P. Watson, L. D. Whitley, and A. E. Howe, "Scheduling space–ground communications for the air force satellite control network," *Journal of Scheduling*, vol. 7, no. 1, pp. 7–34, Jan 2004. [Online]. Available: https://doi.org/10.1023/B:JOSH.0000013053.32600.3c

[53] P. Soma, S. Venkateswarlu, S. Santhalakshmi, T. Bagchi, and S. Kumar, "Multi-satellite scheduling using genetic algorithms," in *Space OPS 2004 Conference*, 2004. [Online]. Available: https://arc.aiaa.org/doi/abs/10.2514/6.2004-743-515

[54] R. Jordan, G. Picardi, J. Plaut, K. Wheeler, D. Kirchner, A. Safaeinili, W. Johnson, R. Seu, D. Calabrese, E. Zampolini, A. Cicchetti, R. Huff, D. Gurnett, A. Ivanov, W. Kofman, R. Orosei, T. Thompson, P. Edenhofer, and O. Bombaci, "The Mars Express MARSIS Sounder Instrument," *Planetary and Space Science*, vol. 57, no. 14, pp. 1975 – 1986, 2009. [Online]. Available: http://www.sciencedirect.com/science/article/pii/S0032063309002803

[55] R. Croci, R. Seu, E. Flamini, and E. Russo, "The SHAllow RADar (SHARAD) Onboard the NASA MRO Mission," *Proceedings of the IEEE*, vol. 99, no. 5, pp. 794–807, May 2011.

[56] T. Ono and H. Oya, "Lunar radar sounder (lrs) experiment on-board the selene spacecraft," *Earth, Planets and Space*, vol. 52, no. 9, pp. 629–637, Sep 2000. [Online]. Available: https://doi.org/10.1186/BF03351671

[57] T. Ono, A. Kumamoto, Y. Kasahara, Y. Yamaguchi, A. Yamaji, T. Kobayashi, S. Oshigami, H. Nakagawa, Y. Goto, K. Hashimoto, Y. Omura, T. Imachi, H. Matsumoto, and H. Oya, "The lunar radar sounder (lrs) onboard the kaguya (selene) spacecraft," *Space Science Reviews*, vol. 154, no. 1, pp. 145–192, Jul 2010. [Online]. Available: https://doi.org/10.1007/s11214-010-9673-8

[58] L. Bruzzone, J. J. Plaut, G. Alberti, D. D. Blankenship, F. Bovolo, B. A. Campbell, D. Castelletti, Y. Gim, A. M. Ilisei, W. Kofman, G. Komatsu, W. McKinnon, G. Mitri, A. Moussessian, C. Notarnicola, R. Orosei, G. W. Patterson, E. Pettinelli, and D. Plettemeier, "Jupiter ICY moon explorer (JUICE): Advances in the design of the radar for Icy Moons (RIME)," in *2015 IEEE International Geoscience and Remote Sensing Symposium (IGARSS)*, July 2015, pp. 1257–1260.

[59] D. Blankenship, T. Ray, J. Plaut, A. Moussessian, W. Patterson, A. Romero-Wolf, C. Grima, D. Young, K. Soderlund, Y. Gim, D. Schroeder, A. Freedman, S. Collins, E. Chapin, J. Hoffman, and REASON Science Team, "REASON for Europa," in *42nd COSPAR Scientific Assembly*, vol. 42, Jul. 2018, pp. B5.3–55–18.

[60] L. Bruzzone, F. Bovolo, S. Thakur, L. Carrer, E. Donini, C. Gerekos, S. Paterna, M. Santoni, and E. Sbalchiero, "Envision mission to venus: Subsurface radar sounding," in *IGARSS 2020 - 2020 IEEE International Geoscience and Remote Sensing Symposium*, 2020, pp. 5960–5963.

[61] L. Carrer and L. Bruzzone, "Solving for ambiguities in radar geophysical exploration of planetary bodies by mimicking bats echolocation," *Nature Communications*, vol. 8, 12 2017.

[62] L. Carrer, "Advanced Signal Processing Methods for Planetary Radar Sounders Data," Ph.D. dissertation, University of Trento, 2018, Chapter 1.

[63] L. Carrer, D. M. Schroeder, A. Romero-Wolf, P. Ries, and L. Bruzzone, "Noise character constraints on passive radio sounding of jupiter's icy moons using jovian decametric radiation," in *IGARSS 2018 - 2018 IEEE International Geoscience and Remote Sensing Symposium*, 2018, pp. 4158–4161.

[64] L. Bruzzone, G. Alberti, C. Catallo, A. Ferro, W. Kofman, and R. Orosei, "Subsurface Radar Sounding of the Jovian Moon Ganymede," *Proceedings of the IEEE*, vol. 99, no. 5, pp. 837–857, May 2011.

[65] L. Carrer, D. M. Schroeder, A. Romero-Wolf, P. A. Ries, and L. Bruzzone, "Analysis of temporal and structural characteristics of jovian radio emissions for passive radar sounding of jupiter's icy moons," *IEEE Transactions on Geoscience and Remote Sensing*, vol. 59, no. 5, pp. 3857–3874, 2021.

[66] K. Deb, A. Pratap, S. Agarwal, and T. Meyarivan, "A fast and elitist multiobjective genetic algorithm: NSGA-II," *IEEE Transactions on Evolutionary Computation*, vol. 6, no. 2, pp. 182–197, April 2002.

[67] C. H. Acton, "Ancillary data services of NASA's Navigation and Ancillary Information Facility," *Planetary and Space Science*, vol. 44, no. 1, pp. 65 – 70, 1996. [Online]. Available: http://www.sciencedirect.com/science/article/pii/0032063395001077

[68] C. Acton, N. Bachman, B. Semenov, and E. Wright, "A look towards the future in the handling of space science mission geometry," *Planetary and Space Science*, vol. 150, pp. 9 – 12, 2018. [Online]. Available: http://www.sciencedirect.com/science/article/pii/S0032063316303129

[69] M. Emmerich and A. Deutz, "A tutorial on multiobjective optimization: fundamentals and evolutionary methods," *Natural Computing*, vol. 17, no. 3, pp. 585 – 609, Sep 2018. [Online]. Available: https://doi.org/10.1007/s11047-018-9685-y

[70] C. Persello and L. Bruzzone, "A novel protocol for accuracy assessment in classification of very high resolution images," *IEEE Transactions on Geoscience and Remote Sensing*, vol. 48, no. 3, pp. 1232 – 1244, March 2010.

[71] L. Pasolli, C. Notarnicola, and L. Bruzzone, "Multi-objective parameter optimization in support vector regression: General formulation and application to the retrieval of soil moisture from remote sensing data," *IEEE Journal of Selected Topics in Applied Earth Observations and Remote Sensing*, vol. 5, no. 5, pp. 1495–1508, Oct 2012.

[72] "JUICE SPICE Kernels Set." [Online]. Available: https://www.cosmos.esa.int/web/spice/spice-for-juice

[73] A. Boutonnet, J. Schoenmaekers, and W. Martens, "JUpiter Icy moons Explorer (JUICE): Consolidated Report on Mission Analysis (CReMA)," October 2015, Issue 3, Revision 0.

[74] A. Sinha, P. Malo, and K. Deb, "A review on bilevel optimization: From classical to evolutionary approaches and applications," *IEEE Transactions on Evolutionary Computation*, vol. 22, no. 2, pp. 276–295, 2018.

[75] H. Hussmann, K. Lingenauber, R. Kallenbach, K. Enya, N. Thomas, L. M. Lara, C. Althaus, H. Araki, T. Behnke, J. M. Castro-Marin, H. Eisenmenger, T. Gerber, M. Herranz de la Revilla, C. Hüttig, K. Ishibashi, J. Jiménez-Ortega, J. Kimura, M. Kobayashi, H.-G. Lötzke, A. Lichopoj, F. Lüdicke, I. Martínez-Navajas, H. Michaelis, N. Namiki, H. Noda, J. Oberst, S. Oshigami, J. P. Rodríguez García, J. Rodrigo, K. Rösner, A. Stark, G. Steinbrügge, P. Thabaut, S. del Togno, K. Touhara, S. Villamil, B. Wendler, K. Wickhusen, and K. Willner, "The Ganymede laser altimeter (GALA): key objectives, instrument design, and performance," *CEAS Space Journal*, vol. 11, no. 4, pp. 381–390, Dec 2019. [Online]. Available: https://doi.org/10.1007/s12567-019-00282-8

[76] P. Palumbo, R. Jaumann, G. Cremonese, H. Hoffmann, S. Debei, V. Corte, A. Holland, L. Lara, J. Castro, M. Herranz, A. Koncz, M. Leese, A. Lichopoj, D. Magrin, I. Martinez-Navajas, E. Epifani, H. Michaelis, R. Ragazzoni, T. Roatsch, and M. Soman, "JANUS: The Visible Camera Onboard the ESA JUICE Mission to the Jovian System," 01 2014.

[77] G. Piccioni, L. Tommasi, Y. Langevin, G. Filacchione, F. Tosi, D. Grassi, F. Poulet, C. Dumesnil, C. R. Degalarreta, A. Bini, G. Bugetti, I. Guerri, and M. Rossi, "Scientific goals and technical challenges of the MAJIS imaging spectrometer for the JUICE mission," in *2019 IEEE 5th International Workshop on Metrology for AeroSpace (MetroAeroSpace)*, 2019, pp. 318–323.

[78] "Juice's instruments," https://www.esa.int/ESA_Multimedia/Images/2019/02/Juice_s_instruments.

[79] K. Deb and H. Jain, "An evolutionary many-objective optimization algorithm using reference-point-based nondominated sorting approach, part i: Solving problems with box constraints," *IEEE Transactions on Evolutionary Computation*, vol. 18, no. 4, pp. 577–601, 2014.